

UNIVERSITY OF SOUTHAMPTON
FACULTY OF ENGINEERING, SCIENCE &
MATHEMATICS

Institute of Sound and Vibration Research



**The Analysis of Muscle Activity during the Gait Cycle
Based Upon Surface Electromyography Measurement
and Signal Processing Methods**

by

Wei Wang

Thesis for the degree of Doctor of Philosophy

April 2006

UNIVERSITY OF SOUTHAMPTON

ABSTRACT

**FACULTY OF ENGINEERING, SCIENCE &
MATHEMATICS**

INSTITUTE OF SOUND & VIBRATION RESEARCH

Doctor of Philosophy

**THE ANALYSIS OF MUSCLE ACTIVITY DURING THE GAIT
CYCLE BASED UPON SURFACE ELECTROMYOGRAPHY
MEASUREMENT AND SIGNAL PROCESSING METHODS**

Wei Wang

In the analysis of different gait patterns during normal and pathological walking, the surface electromyography (EMG) offers a safe and non-invasive approach to assess the muscle activity and function. The correlation between the surface EMG and gait analysis is addressed in this study to provide valuable information on muscle activity of clinical interest. The history and characteristics of the surface EMG during various clinical applications are reviewed at the beginning of this thesis. Physiological details, measurement, and acquisition system of the surface EMG are introduced. The fundamental concepts of gait analysis, such as gait phases and muscle control during different gait patterns are also described. To assess new methods and algorithms used to explore the muscle activity during the gait cycle, a model is generated with a multiple-layer structure, which contains most of features of the surface EMG, such as the fibre distribution, motor unit type, location and recruitment, tissue anisotropy, electrode configuration, and gait phases. A series of simulated surface EMG signals during the gait cycle are then produced by modifying the values of existing modular parameters depending upon the anatomical conditions and detection system configuration. Comparing the simulated signals with real EMG data, the results illustrate that the simulated signals are able to reproduce the surface EMG signals. The model has the potential to facilitate the assessment of algorithms or methods that are used to process normal or abnormal surface EMG signals during normal or pathological gait. Based upon the simulation model, an algorithm to detect the timing of muscle activation is developed in order to overcome shortcomings of approaches proposed previously, and is then used to process the real raw surface EMG signals recorded from the lower limb muscles during gait. The performance of the algorithm indicates that it is more suitable than previous methods for the estimation of muscle activation intervals.

CONTENTS

ABSTRACT.....	i
CHAPTER 1 INTRODUCTION	1
1.1 AN OVERVIEW OF SURFACE EMG	2
1.2 THE HISTORY OF ELECTRODIAGNOSTIC METHODS	3
1.3 THE DEVELOPMENT OF THE SURFACE EMG	4
1.4 THE CHARACTERISTICS OF SURFACE EMG.....	12
1.4.1 <i>The Advantages of Surface EMG.....</i>	<i>12</i>
1.4.2 <i>The Disadvantages of Surface EMG</i>	<i>14</i>
1.5 SURFACE EMG APPLICATIONS	15
1.5.1 <i>Surface EMG Applications in Bio-feedback and Rehabilitation</i>	<i>15</i>
1.5.2 <i>Surface EMG Applications in Kinesiology and Neurology.....</i>	<i>16</i>
1.6 OBJECTIVE OF THIS STUDY.....	17
1.7 MAJOR CONTRIBUTIONS OF THIS STUDY.....	18
1.8 SUMMARY.....	19
CHAPTER 2 ANATOMICAL AND PHYSIOLOGICAL BASIS OF THE SURFACE EMG	20
2.1 INTRODUCTION	20
2.2 NEUROMUSCULAR SYSTEM.....	21
2.3 MUSCLE: TYPES AND STRUCTURE	23
2.3.1 <i>Types of Muscle.....</i>	<i>23</i>
2.3.2 <i>Structure of Skeletal Muscle.....</i>	<i>24</i>
2.4 TYPES OF MUSCLE CONTRACTIONS	26
2.5 HOW MUSCLE FIBRES WORK.....	28
2.5.1 <i>Muscle Fibre Work.....</i>	<i>28</i>
2.5.2 <i>Categories of Muscle Fibres.....</i>	<i>29</i>
2.6 THE MOTOR UNIT: PROPERTIES AND RECRUITMENT	29
2.6.1 <i>The Motor Unit.....</i>	<i>29</i>
2.6.2 <i>Territories of the Motor Unit.....</i>	<i>30</i>
2.6.3 <i>Motor Unit Recruitment & Firing Frequency</i>	<i>32</i>
2.7 SUMMARY.....	33
CHAPTER 3 SURFACE EMG AND GAIT ANALYSIS.....	34
3.1 INTRODUCTION	34
3.2 GAIT CYCLE.....	34
3.3 PHASES OF GAIT.....	35
3.4 BASIC FUNCTIONS OF THE GAIT CYCLE	37
3.5 MUSCLE CONTROL DURING NORMAL GAIT	39
3.5.1 <i>The Lower Limb Muscles.....</i>	<i>39</i>
3.5.2 <i>Muscle Control.....</i>	<i>41</i>
3.6 SURFACE EMG APPLICATIONS IN GAIT ANALYSIS	41
3.7 SUMMARY.....	42

CHAPTER 4	SURFACE EMG DETECTION AND MEASUREMENT.....	44
4.1	INTRODUCTION	44
4.2	ELECTRODES.....	45
4.2.1	<i>Electrodes: Types and Properties.....</i>	45
4.2.2	<i>Surface Electrodes.....</i>	45
4.2.3	<i>Surface Electrodes Placement.....</i>	47
4.3	DIFFERENTIAL AMPLIFIER	47
4.3.1	<i>Structure of the Differential Amplifier.....</i>	48
4.3.2	<i>Common Mode Rejection Ratio.....</i>	49
4.3.3	<i>Input Impedance.....</i>	50
4.3.4	<i>Specification of the Differential Amplifier.....</i>	51
4.4	NOISES AND ARTEFACTS.....	52
4.5	FILTERING.....	53
4.6	SUMMARY.....	54
CHAPTER 5	SURFACE EMG SIGNAL PROCESSING METHODS.....	55
5.1	OVERVIEW	55
5.2	SURFACE EMG SIGNAL INTERPRETATION	56
5.2.1	<i>Relative Intensity of Muscle Activity.....</i>	56
5.2.2	<i>Muscle Activation Intervals.....</i>	56
5.2.3	<i>Muscle Function: Muscle Fatigue.....</i>	57
5.3	SAMPLING AND A/D CONVERSION.....	57
5.4	SURFACE EMG QUANTIFICATION.....	58
5.4.1	<i>Surface EMG Quantification during Non-dynamic Contractions.....</i>	58
5.4.2	<i>Surface EMG Quantification during Dynamic Contractions.....</i>	59
5.5	SURFACE EMG NORMALIZATION	60
5.6	SURFACE EMG SPECTRAL ANALYSIS	61
5.6.1	<i>Fast Fourier Transform (FFT).....</i>	62
5.6.2	<i>Spectral Estimation of Surface EMG.....</i>	62
5.7	SUMMARY.....	64
CHAPTER 6	SURFACE EMG COLLECTION DURING DYNAMIC MOVEMENT	66
6.1	OVERVIEW	66
6.2	ETHICS APPROVALS	67
6.3	PARTICIPANTS RECRUITMENT.....	68
6.3.1	<i>Sample Size and Recruitment.....</i>	68
6.3.2	<i>Setting.....</i>	68
6.4	MEASUREMENT AND INSTRUMENTATION.....	69
6.4.1	<i>Participants Information.....</i>	69
6.4.2	<i>Signal Measurement.....</i>	70
6.4.3	<i>Instrumentation.....</i>	74
6.5	MANAGEMENT OF THE EXPERIMENT.....	76
6.6	RESULTS ANALYSIS	76
6.7	SUMMARY.....	79
CHAPTER 7	SURFACE EMG SIMULATION MODELLING.....	81
7.1	OVERVIEW	81
7.2	SURFACE EMG SIMULATION MODELS: PROPERTIES AND APPLICATIONS	82
7.3	A MULTIPLE-LAYER MODEL OF SURFACE EMG.....	83
7.4	METHOD TO GENERATE THE SURFACE EMG SIGNAL FROM THE MODEL.....	84
7.5	SINGLE FIBRE ACTION POTENTIAL SIMULATION.....	90
7.5.1	<i>Muscle Fibre Characteristics and Distribution.....</i>	90
7.5.2	<i>Method to Simulate Single Fibre Action Potential.....</i>	90
7.6	MOTOR UNIT ACTION POTENTIAL AND VOLUNTARY CONTRACTION SIMULATION	92

7.6.1	<i>The Motor Unit Distribution</i>	92
7.6.2	<i>Principles of the Motor Unit Recruitment</i>	93
7.6.3	<i>Method to Simulate Motor Unit Action Potential</i>	95
7.6.4	<i>Method to Simulate Motor Unit Action Potential Trains and Voluntary Contraction</i>	97
7.7	SURFACE EMG SIMULATION DURING THE GAIT CYCLE	99
7.7.1	<i>Parameters of the Gait Cycle</i>	99
7.7.2	<i>Method to Generate the Simulated Surface EMG Signal during the Gait Cycle</i>	100
7.8	SIMULATION RESULTS	101
7.8.1	<i>Simulated Single Fibre Action Potential</i>	101
7.8.2	<i>Simulated Motor Unit Action Potential</i>	102
7.8.3	<i>Simulated Surface EMG during Voluntary Muscle Contraction</i>	103
7.8.4	<i>Simulated Surface EMG during the Gait Cycle</i>	106
7.9	COMPARISON BETWEEN THE SIMULATED SURFACE EMG AND REAL SURFACE EMG RECORDED FROM GAIT EXPERIMENTS.....	110
7.10	DISCUSSION OF THE SIMULATION MODEL.....	114
7.11	SUMMARY.....	115
CHAPTER 8 ESTIMATION OF MUSCLE ACTIVATION TIMING BASED UPON SURFACE EMG ANALYSIS		117
8.1	OVERVIEW	117
8.2	INTRODUCTION TO DETECTION OF MUSCLE ACTIVATION INTERVALS	118
8.3	APPROACHES AND ALGORITHMS USED IN PRESENT CLINICAL RESEARCH.....	120
8.3.1	<i>Visual Determination and its Limitations</i>	120
8.3.2	<i>Methods with a Fixed Threshold</i>	121
8.3.2.1	Fixed Threshold Algorithm	121
8.3.2.2	Limitations of the Single-threshold Algorithm	122
8.3.3	<i>Statistical Method: Double-threshold Algorithm</i>	125
8.3.3.1	Double-threshold Algorithm.....	125
8.3.3.2	Derivation of the Double-threshold Algorithm.....	127
8.3.3.3	Performance of the Double-threshold Algorithm Applied to Phenomenologically Simulated Surface EMG Signals	128
8.3.3.4	Limitations of the Double-threshold Algorithm	132
8.3.4	<i>Other Methods Used in Clinical Research</i>	135
8.4	A NOVEL ALGORITHM TO DETECT THE MUSCLE ACTIVATION TIMING.....	136
8.4.1	<i>Overview of the Algorithm</i>	136
8.4.2	<i>Derivation of the Algorithm</i>	137
8.4.3	<i>Selection of the Basic Parameters of the Algorithm</i>	139
8.4.3.1	Determination of the Length of the Observation Window.....	140
8.4.3.2	Calculation of the Initial Threshold	140
8.4.3.3	Calculation of the Final Threshold	141
8.4.4	<i>The Post Processor</i>	147
8.4.5	<i>Output of the Algorithm</i>	149
8.5	STATISTICAL ANALYSIS OF THE ALGORITHM.....	153
8.6	APPLICATIONS OF THE ALGORITHM IN THE ANALYSIS OF THE MUSCLE ACTIVATION INTERVALS	154
8.6.1	<i>Detection the On-Off Timing of Muscle Activation of the Simulated Surface EMG Signals</i>	154
8.6.2	<i>Detection of On-Off Timing of Muscle Activation of Real Surface EMG Signals Recorded from the Gait Experiment</i>	159
8.7	COMPARISON WITH OTHER METHODS	162
8.7.1	<i>Comparison with the Single-threshold Algorithm</i>	163
8.7.2	<i>Comparison with the Double-threshold Algorithm</i>	168
8.8	RESULTS AND DISCUSSION.....	172
8.9	SUMMARY.....	174
CHAPTER 9 CONCLUSIONS & FUTURE WORK		175

List of Figures

Figure 2-1 A typical motor neuron and motor endplate.....	22
Figure 2-2 Structure of skeletal muscle.....	25
Figure 2-3 The structure of a sarcomere that is the basic anatomical unit of muscles.....	26
Figure 2-4 Motor unit territories on the cross-section of the muscle and their contributions to the surface EMG signal.....	31
Figure 3-1 Divisions of the gait cycle and the subdivisions of stance and swing phases.....	36
Figure 3-2 Tibialis anterior and gastrocnemius. (a) Right tibialis anterior, anterior view; (b) Right gastrocnemius, posterior view.....	40
Figure 5-1 The ensemble averaging method in the surface EMG quantification during dynamic contractions.....	60
Figure 6-1 The experimental setup and data recorded.....	74
Figure 6-2 The Noraxon EMG & Sensor System and its accessories.....	74
Figure 6-3 The Noraxon Multi-Mode Foot Switch System.....	75
Figure 6-4 The Vicon Motion Analysis System and the BioDex Rehabilitation Treadmill.....	75
Figure 6-5 The processed surface EMG signals, gait cycle, and body movement.....	79
Figure 7-1 The multiple-layer model comprising muscle, fat and skin layers.....	84
Figure 7-2 The timing of muscle activation and locations of muscle maximum contraction during the different gait phases.....	100
Figure 7-3 Single fibre action potential of the tibialis anterior muscle.....	102
Figure 7-4 Motor unit action potential of the tibialis anterior muscle.....	103
Figure 7-5 The influence of the motor unit distribution and features of recruitment on the its potential.....	104
Figure 7-6 The motor unit action potential trains of the tibialis anterior muscle.....	105
Figure 7-7 The simulation EMG signal of the tibialis anterior muscle in voluntary contraction and corresponding power spectral density (400 motor units).....	106
Figure 7-8 The simulated surface EMG signals of the tibialis anterior and gastrocnemius medialis muscles during the gait cycle, including four cycles.....	107
Figure 7-9 The simulated surface EMG signals of tibialis anterior muscle during one gait cycle and its characteristics.....	109
Figure 7-10 The simulated surface EMG signals of gastrocnemius medialis muscle during one gait cycle and its characteristics.....	110
Figure 7-11 The surface EMG signals during the one gait cycle and their characteristics, which are collected from the tibialis anterior and gastrocnemius medialis muscles during the gait experiment.....	113
Figure 8-1 Flowchart of the algorithm with a fixed threshold.....	122
Figure 8-2 Errors produced by using the fixed threshold algorithm.....	125
Figure 8-3 Flowchart of the double-threshold algorithm.....	126
Figure 8-4 The performance of the double-threshold algorithm applied to the simulated surface EMG signal produced by the phenomenological model.....	131
Figure 8-5 Errors produced by using the double-threshold algorithm to detect the timing of muscle activation for the simulated surface EMG signals produced by the physically-based model.....	134
Figure 8-6 Flowchart of the power-threshold algorithm to detect the on-off timing of muscle contraction.....	139
Figure 8-7 The relationship between the final threshold, the length of the observation window and the threshold coefficient. In this case, the fixed signal-to-noise of the simulated EMG signals is 8 dB.....	142

<i>Figure 8-8 The performance of the algorithm with the length of observation window $w = 8$ and the threshold coefficient $\lambda = 1.8$, in the processing of the simulated EMG signals with signal-to-noise ratio (a) 8 dB, (b) 10 dB and (c) 20 dB.</i>	<i>147</i>
<i>Figure 8-9 The complete algorithm.....</i>	<i>153</i>
<i>Figure 8-10 The performance of the algorithm on the simulated surface EMG signals with SNR = 3 dB, 6 dB, 8 dB, 10 dB, and 20 dB produced by the physically-based model.</i>	<i>158</i>
<i>Figure 8-11 The performance of the power-threshold algorithm on the real surface EMG signal recorded from the gait experiment.</i>	<i>161</i>
<i>Figure 8-12 The results of the single-threshold algorithm on the simulated surface EMG signals with SNR = 3 dB, 6 dB, 8 dB, 10 dB 20 dB produced by the physically-based model.</i>	<i>166</i>
<i>Figure 8-13 The results of the double-threshold algorithm on the simulated surface EMG signals with SNR = 3 dB, 6 dB, 8 dB, 10 dB and 20 dB produced by the physically-based model.</i>	<i>171</i>

List of Tables

<i>Table 3-1: The time length of the gait cycle, stance and swing phases of normal adult men and women during free walking.</i>	37
<i>Table 4-1: A typical specification of a differential amplifier for EMG recording.</i>	52
<i>Table 7-1 The parameters of the simulation model.</i>	86
<i>Table 7-2 The characteristics of the simulated surface EMG signals and the real surface EMG signals collected during the gait experiment.</i>	114
<i>Table 8-1 Bias and standard deviation of the onset and cessation timing of muscle activation produced by the double-threshold algorithm applied to the simulated surface EMG signals during the gait cycle, which are originated from the phenomenological model.</i>	132
<i>Table 8-2 Bias and standard deviation of the onset and cessation timing produced by the double-threshold algorithm applied to the simulated signals generated by the physically-based model.</i>	135
<i>Table 8-3 The standard deviation of the timing of muscle activation for different lengths of the observation window (w) and different threshold coefficients (λ) based upon the simulated surface EMG signal of a fixed signal-to-noise ratio.</i>	144
<i>Table 8-4 The standard deviation of the timing of muscle activation by using the algorithm. In this case, SNR = 3 dB, 6 dB, 8 dB, 10 dB, and 20 dB; the observation window w is 8 samples.</i>	158
<i>Table 8-5 The standard deviation of the timing of muscle activation produced by applying the algorithm to the real surface EMG data recorded from the tibialis anterior muscle of the healthy adults.</i>	162
<i>Table 8-6 The values of standard deviation of onset and cessation timing of the simulated signals with SNR = 3 dB, 6 dB, 8 dB, 10 dB and 20 dB are calculated by the use of the single-threshold algorithm with different threshold coefficients γ. In this case, $\gamma = 2.0, 2.2, 2.4, 2.6, 2.8, 3.0$.</i>	167
<i>Table 8-7 The bias and standard deviation of onset and cessation timing of muscle activation by using the single-threshold algorithm to analyse the simulated surface EMG signals produced by the physically-based model.</i>	168
<i>Table 8-8 The bias and standard deviation of onset and cessation timing of muscle activation by using the double-threshold algorithm.</i>	172

Acknowledgements

First and foremost, I would like to express my gratitude to Professor Robert Allen for his supervision and guidance in conducting this research, and to Dr Antonio De Stefano for his constructive advice in countless discussions. My gratitude also to Dr Victoria Yule and Dr Anna Barney for their advice and technical assistance.

My sincere appreciation to the entire team at the Signal Processing and Control Group in the Institute of Sound and Vibration Research, with special thanks to Dr David Simpson for his valuable advice. My thanks as well to Maureen Strickland and Joyce Shotter for their support and assistance.

I would like to acknowledge the sponsorship provided by Universities UK and Institute of Sound and Vibration Research.

And finally, special thanks to my mum, dad, and sister for their support and encouragement throughout the last many years. Many thanks also to my trusted and talented friends for their support and truly understanding.

Chapter 1 Introduction

The correlation between the surface electromyography (EMG) signal and gait analysis is addressed in this study to provide valuable information of clinical interest regarding muscle activity during dynamic movements. Features of the surface EMG, EMG measurement and instrumentation system, and the characteristics of gait phases are described at the beginning of this thesis. A model is presented which simulates the surface EMG signal during dynamic movements and is used to assess new approaches to extract appropriate and accurate information from the raw surface EMG data. An algorithm to detect the muscle activation intervals is derived on the basis of the simulated surface EMG signals and is applied to real EMG data recorded from the lower limb muscles during normal walking.

This chapter introduces surface EMG development, characteristics, and applications. The concept of the surface EMG is described in Section 1.1. Section 1.2 introduces the history of electrodiagnostic techniques. The development of the Surface EMG and its advantages and disadvantages are presented. This will provide the background for the emergence of the use of

the surface EMG in clinical research. Surface EMG applications in kinesiology, rehabilitation, physiology, sports medicine and neurology are enumerated in Section 1.5. The objectives of this study are presented in Section 1.6 and the main contributions are set forth in Section 1.7. Since this project crosses traditional subject boundaries, a glossary of terms is provided in Appendix II to help engineering readers unfamiliar with the biology and vice versa.

1.1 An Overview of Surface EMG

When muscles contract, microvolt level electrical signals are generated and can be measured by attaching surface electrodes over the muscle. The electrical signals, referred to as the surface EMG, uniquely provide a non-invasive and painless means of monitoring direct and associated muscle activity.

The surface EMG recording offers a safe technique to show the electrical activity of nerves and muscles. Both the magnitude and timing pattern of muscle activity can be displayed and allow objective quantification of muscle function and possibly differentiate the various aspects of muscle activity. Researchers and clinicians use the surface EMG to assess the functional status of skeletal muscles and aid in neuromuscular training and rehabilitation.

The surface EMG is used commonly in practice. For example, physical therapists employ the surface EMG to address movement dysfunction. Rehabilitation therapists treat patients who learn to relax overly tense muscles or activate weak muscles much better with the surface EMG feedback. Patients might be engaged by the surface EMG feedback display and may understand patterns of movement control. Neurologists use the

surface EMG to enhance diagnosis of muscle dysfunction as well as monitor the influences of medicines and surgical interventions designed to impact on muscle activity. The surface EMG provides a valuable aid for clinicians to objectively quantify and document muscle activity during examination procedures and the performance of functional tasks.

1.2 The History of Electrodiagnostic Methods

The surface EMG has been developed out of the discovery of *electrodiagnostic techniques* for the study of nerve and muscle. The electrodiagnostic techniques were established in the course of the past 100 years and have achieved widespread use in clinical diagnosis since the 1930s (*Lenman, J A R, Ritchie, A E, and Simpson, J A, 1987*). Nerve and muscle are inaccessible from the surface of the body; their function can be studied only through the aid of appropriate instruments and techniques. Two categories of techniques, the artificial electrical stimulation of nerve and muscle and the recording of electrical potentials from muscle and nerve activation, are used to describe muscle activities objectively (*Lenman, J A R, Ritchie, A E, and Simpson, J A, 1987*).

Electrical stimulation, a technique to determine the excitability of the muscle, was first described by Adrian (*Adrian, E D, 1916*). A further application of stimulation techniques, measurement of conduction velocity along peripheral nerves, was introduced during animal experiments by Berry *et al.* and Sanders and Whitteridge (*Berry, C M, Grundfest, H, and Hinsey, J C, 1944; Sanders, F K and Whitteridge, D, 1946*). The recording of electrical potentials from muscle and nerve activation comprises evoked potentials and action potentials. The evoked potential, also known as an evoked response, is a diagnostic aid for evaluation of the function of the central nervous

system and is regularly recorded during nerve conduction measurements. The action potentials are measured during muscle spontaneous or voluntary activity. The earliest study of muscle and nerve active potentials was made by Piper (*Lenman, J A R, Ritchie, A E, and Simpson, J A, 1987*). The action potentials during voluntary contraction were recorded by using surface electrodes and a string galvanometer in Piper's work, which was the earliest extensive study of human electromyography (*Lenman, J A R, Ritchie, A E, and Simpson, J A, 1987*). Much information has been presented regarding the anatomy and physiology of different muscles with progress in modern apparatus. The study of the action potentials of motor units and single muscle fibres became possible when Adrian and Bronk introduced the concentric needle electrode in the electrodiagnostic techniques (*Adrian, E D and Bronk, D W, 1929*). In recent years, many refined instruments have been developed and quantitative analysis of the data obtained has become possible. These electrodiagnostic methods form the basis of surface EMG as it exists today.

1.3 The Development of the Surface EMG

Since the process of the electrodiagnostic technology has had such a dramatic impact on medical diagnosis and therapy, it has become intimately involved in muscle dysfunction treatment. As a result, the surface EMG has emerged as an integrating technique for two disciplines, medicine and engineering, and has assisted in the analysis of normal and pathological muscle activity by providing accurate signal acquisition and appropriate signal processing methods. Since the 19th century, clinicians and researchers have developed the surface EMG technique and sought new solutions for the various problems confronting the neuromuscular system. The purpose of this section is to provide a broad overview of the role of the surface EMG in the study of neuromuscular system, highlight the basic roles the surface EMG

signal processing plays, and present a view of the professional status of the field.

The development of the surface EMG can be traced back to the mid-1800's. In the early part of the 19th century, the techniques of using electricity to stimulate muscles were exploited and gained wide attention. Some people conducted this novel technique to study muscle function. The first systematic study of the dynamics and function of the muscle by using electrical stimulation was made by Duchenne and colleagues (*Duchenne, G B and Kaplan, E B, 1949*). Equipment used to measure electrical currents and muscle activity, the *galvanometer*, was invented in the early of the 19th century. In 1849, DuBois-Reymond documented the first evidence of electrical activity of human muscles during voluntary contraction (*Cram, J R, Kasman, G S, and Holtz, J, 1998*). In DuBois-Reymond's experiment, he placed blotting cloth on each of the hands or forearms of his participants and asked them to immerse their hands or forearms into separate vats of saline solution when the electrodes were connected to the galvanometer. Consistent and predictable deflections were observed whenever the participants flexed their hand or arm. In 1917, the study of Pratt demonstrated that the magnitude of the energy of muscle contraction was due to individual muscle and muscle fibre recruitment, rather than due to the size of the neural impulse (*Pratt, F H, 1917*). By 1922, Gasser *et al.* had introduced the cathode ray oscilloscope to the study of muscle function and showed electrical signals from muscles (*Gasser, H S and Newcomer, H S, 1921*). The studies mentioned above established the foundations of the surface EMG technique.

During the 1930s through the 1950s, the surface EMG was used more widely for the study of normal and abnormal muscle function. Jacobson used the surface EMG to demonstrate the influences of imagination and emotion on a variety of muscles (*Jacobson, E, 1934*). Reusch *et al.* observed

muscular tension by the analysis of patterns of the surface EMG recorded from the resting forearm (*Reusch, J, Cobb, S, and Finesinger, J E, 1941*). Inman and his colleagues used the surface EMG to study dynamic movement and conduct a highly regarded study on shoulder movements (*Inman, V T, Saunders, J B, and Abbott, L C, 1944*). Price and his colleagues made use of the surface EMG activation patterns to study back pain (*Price, J P, Clare, M H, and Ewerhardt, R H, 1948*). Malmo observed psychotic and neurotic patients by recording and comparing the forearm surface EMG (*Malmo, R B et al., 1951*). Furthermore, Davis conducted much of the surface EMG research and constructed the first surface EMG electrode atlas to assist in the standardization of the surface EMG recording (*Davis, R C, 1952*). Floyd and Silver analysed the effects of flexion of the trunk on spine muscles by using the surface EMG patterns (*Floyd, W F and Silver, P, 1955*). In addition, Whatmore and Ellis introduced the surface EMG to the study of the schizophrenic subjects and noted that levels of surface EMG in the forehead, forearm and leg muscles of schizophrenic patients are higher than those of normal subjects (*Whatmore, G and Ellis, R M, 1958*). As a result, the surface EMG technique may provide a valuable aid for researchers in the study of normal and pathological muscle activities and functions.

During the 1960s and through the 1970s, the surface EMG technique began to rapidly expand. It was introduced to the technique of biofeedback for the treatment of specific neuromuscular disorders. The study of Basmajian on single motor unit training of the neuromuscular system by using fine wire electrodes rather than surface electrodes, which firstly, and clearly, demonstrated that the neuromuscular system could be trained using EMG feedback techniques (*Basmajian, J V, 1963*). He had compiled all of the information available on EMG techniques into his book *Muscle Alive* (*Basmajian, J V, 1967*). Basmajian also formed an international forum to share information on surface EMG in 1965. This forum still exists today and presents a journal that specifically discusses the surface EMG technique:

Journal of Electromyography & Kinesiology. From Basmajian's work, the study of the surface EMG was further advanced by Green *et al.*. They modified Basmajian's single motor unit training method and used the surface EMG in relaxation training (Green, E E *et al.*, 1969). Several years later, surface EMG techniques became more and more popular during the studies of specific neuromuscular disorders. For example, Budzynski *et al.* applied the surface EMG to feedback techniques for the treatment of muscle contraction headaches (Budzynski, T, Stoyva, J, and Adler, C, 1970). Furthermore, Booker *et al.* developed neuromuscular re-education techniques by using surface EMG biofeedback in the therapy of patients with different neuromuscular conditions (Booker, H E, Rubow, R T, and Coleman, P J, 1969). In addition, Johnson and Garton used the surface EMG to study the restoration of function of hemiplegic patients (Johnson, H E and Garton, W H, 1973). Hence, the surface EMG became an important tool for the biofeedback technique during the treatment of neuromuscular diseases.

During the 1980s, some researchers and clinicians made attempts to extract more information from the surface EMG signal by using new signal processing methods. For example, Yang and Winter examined the effect of four amplitude normalization methods on variability of surface EMG profiles during the study of normal gait (Yang, J F and Winter, D A, 1984). One year later, a method of linear electrode arrays and double differential amplification techniques to the study of the neuromuscular system had been introduced and allowed the researcher to investigate the electrophysiological characteristics of the motor unit action potential (Cram, J R, 2003). Nandedkar and colleagues utilized simulation techniques to address the surface EMG interference pattern in normal muscle (Nandedkar, S D, Sanders, D B, and Stalberg, E V, 1986). Two years later, Cram encouraged clinicians to apply the diagnostic information extracted from the surface EMG signal to the treatment of pain-related disorders (Cram, J R, 1988).

Since 1990, the surface EMG signal analysis and processing methods have been developed widely and rapidly. Gamet *et al.* studied the influence of motor unit recruitment on the electromyographic spectral content by calculating the most representative spectral parameters such as, EMG total power, mean and median power frequencies (Gamet, D *et al.*, 1990). Nandedkar *et al.* described a method to make automatic measurements of the amplitude of the surface EMG envelope and this method was tested on recordings of the EMG interference pattern from the biceps muscle of normal subjects (Nandedkar, S D and Sanders, D B, 1990). Priez *et al.* addressed a method of quantifying Duchenne muscular dystrophy by analysing the surface EMG signals. Spectral parameters were first computed from digitised EMG, and then a polynomial model was deduced from the evolution of each parameter (Priez, A, Duchene, J, and Goubel, F, 1992). By 1993, standing on top of the studies mentioned above, Duchene *et al.* had summarized the various processing methods used for the surface EMG, such as, signal acquisition, random feature extraction, time and spectral parameter determination, and statistical testing (Duchene, J and Goubel, F, 1993). Moreover, several years later, Merletti *et al.* presented an overview of techniques suitable for the estimation, interpretation and understanding of time variations that affect the surface EMG signal during isometric contractions (Merletti, R and LoConte, L R, 1997). The work of Duchene *et al.* and Merletti *et al.* firstly shed light on key methods and algorithms for surface EMG signal processing.

Several years later, Bonato summarized and discussed a number of techniques recently proposed for surface EMG signal processing (Bonato, P, 2001). He also developed a method to define the instantaneous median and mean frequency during cyclic dynamic contractions by using Cohen class time-frequency transforms and proved that the time-dependent shift in the spectral content of the surface EMG signal was a useful tool for assessing localized muscle fatigue (Bonato, P *et al.*, 2001). Increasingly signal

processing methods were used to analyse the surface EMG signal. First, the study of D'Alessio and Conforto presented a fully automatic estimation technique to extract the envelope of the surface EMG signal (*D'Alessio, T and Conforto, S, 2001*). Second, Merletti utilized spectral and temporal variables of the surface EMG signal to investigate the effects of the age-related central and peripheral mechanisms on muscle fatigue (*Merletti, R et al., 2002*). Third, a review of data acquisition and signal processing issues relative to producing an amplitude estimate of the surface EMG signal was addressed in Clancy *et al.*'s paper (*Clancy, E A, Morin, E L, and Merletti, R, 2002*). Furthermore, Merlo and colleagues described an algorithm to estimate on-off timing of muscle activation during movement, which is based on the identification of single motor unit action potentials from the surface EMG signal with the use of the continuous wavelet transform (*Merlo, A, Farina, D, and Merletti, R, 2003*).

Recently, the surface EMG signal processing has become increasingly important as a non-invasive method to study the features of motor units and muscle fibres. For example, the motor unit firing patterns on the basis of topographical information from 128-channel high-density surface EMG signals was reported by the Kleine and colleagues' trails (*Kleine, B U et al., 2000*). Farina and colleagues developed an improved spike triggered averaging technique for the assessment of control properties and conduction velocity of single motor units during voluntary muscle contractions based upon the detection of multi-channel surface EMG signals (*Farina, D et al., 2002*). The study of Farina also described the methods currently available for estimating muscle fibre conduction velocity from the surface EMG signal (*Farina, D and Merletti, R, 2004*). The study of Gazzoni *et al.* presented an automatic system for the detection and classification of motor unit action potentials from multi-channel surface EMG signals (*Gazzoni, M, Farina, D, and Merletti, R, 2004*). In this method, the segmentation phase was based upon the matched Continuous Wavelet Transform while the

classification was performed by a multi-channel neural network. Furthermore, Schulte *et al.* demonstrated the influence of fibre shortening on estimates of conduction velocity and mean power spectral frequency from the analysis of the surface EMG signal (Schulte, E *et al.*, 2004). In addition, Saitou *et al.* described non-invasively extracted information about the size and muscle fibre density of muscular units through the inverse analysis of the surface EMG signal (Saitou, K, Masuda, T, and Okada, M, 2004). Merlo *et al.* utilized time-frequency analysis methods, which compared the direct estimation of average muscle fibre conduction velocity with instantaneous mean frequency of the surface EMG signal, to assess muscle fibre membrane properties during dynamic contractions (Merlo, E *et al.*, 2005). To summarize, the surface EMG can be used to analyse motor units and muscle fibres by using appropriate signal processing methods and acquisition configurations.

Over the years, many publications have been created, which focused on the clinically applied aspects of the surface EMG. A book by Lenman *et al.* provided a concise account of clinical electromyography for those working in the fields of neurology, physical medicine, and orthopaedic surgery (Lenman, J A R, Ritchie, A E, and Simpson, J A, 1987). Brown edited a book covering the application and analysis of electromyography with regard to specific clinical syndromes and featuring the advances in electrophysiologic diagnosis (Brown, W F, 1993). The book by Cram *et al.* chiefly addressed the electrode atlas to assist the practitioner in understanding the energy emitted by muscles (Cram, J R, Kasman, G S, and Holtz, J, 1998)

Furthermore, the European, American and international academic communities have provided a strong fundamental basis for exchanging knowledge and experience on basic and applied aspects of the surface EMG and helping in breakdown of present barriers which prevent useful information exchange and enhance widespread use of the surface EMG.

Surface EMG for Non-Invasive Assessment of Muscles (SENIAM), funded by the European Commission, is one of the concerted organisations. It enables scientists and clinicians working with the surface EMG technique to exchange experiences. In 1996, Merletti organised the first general workshop of SENIAM in Italy (Hermens, H J, Merletti, R, and Freriks, B, 1996). A number of experts came from the 16 partners of the concerted action from 9 different countries to address their specific areas of expertise. Through this effort, several publications have been created, for example, *European Recommendations for Surface Electromyography* (Hermens, H J et al., 1999a), *The State of the Art on Signal Processing Methods for Surface Electromyography* (Hermens, H J et al., 1999b) and *State of the Art on Modelling Methods for Surface Electromyography* (Hermens, H J et al., 1998).

Another well-known group of DeLuca and his colleagues at the Neuromuscular Research Institute in Boston have made contributions to the surface EMG techniques and applications which cannot be overlooked. Much of their work is in biomechanics and signal analysis related to neuromuscular diseases (DeLuca, C J et al., 1982a; DeLuca, C J et al., 1982b; DeLuca, C J, 1993; DeLuca, C J, 1995; DeLuca, C J, 1997; DeLuca, C J and Jabre, J F, 1985; DeLuca, C J and Jabre, J F, 1986; DeLuca, C J and Merletti, R, 1988).

In addition, the study of Dimitrova and Dimitrov at the Centre of Biomedical Engineering ‘Ivan Daskalov’ in Bulgarian Academy of Science have contributed to the understanding of muscle fatigue (Dimitrova, N A and Dimitrov, G V, 2002; Dimitrova, N A and Dimitrov, G V, 2003), the modelling of motor unit action potential and muscle contraction (Dimitrov, G V et al., 2003; Dimitrov, G V and Dimitrova, N A, 1998), and the analysis of characteristic frequencies of muscle fibres potentials (Dimitrova, N A, Dimitrov, G V, and Nikitin, O A, 2001).

The surface EMG technique crosses many disciplines ranging from manual therapies and psychology to biomedical engineering. This thesis reviews the application of EMG techniques and associated signal processing to gait analysis and in particular to studies of muscle activity during both normal and pathological gait.

1.4 The Characteristics of Surface EMG

1.4.1 The Advantages of Surface EMG

The use of the surface EMG has many advantages. First, the surface EMG technique provides a safe and non-invasive approach to assess the muscle activity and function by using the surface electrode rather than the needle or wire electrode inserting into the skin or muscles to monitor and record the electrical activity of individual muscle. The surface EMG offers a recording of the amplitude and timing of muscle activity with far greater precision than the muscle activation timing, intensity and force obtained by a clinician's or researcher's eyes and hands. An entire range of activity levels can be monitored and displayed for inspection, from amplitudes associated with activation of a few motor units to the activity of particular muscles or muscle groups. It can display both voluntary and involuntary muscle activity in addition to externally stimulated muscle action potentials, for example, motor evoked potentials after central or peripheral nerve stimulation (*Pullman, S L et al., 2000*). Furthermore, the surface EMG method tends to be readily accepted by patients because it is non-invasive, painless, and generally quite safe.

Second, it is more suitable for recording the muscle activity during dynamic movements. In many studies of neuromuscular diseases affecting movement,

balance, or reaction times, the needle or wire electrode may produce pain and be uncomfortable. Therefore, during investigations of movement control and psycho-physiological phenomena, substitution of the surface EMG for the needle or wire EMG is considered as a more acceptable and reliable method to investigate and quantify muscle function for kinesiology analysis of movement disorders, evaluating gait and posture disturbances, and estimating psycho-physiological measures of reaction and movement time.

Third, it is easy for clinicians and researchers to learn and perform the surface EMG procedure. In comparison with other ways of muscle monitoring, the surface EMG method is much more convenient. Instrument set-up becomes simple once the user is experienced. For instance, attaching the surface electrode to the target muscles or muscle groups is an easy procedure for the researcher or for the patient who is not a clinical professional. In contrast, the needle or wire electrode must be inserted by a qualified practitioner. Moreover, the portable surface EMG units are simply incorporated into therapeutic exercise programs taking place in the clinic, gymnasium, or home.

Furthermore, the diagnostic information extracted from the surface EMG signal can be easily feedback to the patient, which provides a valuable way to re-educate neuromuscular system in the rehabilitation studies. The surface EMG recording is often used as a means of feedback for helping the patient to understand the patterns of movement control and learn muscle function and activity. The patient is engaged by the surface EMG feedback display and may be able to control muscle activity in order to reduce pain and increase function. An example would be a patient with muscle hyperactivity using feedback cues to reduce muscle output (*Kasman, G, 2002*). The feedback may assist a patient who has neck pain and upper trapezius hyperactivity in improving posture or self-regulating response to emotional

stress factors. On the other hand, a patient with muscle hypoactivity could attend to the surface EMG feedback to learn to increase muscle recruitment.

In addition, with advances in apparatus, signal acquisition, and signal processing algorithms, the surface EMG recording becomes a rich source of information for the researcher or clinician to investigate neural control strategies (*Farina, D, Merletti, R, and Enoka, R M, 2004*), distinguish individual motor units and observe properties of the motor unit action potentials (*Drost, G et al., 2004; Gazzoni, M, Farina, D, and Merletti, R, 2004*), and debate how to measure muscle fibre conduction velocity in the best way (*Farina, D and Merletti, R, 2004; Schulte, E et al., 2004*) . To conclude, as a non-invasive, safe, painless, and multidisciplinary technique, the surface EMG is widely used to objectively quantify and document muscle activity as well as the performance of muscle functional tasks during a variety of clinical applications.

1.4.2 The Disadvantages of Surface EMG

Like any biomedical engineering technology, the surface EMG has limitations. Electrical cross-talk, a phenomenon where electrical signals from one muscle group travel into the recording area of another muscle group, is one such limitation. The surface EMG cannot identify the origin of the electrical signals where two or more muscles, which lie in close proximity to each other, are active at the same time.

Another weakness of the surface EMG technique is that the electrical signals in the surface EMG tracing are often attenuated by intervening tissue, such as fat, particularly when muscles or muscle groups are 10 mm or more below the surface of the skin (*Fuglevand, A J et al., 1992*). Furthermore, the limited spatial resolution of the surface EMG signals results in poor fidelity recording of high-frequency signals, for example, fibrillation potentials and

positive sharp waves (*Turker, K S, 1993*). Importantly, the surface EMG is worse than needle EMG in recording evidence of denervation at rest (*Pullman, S L et al., 2000*).

In addition, a final shortcoming is that the surface EMG technique is not a measure of force, strength, pain, anxiety, joint position, muscle length or anything else other than voltage which is representative of muscle recruitment. It is simply a measure of the electrical signals produced by muscles or muscle groups as they contract and do work.

1.5 Surface EMG Applications

This section focuses on different applications of the surface EMG technique in the fields of kinesiology, rehabilitation, physiology, bio-feedback, neurology, fatigue studies, sports medicine, and ergonomics. A deeper insight into the variety and the differences of the signal processing methods and parameter extraction techniques in the different applications of the surface EMG is shown.

1.5.1 Surface EMG Applications in Bio-feedback and Rehabilitation

Physical therapists routinely use the surface EMG technique to examine movement dysfunction of patients who have musculoskeletal and neuromuscular impairments. Rehabilitation nurses and therapists usually monitor and treat the muscle action of patients with the surface EMG feedback. To date, a large number of projects have been carried out in the field of bio-feedback and rehabilitation. For instance, the study of Armagan and colleagues on the functional recovery of the hemiplegic hand, demonstrated the potential benefits of the surface EMG biofeedback in

conjunction with neurophysiological rehabilitation techniques to maximize the hand function in hemiplegic patients (*Armagan, O, Tascioglu, F, and Oner, C, 2003*). Brucker and Bulaeva applied the surface EMG technique during the treatment of patients with spinal cord injury. The results suggested the efficacy of the surface EMG biofeedback for increasing voluntary responses from the triceps muscles of long term cervical spinal cord injured individuals (*Brucker, B S and Bulaeva, N V, 1996*).

Furthermore, Erler *et al.* evaluated the therapeutic effect of a special type of hydrotherapy on patients with a total of knee arthroplasty based upon the surface EMG investigations, and showed their technique might lead to better muscular coordination and strength, which could provoke a better stabilization of the knee joint (*Erler, K et al., 2001*). Ferrario *et al.* compared the surface EMG characteristics of masticatory muscles in patients with fixed implanted-supported prostheses and implant overdentures and showed that two types of implant-supported prostheses were functionally equivalent (*Ferrario, V F et al., 2004*). In addition, one of Merletti *et al.*'s projects focused on processing and interpretation of multi-channel surface EMG recorded from the external anal sphincter muscle. The technological innovation presented was promising for a further insight into the examination of pelvic floor pathologies and rehabilitation treatments (*Merletti, R et al., 2004*).

1.5.2 Surface EMG Applications in Kinesiology and Neurology

The surface EMG technique is considered as an acceptable method for kinesiology analysis of movement dysfunctions. It is routinely used to measure nerve conduction velocity after electrical stimulation of a peripheral nerve (*Pullman, S L et al., 2000*). It is also a valuable tool for the neurophysiological analysis of movement disorders, such as tremor,

myoclonus, dystonia, and dyskinesia, the evaluation of gait and posture, and the assessment of psychophysical measurements of reaction and movement time. Through measurement of frequency and amplitude of muscle activity, the surface EMG may provide information about motor unit recruitment and synchronization and can also reveal whether involved muscles discharge simultaneously or alternately. Recently, Staudenmann and colleagues optimized muscle force estimation with the aid of a high-density EMG electrode gird (*Staudenmann, D et al., 2005*). Jonkers *et al.* applied surface EMG analysis methods to identify muscle group activity profiles and potential overload risks (*Jonkers, I et al., 2004*).

1.6 Objective of this Study

The correlation between the surface EMG signal and the study of dynamic movements, especially gait analysis, can provide much valuable information and further data of clinical interest of the role of motor control and muscle activity. The knowledge of physiological details of the surface EMG needs to be furthered. The approaches and algorithms used to process the surface EMG signal also require improvement in order that the clinician may ensure better and more reliable information on the functional effects of muscular action in various areas of clinical research.

As a result, the purpose of this study is to address the features, measurement and instrumentation of the surface EMG, present a simulation model of the surface EMG signal during dynamic movements, and improve the signal processing algorithm based upon the simulated and real signals in order to assess the muscle activity as well as the performance of muscle functional tasks. The physiological basis of the surface EMG signal will be introduced in Chapter 2. The basic concepts of the gait cycle, features of the gait phases, and muscle control during walking will be described in Chapters 3.

Measurement, electrode configuration, and acquisition system will be addressed in Chapter 4. A model generated from the physically-based structure, which is used to examine new algorithms to illustrate the features of muscle activity, is chiefly described in Chapter 7. By adapting the values of parameters appropriately, the model also has potential in combination with information related to different movements. Chapter 5 mainly presents the surface EMG signal processing methods for clinical application. A novel algorithm to estimate the muscle activation timing is derived and discussed in Chapter 8. All real surface EMG data presented in this study are obtained from a series of gait trials which are described in Chapter 6.

1.7 Major Contributions of this Study

The key contributions involve:

- Producing a simulation model of the surface EMG signal for the analysis of muscle activity during the gait cycle. A multiple-layer structure model covers the majority of the characteristics of the surface EMG, such as the fibre distribution, motor unit type, location and recruitment, tissue anisotropy, electrode configuration and gait phases. A series of simulated results of, for example, the single fibre action potential, motor unit action potential, motor unit action potential trains and surface EMG signal during voluntary contraction are generated by input or modification of the values of the parameters contained in the model. The simulated surface EMG signals from the lower limb muscles during walking are also created. The validation of the model is performed by comparison between the simulated signals and real surface EMG signals recorded from a gait experiment.

- Presenting a power-threshold algorithm to estimate the muscle activation intervals. Derivation of the algorithm and selection of parameters are described. The features, especially limitations of methods proposed previously are discussed based upon the simulated surface EMG signals originated from the physically-based model. The performance of the algorithm is illustrated by application to real surface EMG signals measured from a gait experiment. In addition, from a comparison between the power-threshold algorithm and the more traditional methods described in the literature, it is evident that the power-threshold algorithm is more suitable for the estimation of the timing of muscle activation during the gait cycle.
- Designing and performing a gait experiment to investigate the muscle activity during dynamic movement. During the experiment, three main signals, surface EMG, foot switches and body movement are measured from healthy adults during normal walking. Surface EMG signals and foot switch data are used to demonstrate the validity of the simulation model and assess the algorithm to estimate muscle activation intervals.

1.8 Summary

In this introductory chapter, the concept of the surface EMG has been introduced. Electrodiagnostic methods and categories of techniques were reviewed. The surface EMG history, development and properties were also described, as well as its applications in bio-feedback, rehabilitation, kinesiology and neurology. The advantages and limitations of the surface EMG have been examined, the purpose of this study stated and the key contributions enumerated.

Chapter 2 Anatomical and Physiological Basis of the Surface EMG

2.1 Introduction

This chapter describes the anatomical and physiological basis of the surface EMG signal. The structure and function of the basic components of the neuromuscular system are presented. An introduction to properties and structures of the skeletal muscles is given in Section 2.3, which is developed further in Section 2.5. The structures and categories of muscle fibre are outlined and muscle fibre action is described. Section 2.4 illustrates types of muscle contractions. The terms to describe the contractions and the types of muscle work are defined. Section 2.6 augments the knowledge of the neuromuscular system from Section 2.1 to formulate the motor unit types, territories, and recruitment during muscle contraction and relaxation.

2.2 Neuromuscular System

In order to present, simulate and process the surface EMG signal during dynamic movements, it is essential to understand the properties of the neuromuscular system and how the muscles work under the nervous system control. The recruitment of muscle would not occur were it not for the nervous system (*Cram, J R, Kasman, G S, and Holtz, J, 1998*). The functions of the nervous system in dynamic movements include both conducting motor commands from the brain to muscles and monitoring changes in the environment both external and internal that affect locomotion (*Tyldesley, B and Grieve, J, I, 2002*).

The basic unit of the nervous system is the *neuron*. A diagram of typical motor neuron and motor endplate is shown in Figure 2-1. Its functions are to generate impulses in response to stimulation and to conduct the impulses between neurons. Neurons are situated in networks or centers in the brain and the spinal cord. Activity in one center can be directed to the particular end and may be conducted to one or many other centers through the neural networks. For instance, the lower motor neuron's axon branches and attaches itself to the muscle fibre at the motor endplate to create neuromuscular synapses. During muscles contraction, a nerve action potential travels down the axon, arrives at the neuromuscular synapses and releases acetylcholine (Ach), which produces the breakdown of the ionic barrier of muscle tissues and allows the action potential signals to pass through the muscle system. Muscle fibres have the ability to shorten to almost half their resting length via a process of 'ratcheting' myosin fibres against the actin fibres in order to produce muscle contraction (*Palastanga, N, Field, D, and Soames, R, 2002*).

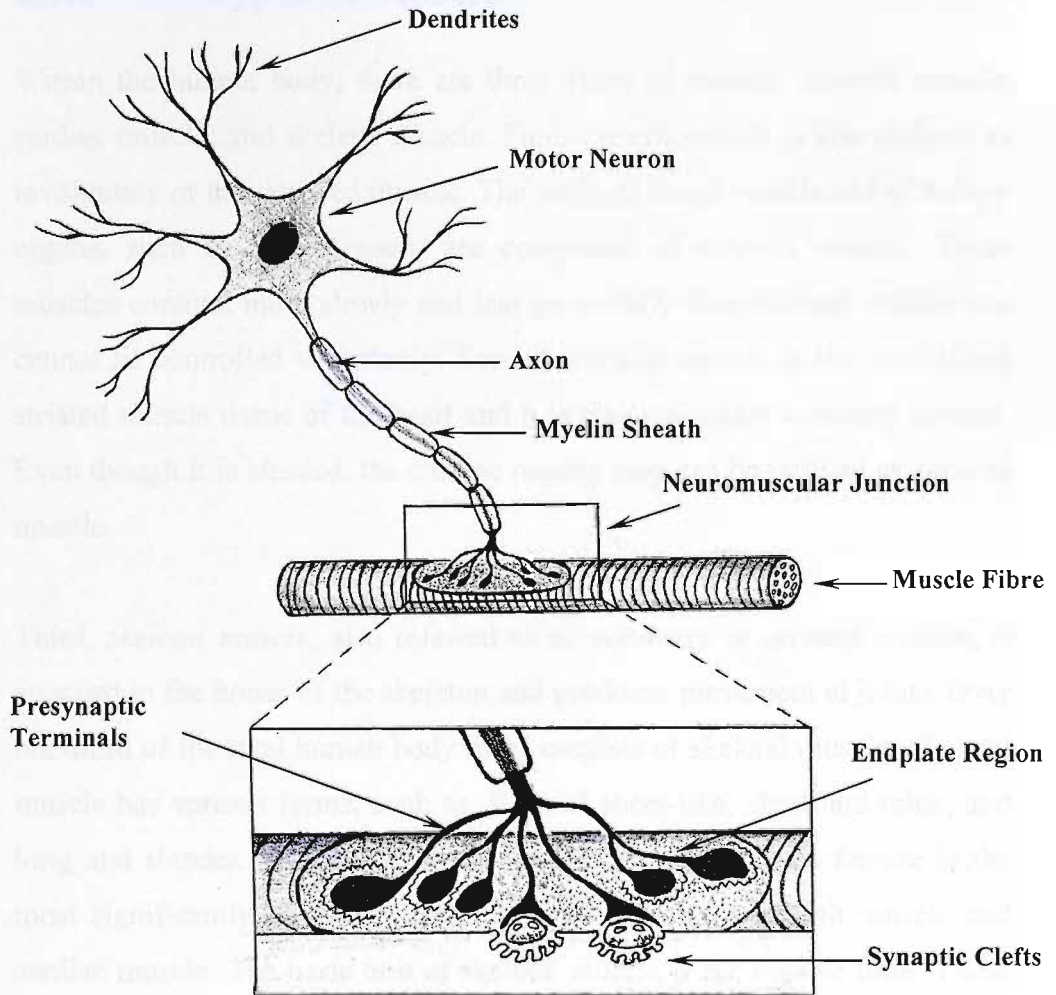


Figure 2-1 A typical motor neuron and motor endplate

Source: adapted from *Noninvasive Instrumentation and Measurement in Medical Diagnosis*, Robert.B. Northrop, CRC Press, London, 2002

2.3 Muscle: Types and Structure

2.3.1 Types of Muscle

Within the human body, there are three kinds of muscle: smooth muscle; cardiac muscle; and skeletal muscle. First, *smooth muscle* is also defined as involuntary or non-striated muscle. The walls of blood vessels and of hollow organs, such as the stomach, are comprised of smooth muscle. These muscles contract more slowly and less powerfully than skeletal muscle and cannot be controlled voluntarily. Second, *cardiac muscle* is the specialized striated muscle tissue of the heart and it is also not under voluntary control. Even though it is striated, the cardiac muscle may not be defined as skeletal muscle.

Third, *skeletal muscle*, also referred to as voluntary or striated muscle, is attached to the bones of the skeleton and produces movement at joints. Over one-third of the total human body mass consists of skeletal muscle. Skeletal muscle has various forms, such as, flat and sheet-like, short and thick, and long and slender. It contracts under voluntary control. This feature is the most significantly different aspect contrasting it with smooth muscle and cardiac muscle. The basic unit of skeletal muscle is the muscle fibre. These non-branching striated muscle fibres are bound together in bundles to form a whole muscle, which can contract to produce and support movement, as well as to resist movement in response to the force of gravity or an added load. Skeletal muscle is the target muscle group in this study. The real and simulated surface EMG signals shown in the thesis are considered as electrical activities produced by particular skeletal muscles during voluntary contractions or relaxations.

2.3.2 Structure of Skeletal Muscle

In order to explore muscle activities, it is helpful to understand the composition of muscle and to examine the structure of muscle from a macroscopic to a microscopic level. The structure of a whole muscle is composed of muscle and connective tissues, and both participate in muscle activities and support muscle functions. On a macroscopic level, a whole muscle consists of muscle fascicles, which are bound together by connective tissue and run in the same direction. A further covering of connective tissue surrounds the whole muscle. Each muscle fascicle is composed of contractile muscle fibres, which are also surrounded by connective tissue, separating them from their neighbours, yet connecting them together. Muscle fibres are long, cylindrical, multinucleated cells of varying length and width (*Palastanga, N, Field, D, and Soames, R, 2002*). The organization of skeletal muscle is given in Figure 2-2.

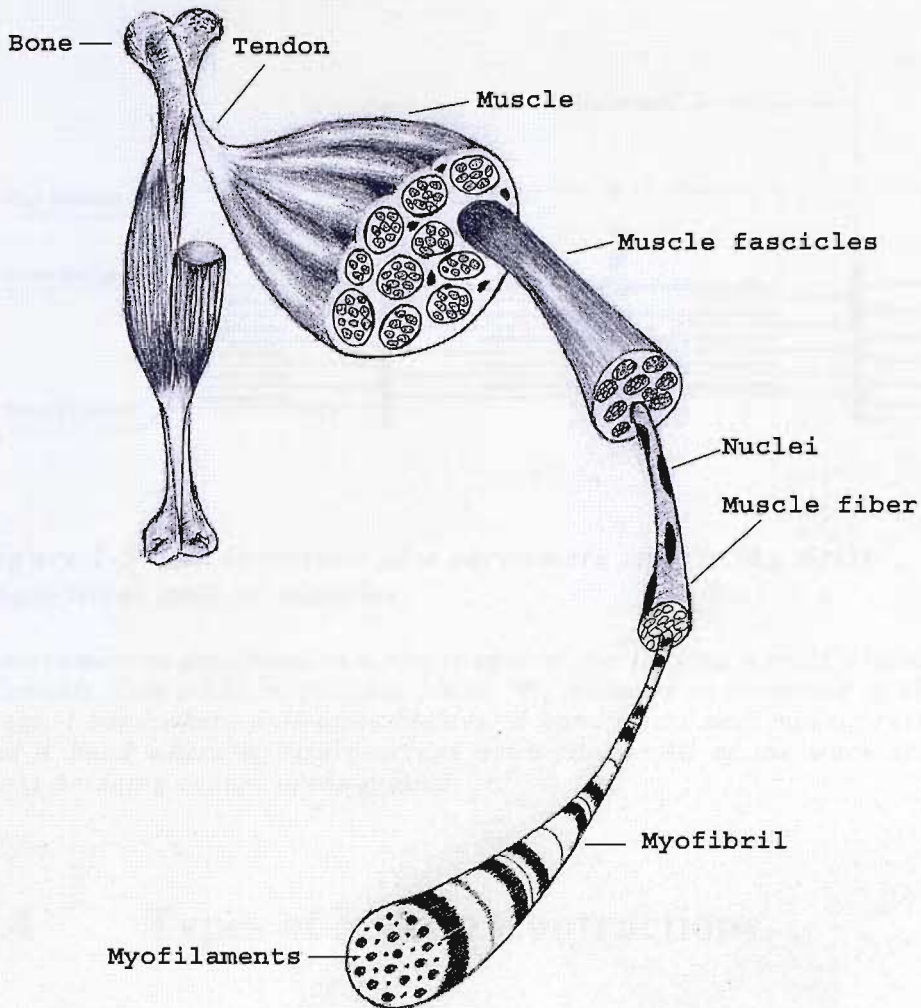


Figure 2-2 Structure of skeletal muscle.

A whole muscle is composed of muscle and connective tissues. The muscle consists of muscle fascicles, which are groups of contractile muscle fibres bound together by connective tissue. Source: adapted from Muscles, Nerves & Movement in Human Occupation, Barbara Tyldesley and June I. Grieve, Blackwell Science, Oxford, 2002.

On a microscopic level, the muscle fibres may be divided into clusters of individual myofibrils, which appear to be braided in light and dark bands under a microscope. Each myofibril contains myosin and actin filaments. The basic structure of the muscle is a sarcomere, which consists of a unit of myosin and actin filaments from one Z-line to the next. The Z-line is the

dark line representing the attachment of actin fibres. The structure of a sarcomere is shown in Figure 2-3.

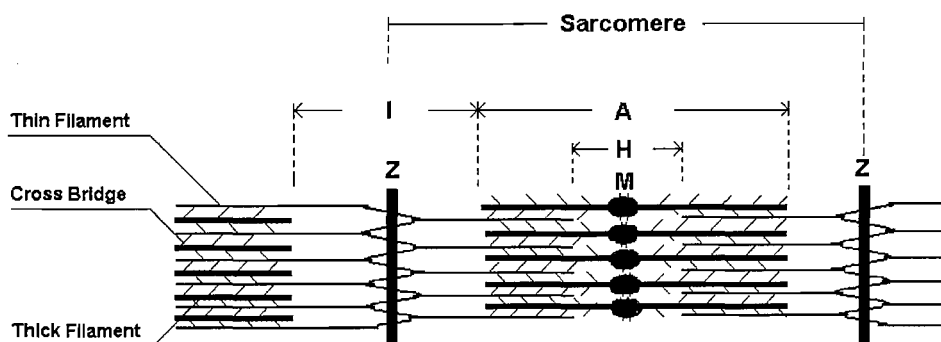


Figure 2-3 *The structure of a sarcomere that is the basic anatomical unit of muscles.*

A sarcomere is described as a single unit of overlapping myosin and actin filaments from z-line to the next z-line. A sarcomere is composed of three areas, I band where only actin resides, H band where only myosin resides and A band where myosin overlaps actin fibres. All of the work of the cross-bridging occurs in the A band.

2.4 Types of Muscle Contractions

The surface EMG patterns recorded from different dynamic movements may differ, depending upon which type of muscle contraction which is being studied. There are two identifiable types of muscle contractions: *isotonic* and *isometric* (Gage, J R, 1991; Palastanga, N, Field, D, and Soames, R, 2002). When a muscle is stimulated, it contracts so as to bring its two ends closer together. Muscle contractions, in which the muscle length obviously changes, although the tension produced remains more or less constant, are termed isotonic. Muscle contractions, in which the muscle length remains unaltered and the tension usually increases in order to overcome the resistance, are termed isometric.

Isotonic contraction comprises two types: *concentric* and *eccentric* (Palastanga, N, Field, D, and Soames, R, 2002). Concentric contraction occurs when the muscle shortens and is usually used to overcome the external resistance. The moving body part is generally accelerated when concentric contraction occurs. Eccentric contraction occurs when the muscle lengthens. Eccentric contraction happens in an already shortened muscle in which the external force is greater than the tension produced by the muscle contraction

Isometric contraction occurs when a constant muscle length is maintained. It is usually used to control posture and stabilize axial body parts during extreme movements. The surface EMG is typically greatest during isometric contraction.

Determined by which type of muscle contraction occurs, the amount of muscular energy is quite different. Muscular energy is greater during an isometric contraction than during a concentric contraction because 20% of the energy efficiency of the movement is used to shorten the muscle during concentric contraction (Cram, J R, Kasman, G S, and Holtz, J, 1998; Perry, J, 1992). The greatest load produced by a concentric contraction is only 80% of the load generated by maximum isometric contraction. The amount of energy produced by an eccentric contraction is greater than the energy produced by an isometric contraction and exceeding it by 10-20%. Consequently, the force produced by a muscle cannot be directly related to amplitude of surface EMG signals without taking account of underlying muscular contraction (Perry, J, 1992).

During the gait cycle, all three types of muscle contraction are involved. Eccentric contraction happens when a limb decelerates during the stance phase. Isometric contraction generates peak values of muscle activity during

the gait cycle. Advancement of the limb during the swing phase is controlled by concentric contraction.

2.5 How Muscle Fibres Work

2.5.1 Muscle Fibre Work

Muscle contraction can be created through the muscle fibres that do their work to shorten their resting lengths. In the excitation sequence, the impulse enters the motor nerve terminal and allows Calcium (Ca^{2+}) ions to penetrate and release Ach from the synaptic vesicles. The role of Ach is to act as a chemical intermediary in the process of transferring excitation from nerve to muscle. The Ach may diffuse across the synaptic cleft and connect with receptors situated in the muscle fibre membrane. The interaction between Ach and receptors can change the permeability of the membrane, then bring about a depolarization and hence fire an impulse. Once initiated, the action potential, which arises in the membrane immediately adjacent to the Ach receptors, propagates in both directions toward the end of the muscle fibre.

The depolarization, which is created by the action potential, spreads to the interior of the muscle fibre through the transverse tubule system, then, causes release of calcium ions by the sarcoplasmic reticulum. The released calcium ions attach to troponin molecules on the thin filaments. At the same time, tropomyosin uncovers the myosin combining with actin. Energized by splitting an *Adenosine Triphosphate (ATP)*, globular heads of myosin molecules may attach to actin. The energy of the activated myosin propels the thick and thin filaments past each other. As a result, contraction occurs and is maintained as long as internal calcium concentration is elevated. A sequence of events that intervene between the occurrences of the action potential in the plasma membrane of the muscle cell and the

activation of the contraction is defined as the process of excitation-contraction coupling. (*Matthews, G G, 1986*).

2.5.2 Categories of Muscle Fibres

Not all muscle fibres in one muscle have a constant time delay between the occurrence of the muscle fibre action potential and the peak of the resulting tension. The range of the delay time is from 10 msec to 200 msec (*Matthews, G G, 1986*). In general, two main types, slow fibres and fast fibres, have been distinguished on the basis of this speed.

Slow fibres, also defined as type I fibres, contain myoglobin that is used to store oxygen and respond to stimulation with a slow twitch. They are resistant to fatigue. The slow fibres predominate in muscles that sustain postural activity and maintain steady contraction, for example, keeping us standing upright.

Fast fibres, referred as type II fibres, have no myoglobin and respond with a fast twitch. They are easily fatigued. The fast fibres are adapted for rapid intense bursts of activity, such as jumping and running. They are common in muscles that require rapid contraction, for example, moving the eyes in quick movements for scanning the words on books.

2.6 The Motor Unit: Properties and Recruitment

2.6.1 The Motor Unit

A single motor neuron in the anterior horn of the spinal cord makes synaptic contact with a number of muscle fibres. One motor neurone, its axon and all the muscle fibres innervated by the branches of the axon form a basic unit of

motor organization called the *motor unit*. The motor unit is the basic level of the neuromuscular system. This means that all movements are controlled by the central nervous system in terms of motor units rather than individual muscle fibres (McComas, A J, 1996).

One motor unit has many branches and innervates a group of muscle fibres. However, a single muscle fibre usually receives synaptic contact from only one motor unit. Various lengths and diameters of branching nerve fibres that spread to each muscle fibre cause the time that the nerve action potential arrives at the endplate to differ. Hence, the activations of muscle fibres within a given motor unit are asynchronous. The motor unit action potential may be generated by gathering the different temporal muscle fibre action potentials.

It is possible to divide motor units into *low-threshold* and *high-threshold* units depending upon the time that the muscle fibres within the unit take to achieve their peak tension. All movements are produced and supported by a combination of the low-threshold and high-threshold motor units. The low-threshold motor units usually contribute to the steady and postural activities, while the high-threshold units are adapted for rapid bursts of movement.

2.6.2 Territories of the Motor Unit

Motor unit recruitment territories may be imagined as small, overlapping circles on the cross-section of the muscle. The level of performance of a muscle at any time is determined by the number of motor units that are recruited. An approximate estimate of the size of motor units within a given muscle is calculated by the innervation's ratio, which is given by the number of muscle fibres in a muscle and the number of motor nerves supplying it (Lenman, J A R, Ritchie, A E, and Simpson, J A, 1987). Figure 2-4 illustrates

the motor unit territories on the cross-section of the muscle and their contributions to the surface EMG signal.

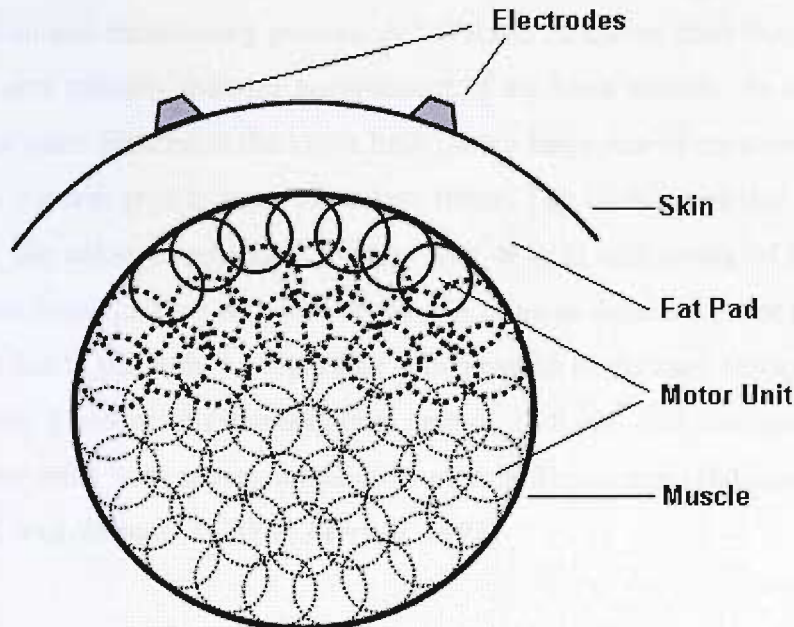


Figure 2-4 Motor unit territories on the cross-section of the muscle and their contributions to the surface EMG signal.

*The motor unit recruitment territories are represented by the small, overlapping circles. Only the heavy, dark motor unit pools contribute substantially to the surface EMG recordings. It is impossible to collect a single motor unit action potential on the surface of the skin by using the surface EMG electrodes. The electrical signals displayed by EMG instruments are the activities of populations of motor units. Source: adapted from *Introduction to surface electromyography*, Jeffrey R. Cram, Aspen, Gaithersburg, 1998.*

The size of the motor unit and the composition of muscle fibres it contains depend upon the function of the muscle rather than its size (Tyldesley, B and Grieve, J, I, 2002). For example, small hand muscles that are employed to control the fine precision movements of the fingers have a small size of motor units including a small number of muscle fibres in each unit. Lumbrical, a small muscle in the hand, plays an important role in controlling the finger position and has a 0.6 cm^2 physiological cross-sectional area that

consists of approximately 95 motor units with approximately 100 muscle fibres each (Palastanga, N, Field, D, and Soames, R, 2002; Perry, J, 1992). In contrast, the muscles in the lower limb are adapted for weighting bearing, locomotion and maintaining posture. All of these functions need much more strength and stability than the requirement of the hand muscle. As a result, the motor units situated in the lower limb have a large size of cross-sectional area and contain greater sizes of muscle fibres. The tibialis anterior muscle supports the ankle at neutral to prevent foot drop in mid-swing of the gait cycle, and in the loading response of the gait cycle to decelerate foot fall and pull the tibia to the body's weight line which results in the knee flexion. This muscle has a moderate cross-sectional area of 13.5 cm² and contains about 445 motor units with approximately 610 muscle fibres each (Palastanga, N, Field, D, and Soames, R, 2002; Perry, J, 1992).

2.6.3 Motor Unit Recruitment & Firing Frequency

A muscle may receive stimulations from hundreds of motor units. The tension of a contracting muscle depends upon the number of motor units and their frequency of firing. Thus, tension in the muscle can be increased by activating additional motor units and increasing their firing frequency. The increase in the number of active motor units is defined as *recruitment* of motor units and is a more important physiological means of producing muscle tension since the firing frequency of motor units varies between fairly narrow limits.

The order of motor unit recruitment abides by the *size principle*. As the tension in the muscle is increased, motor units including a small number of muscle fibres are recruited first; larger motor units are activated later. The low-threshold and small motor units are recruited at the beginning of muscle contractions and this may ensure that the added increments of tension are

small. As tension demand increases, larger motor units are activated to achieve a significant difference, resulting in larger increments of tension.

The range of firing frequency of human muscle fibres is between 8 Hz and 50 Hz (*Cram, J R, Kasman, G S, and Holtz, J, 1998*). Each motor unit has a relatively restricted range of firing frequency, and a particular motor unit has a particular firing frequency at different tensions (*Lenman, J A R, Ritchie, A E, and Simpson, J A, 1987*). Accompanying an increase in tension, the firing frequency of motor units varies from a lower to a higher level. When both additional motor unit recruitment and firing frequency increase come into being, the stronger are the amplitude and power of the surface EMG signal.

2.7 Summary

This chapter has covered the anatomical and physiological basis of the surface EMG. The structure and properties of the basic units of the musculoskeletal and nervous system have been shown. It began by describing the properties of neuromuscular system. The structure of the muscle was illustrated from a macroscopic to a microscopic level. The types of muscles, muscle fibres and motor units have been defined, respectively. Muscle contractions were classified as two identifiable types, isotonic and isometric, in Section 2.4. How muscle fibres work was then examined. The concept of the motor unit was introduced in Section 2.6 and its characteristics, territory, recruitment and firing frequency described.

Chapter 3 Surface EMG and Gait Analysis

3.1 Introduction

This chapter presents the key definitions and concepts of gait analysis. The gait cycle, phases of gait, basic functions of the gait cycle, and muscle control during normal gait are set forth. Section 3.6 describes a number of applications of the surface EMG technique in gait analysis.

3.2 Gait Cycle

The *gait cycle* is a fundamentally important term in gait analysis. When the body attempts to move forward, one limb performs the support function while the other one moves itself to the new support site. The two limbs then exchange their roles. Walking is composed of a series of repetitious sequences of limb functions both moving the body forward and maintaining

body stability. A single sequence of these functions accomplished by one limb is defined as a gait cycle (*Perry, J, 1992*). There is no specific onset or cessation point in a gait cycle. In this study, an initial floor contact with the heel is selected as the onset of a gait cycle, because the moment of the initial contact is easier to identify than other events. In other words, a complete gait cycle begins when the heel of one foot contacts the ground and ends when it contacts the ground again.

3.3 Phases of Gait

Each gait cycle is divided into two major phases, *stance phase* and *swing phase*. Stance phase describes the period during which the foot is on the ground. Correspondingly, swing phase represents the period during which the foot is in the air and limb moves forwards. Stance phase starts at the initial contact and is divided into four intervals, loading response, mid-stance, terminal stance and pre-swing. Swing phase begins when the foot has risen from the ground and is separated into three intervals, initial swing, mid-swing and terminal swing. Divisions of the gait cycle and subdivisions of stance and swing phases are shown in Figure 3-1.

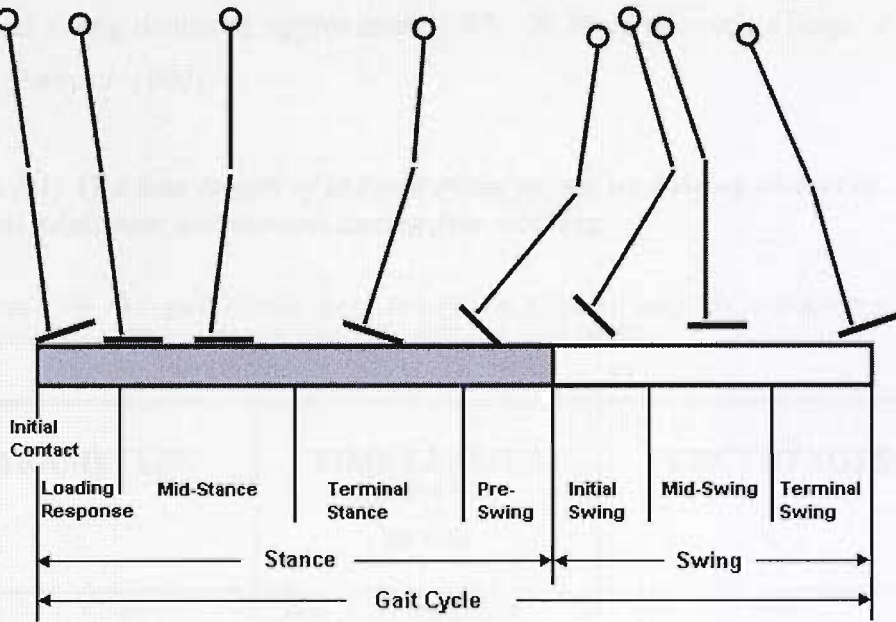


Figure 3-1 Divisions of the gait cycle and the subdivisions of stance and swing phases.

Shaded bar represents the duration of stance, clear bar indicates the duration of swing. Stance phase includes four intervals: loading response, mid-stance, terminal stance and pre-swing; swing phase is divided into three intervals: initial swing, mid-swing, and terminal swing. Limb segments illustrate the onset of stance phase with initial contact, end of stance with toe-off, and end of swing with floor contact again.

Events in the gait cycle are described as occurring at specific percentages of the cycle (Gage, JR, 1991). In general, initial contact is defined as occurring at 0 % and 100 % of the cycle. Because toe-off happens at approximately 60 % of the cycle during normal walking, stance phase represents approximately 60 % of the gait cycle and swing phase represents about 40 %. Table 3-1 indicates the time length of the gait cycle, stance and swing phases of normal men and women during free walking (Brown, B H, 1999). The loading response interval is 2-10 % of the cycle, mid-stance occurs at approximately 10-30 % of the cycle, terminal stance is defined as happening at approximately 30-50 % of the cycle, pre-swing's interval describes about 50-60 % of the cycle, initial swing's interval represents approximately 60-73

% of the cycle, mid-swing's interval is about 73-87 % of the cycle, and terminal swing occurs at approximately 87-100 % of the cycle (*Gage, J R, 1991; Perry, J, 1992*).

Table 3-1: The time length of the gait cycle, stance and swing phases of normal adult men and women during free walking.

Intervals in the gait cycle are described sequentially as occurring at percentages of the cycle. A cycle is defined as 100 %.

PARAMETERS	TIME LENGTH (MEAN ± 1 SD)	PERCENTAGES
	SECOND	%
Gait cycle	Men: 1.06 ± 0.09	100
	Women: 1.03 ± 0.08	100
Stance phase	Men: 0.65 ± 0.07	61.3
	Women: 0.64 ± 0.06	62.1
Swing phase	Men: 0.41 ± 0.04	38.7
	Women: 0.39 ± 0.03	37.9

3.4 Basic Functions of the Gait Cycle

Each of the intervals of gait phases has a functional objective. The sequential combination of the eight intervals of the gait phases enables support and advancement of the limb to accomplish three basic functions: weight acceptance, single limb support and limb advancement (*Perry, J, 1992*).

Weight acceptance is the most demanding task in the cycle. It includes three functional patterns, shock absorption, initial stability and the preservation of progression. Two intervals, initial contact and loading response, are involved in this functional task. Initial contact enables the limb to position in order to start the gait cycle with heel-down. Loading response is a period of deceleration and occurs immediately after initial contact. It corresponds to

the cycle's first period of double limb support. The shock of impact is absorbed during this interval.

Single limb support occurs after loading response and continues until the opposite foot contacts the ground again. Two intervals, mid-stance and terminal stance, are involved in this functional task. Mid-stance begins with contralateral toe-off and ends when the centre of gravity is over the supporting foot. It has a responsibility for limb and trunk stability. Terminal stance begins when the centre of gravity is over the reference foot and ends with the contralateral foot-down. It is able to position the trunk beyond the supporting foot.

Limb advancement is a significant functional task in the gait cycle. It concludes two mainly functional patterns, advancing the limb and preparatory posturing begins in the stance phase. Four intervals, pre-swing, initial swing, mid-swing and terminal swing are involved in this task. Pre-swing begins with contralateral initial contact and ends with ipsilateral toe-off. It corresponds to the cycle's second period of double limb support and is responsible for weight release and swing preparation. Initial swing begins with lift of the foot from the ground and continues until maximum knee flexion occurs. The objectives of this interval include both foot clearance and limb advancement from its trailing position. Mid-swing begins at maximum knee flexion and ends when the tibia is vertical to the ground. The swinging limb is forward during this interval. Terminal swing begins when the tibia is perpendicular and ends when the foot contacts the ground again. This interval has responsibilities for completing limb advancement and preparing the limb for next stance.

3.5 Muscle Control during Normal Gait

3.5.1 The Lower Limb Muscles

During walking, all the muscles of the lower limb play an important role in maintaining the balance of the upright body and transferring the body from one position to another. Three main functions are involved in the gait cycle. These are support, swing and propulsion (*Tyldesley, B and Grieve, J, I, 2002*). Many muscles participate in these functions, for example, quadriceps femoris sartorius of the anterior thigh, adductor magnus and gracilis of the medical thigh, tibialis anterior and extensor hallucis of the anterior lower leg, gastrocnemius and soleus of the posterior lower leg, and peroneus longus and brevis of the lateral leg (*Gosling, J A et al., 1994*).

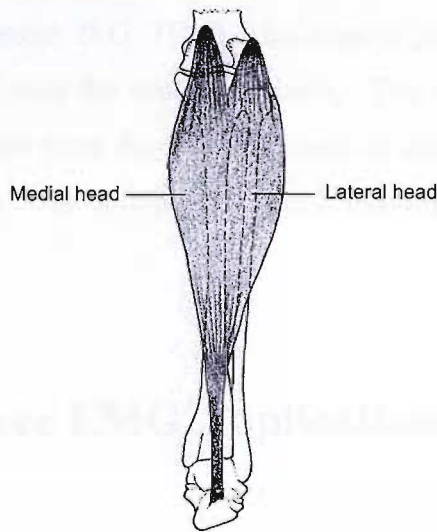
In walking, tibialis anterior and gastrocnemius muscles make an important contribution to support and propulsion. Tibialis anterior is concerned with balancing the body. As with other muscles in the lower limb, it takes responsibility for maintaining body balance during activities of the upper part of the body which change the center of gravity. It works with the surrounding muscles to dorsiflex the foot to prevent the toes catching the ground when the lower limb is carrier forward during the swing phase. Gastrocnemius offers a considerable amount of the propelling force for locomotion. Together with soleus, it is responsible for the chief plantarflexor of the ankle joint. It is also one of the most powerful muscle groups in the body (*Palastanga, N, Field, D, and Soames, R, 2002*). As a result, in this study, the tibialis anterior and gastrocnemius, specifically including gastrocnemius medialis head and gastrocnemius lateral head, are selected to illustrate surface EMG signals in the analysis of muscle activities during the gait cycle. Figure 3-2 shows tibialis anterior and gastrocnemius muscles.

3.5.1 Muscle Control

In the gait cycle, the tibialis anterior muscle is active during the swing phase, particularly during the heel strike and toe-off phases. It contracts to prevent the foot from dropping and to control the foot's position during the swing phase. The muscle also plays a role in the stance phase, particularly during the heel strike and toe-off phases. It contracts to control the foot's position and to prevent the foot from dropping. The muscle is also active during the swing phase, particularly during the heel strike and toe-off phases. It contracts to control the foot's position and to prevent the foot from dropping.



(a)



(b)

Figure 3-2 *Tibialis anterior and gastrocnemius. (a) Right tibialis anterior, anterior view; (b) Right gastrocnemius, posterior view.*

Source: redrawn from *Anatomy and human movement: structure and function*. Nigel Palastanga, Butterworth – Heinemann, Oxford, 2002.

3.5.2 Muscle Control

In the gait cycle, the tibialis anterior muscle is activated at initial contact, controlling the heel rocker, and continues to be active during loading response, decelerating footfall and flexing the knee. The tibialis anterior muscle group is most active at the heel strike and primarily serves to prevent 'foot slap'. It also assists the toes in clearing the floor during swing phase of the gait cycle (*Basmajian, J V, 1967*). It is recruited to control the limb advancement during initial swing, mid-swing and terminal swing.

The gastrocnemius muscle group is activated during mid-stance and terminal stance, providing more than 80 % of the acceleration force necessary to maintain steady state walking. It also assists in plantar flexion in controlling the forward movement of the leg over the fixed foot during ambulation (*Travell, J G and Simons, D G, 1983*). This muscle group is affected by the position of the body over the centre of gravity. The muscle is quiet in the neutral posture, but the more forward it is over its axis, the more active the muscle becomes. It is most active when one is standing on the toes (*Okada, M, 1973*).

3.6 Surface EMG Applications in Gait Analysis

Modern gait analysis began with the studies of Inman (*Inman, V T, 1981; Inman, V T, 1993*) and became a valuable clinical method through the pioneering efforts of Perry (*Perry, J et al., 1975; Perry, J, 1993; Perry, J et al., 1993; Perry, J, 1994; Perry, J et al., 1995; Perry, J et al., 1996; Perry, J, 1999; Perry, J et al., 2003*) and Sutherland (*Sutherland, D H, 1978; Sutherland, D H et al., 1980; Sutherland, D H et al., 1981; Sutherland, D H et al., 1996; Sutherland, D H et al., 1997; Sutherland, D H, 2001;*

Sutherland, D H, 2002; Sutherland, D H, 2005; Sutherland, D H and Cooper, L, 1977; Sutherland, D H and Davids, J R, 1993; Sutherland, D H and Lescooper, A S, 1978). These pioneers indicated that the clinical value of relating muscle function to phases of the gait cycle, which resulted in procedures to improve the gait cycle of those suffering from neuromuscular disorders.

The surface EMG technique is a useful, safe and non-invasive tool for clinicians and researchers to analyse the normal and pathological gait. (*Brach, J S et al., 2001; Buurke, J H et al., 2004; Buurke, J H et al., 2005; Lauer, R T et al., 2005; Levin, O S et al., 2003; Lim, H K et al., 2005; Roetenberg, D et al., 2003; Trueblood, P R, 2001*). It can provide an representation of muscle activation during different intervals of the gait cycle by using proper measurement and instrumentation. Diagnosis can be based upon the analysis of the surface EMG signal and consequently it is extremely important to have appropriate instrumentation, techniques, and signal processing methods that offer high quality EMG signals.

3.7 Summary

This chapter described applications of the surface EMG technique in the study of the gait cycle. The chief concepts and definitions of gait analysis, such as the gait cycle, the phases of the gait cycle, and the intervals of the gait phases have been introduced. Three basic functions of the gait, weight support, single limb support, and limb advancement, were described in Section 3.4. The muscles of the lower limb, especially the tibialis anterior and gastrocnemius, which are two extremely important muscle groups to contribute to the movements, have been examined in detail in Section 3.5. The functions of all muscles of the lower limb (support, swing and propulsion) involved in the gait cycle, were also described. All definitions of

gait analysis given in this chapter provide basic information for the generation of a simulation model and the derivation of an algorithm to examine the muscle activity.

Knowledge for the 21st Century

Department of Electrical and Electronic Engineering

Chapter 4 Surface EMG Detection and Measurement

4.1 Introduction

This chapter provides brief definitions and explanations of some fundamentals of the surface EMG measurement and instrumentation. Electrodes used to measure myoelectrical signals are introduced and shown to be described by their types and properties. The differential amplifier and its configuration are covered. The basic terms of the bioelectrical amplifier, especially input impedance and common mode rejection, are described in detail. Notch and band-pass filters used to improve the quality of myoelectrical signals are also presented. Common sources of noise and artefact, contaminating the recordings of the electromyographer, are described in Section 4.4. Popular methods and techniques used to separate useful myoelectrical signals from other bioelectrical signals and corrupting noise components are also given in this section.

4.2 Electrodes

4.2.1 Electrodes: Types and Properties

The EMG signal can be recorded by two types of electrodes. Surface electrodes are used to extract the myoelectrical signal on the surface of the skin. Wire or needle electrodes are inserted into the muscle to record from single motor units, or even individual muscle fibres. Needle or wire electrodes are insecure and uncomfortable for use during the study of dynamic movement. Moreover, the objective of this study is focused on the surface EMG signal processing. Selection of suitable surface electrodes is a basic and important step in measurement.

4.2.2 Surface Electrodes

A number of specially designed types of surface electrodes are used by researchers. The most common surface electrodes are Ag-AgCl electrodes. The Ag-AgCl electrode is generally described as $\text{Ag}^+|\text{AgCl}|\text{Cl}^-$ (Togawa, T and Tamura, T, 1997). The choices lie on the types of surface electrodes of which there are a variety available with different characteristics.

The size of a surface electrode is a significant factor in making the selection (Hermens, H J et al., 1999a). An electrode that has a smaller detection area can obtain closer inter-electrode space for recording the signal from smaller muscles, such as the facial muscles. These electrodes might be 0.5 cm in diameter and be set at an inter-electrode distance of 1 cm. An electrode that has a larger detection area of, say 1 cm diameter and might be placed an inter-electrode distance of 2 cm, is suitable for larger muscles and is popular in many applications, for example, collecting surface EMG signals from the limbs. With an increase of the inter-electrode distance to more than 3 cm, the

signal from the broader muscle region would be recorded, but the specificity of the recording for the target muscle will decrease.

Surface electrodes can be divided into direct contact electrodes and floating electrodes according to contact methods between electrodes and the skin. A direct contact electrode can be directly placed on the skin and attached by tape. In general, a direct contact electrode is 0.5 to 1 cm in diameter and made of a disposable silver-impregnated plastic that is covered by a thin layer of silver chloride in order to maintain a stable electrical potential on the skin (*Cram, J R, Kasman, G S, and Holtz, J, 1998*). This electrode is suitable for 'quiet' surface EMG collection. Because the electrode is directly placed on the skin, it is easily contaminated by artefacts. It is not satisfactory for recording of dynamic movement. A floating electrode does not directly contact the skin when it is attached on the body. It is kept in a small cup that maintains the electrode above the skin by a millimetre or so and is filled with an electrolytic medium. An electrode paste or gel is used as a bridge to transfer the electrical signal between the electrode and the skin. Because the electrolytic cushion absorbs the movement of electrode on the skin's surface, the floating electrode is preferable for recording the surface EMG signal during dynamic movement.

Another surface electrode, the active electrode, has a built-in amplifier and integrated circuitry and supplies improved impedance for the subsequent processing (*Basmajian, J V and De Luca, C J, 1985*). An active electrode may provide higher impedance, and hence, skin preparation and gels are not necessary for surface EMG recording. The active electrode is fast becoming a popular choice for clinical applications. In this research, however, the floating electrode is chosen to record the surface EMG during the gait experiment described in Chapter 6. since, the gait laboratory in the School of Health Professions and Rehabilitation Sciences uses these electrodes routinely.

4.2.3 Surface Electrodes Placement

Electrode placement is an extremely important factor for surface EMG measurement since the amplitude and shape of the signal will be altered with a change of electrode position.

In gait analysis, for recording the surface EMG signal from the tibialis anterior, two electrodes are placed 2 cm apart, parallel to and just lateral to the medial shaft of the tibia, at approximately one quarter to one third the distance between the knee and ankle. In general, the location of electrodes is 1/3 on the line between the tip of the fibula and the tip of the medial malleolus. The reference electrode needs to be placed at or around the ankle or the spinous process of 7th cervical vertebra (*Hermens, H J et al., 1999a*).

There are two ways to place the electrode for collecting the signal from the gastrocnemius muscle. One way is to place two electrodes on each part of muscle, medial and lateral. The other is to record the signal from medial and lateral head, respectively. It is essential to use four electrodes and locate two of them 2 cm apart, parallel to muscle fibres. In general, the location of two electrodes for recording the medial head activity is on the most prominent bulge of the muscle. Two electrodes used to record the lateral head activity need to be placed at 1/3 of the line between the head of the fibula and the heel. The latter way is chosen for this study in order to record the surface EMG signals from two heads respectively.

4.3 Differential Amplifier

The electrical signal generated by muscle activity is reduced due to the impedance of the body tissue when it passes through the tissue and skin. The body tissue can be considered as a low-pass filter since it absorbs higher-

frequency components of the signal. The further the signal propagates through body tissue, the more the higher-frequency components of signal may be lost.

The myoelectrical signal has a very small value. The amplitude of the signal is generally measured in microvolts. It is essential to use very sensitive instruments to detect and amplify this signal so that it can be recorded and analysed. Furthermore, since the frequency range of the surface EMG signal is between 8 Hz and 500 Hz (*Cram, J R, Kasman, G S, and Holtz, J, 1998*), it may be easily contaminated by other electromagnetic signals in the recording environment.

In the early days of the surface EMG, a recording was conducted in a 'copper room' that could screen the environmental electrical noise. In the middle of the 19th century, the concept of the differential amplifier was introduced in the recording of the surface EMG. The introduction of the differential amplifier meant that the 'copper room' was not necessary for recording the signal and brought the surface EMG signal from the field of the researchers to the realm of the clinicians.

4.3.1 Structure of the Differential Amplifier

Differential amplifiers (DA) are widely used for bio-potential recording based upon their ability to decrease or eliminate common mode interference and noise. Two signal inputs (V_{in} and V_{in}') and one reference input (V_{ref}) are necessary for a differential amplifier. In other words, three surface electrodes are essential for recording myoelectrical signals from muscles. Two of them are recording electrodes that are placed parallel to the muscle fibres and slightly off the center of the belly of the muscle of interest; one is a reference electrode. It needs to be placed at a location with good electrical contact with the body. A number of reference electrode locations are

preferred in practical applications, depending on the muscles from which the surface EMG signal is recorded. It is generally accepted that reference electrodes can be placed on electrically inactive tissue.

The myoelectrical signals picked up by the two recording electrodes are compared to the ‘signal’ from the reference electrode. The part of the signal that is unique to each recording electrode can pass through the amplifier; the amplifier eliminates the part of signal that is common to both recording electrodes. Because the distances between the two recording electrode sites and the endplate of muscle fibres are different, the time that the action potentials arrive at the position of the electrodes can vary. Hence, the signal arising from the action potentials is unique. However, external electromagnetic noise, such as the 50 or 60 cycle mains interference is identical at the two recording electrodes and will be largely removed by the common mode rejection of the amplifier.

4.3.2 Common Mode Rejection Ratio

Unwanted signals such as noise and artefacts, which is common to both inputs of the differential amplifier, is described as a *common-mode signal* and defined formally as:

$$V_{in_comm} \equiv \frac{(V_{in} + V'_{in})}{2} \quad 4.1$$

The bio-potential signal, which is unique to both inputs of the differential amplifier, is called as a *difference-mode input signal*, and is expressed similarly as:

$$V_{in_diff} \equiv \frac{(V_{in} - V'_{in})}{2} \quad 4.2$$

The output of the differential amplifier can be described in terms of V_{in_comm} and V_{in_diff}

$$V_{out} = V_{in_diff} \cdot A_{diff} + V_{in_comm} \cdot A_{comm} \quad 4.3$$

Where, A_{comm} is the common mode gain, A_{diff} is difference mode gain. Generally, the value of A_{comm} is very small, an ideal differential amplifier has $A_{comm} \rightarrow 0$. The value of A_{diff} depends on the specification of the amplifier.

The *common mode rejection ratio* (CMRR) is used to describe the common mode rejection ability of the differential amplifier (*Northrop, R B, 2003*). It is defined by the equation 4.4, usually given in dB,

$$CMRR(dB) \equiv 20 \log_{10} \left(\frac{A_{diff}}{A_{comm}} \right) \quad 4.4$$

The CMRR is a function of frequency. It has a large value at low frequencies and decreases steadily at high frequencies. A typical value is from 90 dB to 140 dB. As a rule, the higher the CMRR, the better the differential amplifier.

4.3.3 Input Impedance

Not only the body tissue, but also the condition of the interface between the sensing electrode and the skin can affect the energy of the signal. The impedance of the skin may vary as the different skin conditions, such as the moisture of the skin, the superficial skin oil content, and the density of the horny, dead cell layer. In the recording of surface EMG, it is important to maintain the impedance of the skin at the electrode site as low as possible and to balance the value of impedance for two recording electrodes. Too

high or too unbalanced a value of skin impedance can cause the common mode rejection of the surface EMG amplifier to be adversely affected.

The maximum ratio (to input impedance) of skin impedance that is allowed in clinical research depends on the input impedance of the surface EMG instrument. In general, the principle of prescribing the maximum ratio of the skin impedance states that the impedance at the interface of electrode and skin should be 10 to 100 times less than the input impedance of the amplifier situated in the surface EMG instrument (*Cram, J R, Kasman, G S, and Holtz, J, 1998*). For instance, if an amplifier has an input impedance of 10 million ohms, the impedance at the interface of skin and electrode should not go beyond 100,000 ohms. As a result, the greater input impedance of the amplifier can provide a higher quality surface EMG signal and overcome to some extent a poor electrode skin connection.

In addition, the amplifier is sensitive to any imbalance impedance between the two electrode sites. The amplifier generally endures up to 20% discrepancy in the impedance between the two electrode sites (*Cram, J R, Kasman, G S, and Holtz, J, 1998*). Discrepancy can occur when one of electrodes loses a good attachment or is placed on an unclean, hairy area of the skin. To avoid these differences between two sites, suitable skin preparation such as cleaning by use of a swab, and shaving hair on the electrode sites needs to be carried out before attaching the electrodes, and researchers should prevent the electrodes from loosening by using the tape to fix the electrode leads during a dynamic evaluation or during treatment sessions.

4.3.4 Specification of the Differential Amplifier

A typical specification (*Brown, B H, 1999*) of the differential amplifier is listed in Table 4-1.

Table 4-1: A typical specification of a differential amplifier for EMG recording.

PARAMETERS	VALUE
Amplification	100
Input impedance	10 M Ω
Common mode rejection ratio	80 dB
Bandwidth	10 Hz – 10 KHz

4.4 Noises and Artefacts

Noise and artefacts are defined as any signals contained in the surface EMG recording that do not represent muscle activity and function. Sources of noise and artefacts for EMG are the ECG (Electrocardiogram), movement, 50 Hz (or 60 Hz) noise, and cross-talk.

A common source of noise is the ECG signal. The amplitude of the ECG signal is much larger than that of the EMG. The ECG signal is clearly shown in the surface EMG tracing when the electrodes are positioned over the muscle groups on the left side of the body, especially near to the heart.

Another major source of noise is movement artefact, which is a direct current shift in the raw surface EMG recording. This happens when the electrodes slips around on the skin during movement. Using a floating electrode instead of a direct contact electrode might reduce this artefact.

Furthermore, a potential source of noise in the recording environment is 50 Hz (or 60 Hz) energy, which arises from the mains power supply through lights and computers. It might also result from poor electrode connection, or may occur when the impedance between the electrode and the skin is too high or unbalanced.

In addition, a possible source of biological artefact is cross-talk. A cross-talk phenomenon occurs when the signal produced by a distant muscle group reaches the electrodes placed over the belly of the target muscle.

To summarize, noise and artefacts are unwanted signals in the surface EMG recording. Many methods such as suitable skin preparation, accurate electrode placement and signal filtering are usually used in order to minimize and eliminate the potential noise components.

4.5 Filtering

Once the surface EMG signal has been magnified by the differential amplifier, it has to be processed by special filters. Most surface EMG instruments contain a notch filter and a band-pass filter. These filters can be implemented both in the electronic circuitry of the equipment and in software.

A 50 Hz (or 60 Hz) notch filter, (i.e. a band-reject filter) with a very narrow band width such as 49 to 51 Hz (or 59 to 61 Hz) and a very steep cut-off slope is used to reject the electrical noise that is between 49 and 51 Hz (or between 59 and 61 Hz).

After the notch filter, a band-pass filter is usually applied to the signal to further attenuate high frequency components and movement artefacts. For general applications of the surface EMG, a typical filter bandwidth is between 10 Hz and 500 Hz (*Hermens, H J et al., 1999a*). The surface EMG usually presents slow variations due to movement artefacts and instability of the electrode-skin attachment and these components tend to lie in the frequency range 0 - 10 Hz, and hence are largely eliminated by the lower

cut-off frequency (3 dB attenuation) of 10 Hz. The upper cut-off frequency (3 dB attenuation) is used to remove the high frequency components in order to reduce the aliasing phenomenon. It is usually near 500 Hz while the sampling frequency is 1000 Hz or higher. During special cases where the high frequency components are of interest, the upper cut-off frequency is 1000 Hz, associated to a sampling frequency higher than 2000 Hz. To summarize, the selection of the filter bandwidth is determined to suit the particular experiments. For gait analysis, a filter bandwidth of 10-500 Hz is appropriate.

4.6 Summary

In this chapter, the types and properties of surface EMG electrodes have been examined. The surface electrode placement in the study of the gait was covered. Section 4.3 discussed the structure of the differential amplifier including the two important parameters, common mode rejection ratio and input impedance. Notch and band-pass filters introduced in Section 4.5 are used to reduce noise and eliminate high frequency components to prevent aliasing. Unwanted signals, noise and artefacts, were described in Section 4.4.

Chapter 5 Surface EMG Signal Processing Methods

5.1 Overview

This chapter describes the properties and parameters of the surface EMG signal. Three main applications of the surface EMG signal processing: estimation of relative intensity, estimation of muscle activation intervals, and estimation of muscle function, are set forth in Section 5.2. The basic steps of the surface EMG signal processing, sampling theorem and analog-to-digital conversion are discussed in Section 5.3. Methods and algorithms of surface EMG signal quantification and normalization are reviewed in detail. Spectral analysis of the surface EMG signal and fast Fourier transform (FFT) are described in Section 5.6.

5.2 Surface EMG Signal Interpretation

5.2.1 Relative Intensity of Muscle Activity

The assessment of the relative intensity of the muscle activity is one of basic applications of the surface EMG signal interpretation. Difference in the relative intensity of muscle activation represents varying levels of muscle developed force. In general, the relative intensity can be estimated by the analysis of parameters such as, amplitude of the signal, peak-to-peak value, and frequency components contained within the signal. For instance, as more muscle strength is required, the firing rates of the motor units could be increased and additional motor units might be recruited. Visually, the surface EMG tracing becomes denser and of larger amplitude. As a result, the differences in the amplitude of the surface EMG signal may illustrate the relative intensity of muscle activity.

5.2.2 Muscle Activation Intervals

Muscle activation intervals, referring to onset and cessation timing of muscle activation, are important factors in the surface EMG signal processing. The evaluation of the timing of muscle activity is widely used in various projects and may assist researchers to examine muscle function. However, there is no standard approach to estimate this parameter (*Hodges, P W and Bui, B H, 1996*). Many methods and algorithms have been proposed in the literature, and their performances vary considerably. The accurate definitions of muscle activation intervals and a variety of signal processing algorithms to extract timing parameters from the raw surface EMG signal are addressed in detail in Chapter 8 of this thesis.

5.2.3 Muscle Function: Muscle Fatigue

The effects of muscle fatigue can be examined by analysing the surface EMG signal. The conduction velocities of the action potentials along the muscle fibres commence slowing down and the muscle starts discharging less frequently when the contraction of a muscle produces enough force for a long enough period of time.

Two basic methods have been used in clinical applications to examine muscle fatigue. One is based upon power spectral approaches. The surface EMG frequency shifts in the power spectrum may provide valuable information for the analysis of the muscle fatigue. It can be used to distinguish between normal muscle and impaired muscle function. The other is the interference pattern analysis approach (*Gabriel, D, Basford, J R, and An, K N, 2001*). The influence of the muscle fatigue can be shown by counting frequencies in the surface EMG.

5.3 Sampling and A/D Conversion

In order to process the surface EMG signal, the signal has to be transformed from an analogue signal to a digital form. *Sampling and Analog-to-digital conversion* (A/D Conversion) need to be used.

The Nyquist Sampling theory (*Baher, H, 1990*) states that an analogue signal can be uniquely reconstructed, without error, from samples taken at equal time intervals when the sampling frequency is at least twice the highest frequency component in the analogue signal. Information (higher frequency's signal) is distorted if the signal contains frequencies higher than half the sampling frequency. Because the frequency contents of the surface EMG signal usually varies from 10 Hz to 500 Hz, the sampling frequency

for the signal must be greater than 1000 Hz. The sampling frequency is usually selected as 1000 Hz, 1500 Hz, or 2000 Hz (better).

After sampling the signal, the amplitude of the signal needs to be processed quantitatively. The quantification of the signal relies on the amplifier gain, the A/D input range and resolution, which cannot be chosen independently. Determined by the desired resolution and the maximal peak-to-peak amplitude of the signal, the number of levels required for the A/D conversion is then calculated. For example, in case of a resolution of 10 μV and 100 mV peak-to-peak amplitude, 14 bits A/D conversion is satisfactory.

5.4 Surface EMG Quantification

The raw surface EMG signal has both positive and negative amplitude values. In order to prevent the positive and negative values cancelling each other when averaging, several signal processing methods such as rectification, integral average, and root mean square are used in surface EMG signal quantification.

5.4.1 Surface EMG Quantification during Non-dynamic Contractions

During non-dynamic contractions, the most commonly used methods to quantify the amplitude of the surface EMG signal are the *Average Rectified (AR)* and the *Root Mean Square (RMS)*. Both methods carry information about the amplitude of the signal and can be applied in the continuous and the discrete time domain (*Hermens, H J et al., 1999a*).

The average rectified calculates the arithmetic mean of the rectified surface EMG signal over a given period of time. The values of the rectified signal

are summated over the period of time required and then divided by the number of values involved in this time. The rectified signal can be obtained by converting all negative amplitude values of the signal into positive values. This method offers information about the area under the signal over the period of time and can be defined by the following equation (Discrete time domain):

$$AR = \frac{\sum_{i=1}^n |x_i|}{N} \quad 5.1$$

The root mean square method is used more generally than the average rectified method and represents the signal by a series of steps, squaring the value, summing the squares, dividing this sum by the number of samples and then taking the square root. It provides information about the mean power of the signal over the period of time and can be expressed by the following equation (Discrete time domain):

$$RMS = \sqrt{\frac{\sum_{i=1}^n x_i^2}{N}} \quad 5.2$$

5.4.2 Surface EMG Quantification during Dynamic Contractions

During dynamic contractions, a number of methods are available for the estimation of the amplitude such as ensemble averaging, which is widely used in signal quantification.

The *Ensemble averaging* is frequently applied to the studies of movement analysis, especially during the gait cycle, to further decrease the amount of estimation uncertainty of the surface EMG signal profiles. By averaging

surface EMG ensembles, the signal of a number of individual cycles N can be normalised with respect to time and amplitude, and averaged as a function of time. The ensemble averaging is shown in Figure 5-1.

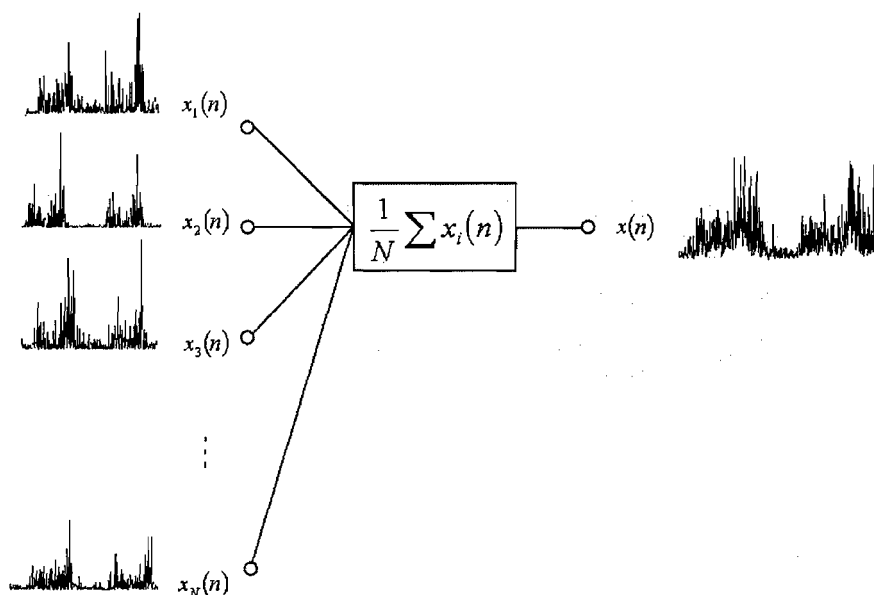


Figure 5-1 The ensemble averaging method in the surface EMG quantification during dynamic contractions.

N is the number of cycles being averaged.

5.5 Surface EMG Normalization

The basic need for normalization is to accommodate the individual variation in many factors that include the number and mixture of motor units, muscle resting length, velocity of muscle contraction, muscle mass, age, sex, subtle change in posture, inter-electrode distance and impedance of skin. As a result, it is impossible to compare the surface EMG signal both within and between individuals directly. Normalization is the essential step before processing and comparing the signal.

There are several methods to normalization, each of which has a reference value of amplitude and calculates all of the other activity as a percentage this reference. The most common method uses the *Maximum Voluntary Contraction (MVC)* as the reference value. For this method, patients may be required to make approximately maximum voluntary contraction for the muscle group of interest. All surface EMG signals are then represented as a percentage of the MVC to indicate the muscle activity. Therefore, the comparison of muscle function within and between individuals becomes possible and understandable. Unfortunately, because the method relies upon a voluntary component of the subject or patient, the examiner is not always sure that the subject has given his or her maximal effort.

To solve this limitation of the MVC method, some approaches that use a reference voluntary contraction rather than the MVC as a baseline have been introduced (*Knutson, L M et al., 1994; Yang, J F and Winter, D A, 1984*). In a dynamic movement such as walking, the peak value of the contraction is described as an anchor (i.e. the baseline). The anchor can be obtained by averaging peak values of muscle contraction during several gait cycles. It is impossible to select one normalization approach for all cases. The best normalization method might be chosen on the basis of the requirement of the task and other conditions in the recording environment.

5.6 Surface EMG Spectral Analysis

The surface EMG signal does not only provide information with respect to its amplitude behaviour, but also contains relevant information in the frequency content. The motor unit firing rate might be reflected in the low frequency range (8-500 Hz) of a power spectral density. The motor unit action potential in terms of its shape and duration could be presented by the

shape of the power spectrum and relevant parameters such as mean or median frequency.

5.6.1 Fast Fourier Transform (FFT)

In general, the *Fourier Transform* is used to decompose a signal into its frequency components. For sampled vector data, the Fourier transform is performed by using the *Discrete Fourier Transform (DFT)*. The *Fast Fourier Transform (FFT)* (Baher, H, 1990; Proakis, J G, 1992) is an efficient algorithm for computing the DFT of a signal that is normally in vector or matrix form. It is particularly applied to fields such as filtering, convolution, frequency analysis and power spectrum estimation. The transform is defined by the following expressions:

$$F(k+1) = \sum_{n=0}^{N-1} f(n+1)W_n^{kn} \quad 5.3$$

$$W_n = e^{-j(2\pi/N)} \quad 5.4$$

Where, $N = \text{length}(f(n))$, is the length of the signal $f(n)$ in the time domain. $F(k)$ represents the signal in frequency domain.

5.6.2 Spectral Estimation of Surface EMG

The main methods to interpret the surface EMG signal in the frequency domain are the Power Spectral Density (PSD) as well as the estimation of Mean or Median Frequency. The power spectral density is derived on the basis of the Fourier transform and is used to describe the distribution (over frequency) of the power contained in a signal.

The power spectrum ($S_{xx}(\omega)$) of a random process (x_n) is mathematically related to the correlation sequence by the discrete Fourier transform. It is defined as:

$$S_{xx}(\omega) = \sum_{m=-\infty}^{\infty} R_{xx}(m) e^{-j\omega m} \quad 5.5$$

or

$$S_{xx}(f) = \sum_{m=-\infty}^{\infty} R_{xx}(m) e^{-2\pi j f m / f_s} \quad 5.6$$

$$\omega = 2\pi f / f_s \quad 5.7$$

Where, f_s is the sampling frequency, $R_{xx}(m)$ is the autocorrelation of a random process (x_n).

The PSD is defined by the following expressions:

$$P_{xx}(\omega) = \frac{S_{xx}(\omega)}{2\pi} \quad 5.8$$

or

$$P_{xx}(f) = \frac{S_{xx}(f)}{f_s} \quad 5.9$$

The average power of a signal over a particular frequency band $[\omega_1, \omega_2]$, $0 \leq \omega_1 < \omega_2 \leq \pi$, can be calculated by integrating the PSD over the band. It is given by the expression:

$$P[\omega_1, \omega_2] = \int_{\omega_1}^{\omega_2} P_{xx}(\omega) d\omega + \int_{-\omega_2}^{-\omega_1} P_{xx}(\omega) d\omega \quad 5.10$$

The parameter $P_{xx}(\omega)$ represents the power content of a signal in an infinitesimally small frequency band. The units of the PSD are power (watts) per unit of frequency (Hertz).

For real signals, the PSD is symmetric, and thus $P_{xx}(\omega)$ for $0 \leq \omega < \pi$ is satisfactory to characterize the PSD. The concept of the one-sided PSD is introduced in order to calculate the average power over the entire Nyquist interval. As a result, the average power of a signal over the frequency band $[\omega_1, \omega_2]$, $0 \leq \omega_1 < \omega_2 \leq \pi$, can be calculated by using the one-sided PSD, and expressed by the following equation:

$$P[\omega_1, \omega_2] = \int_{\omega_1}^{\omega_2} 2 \cdot P_{xx}(\omega) d\omega \quad 5.11$$

5.7 Summary

In this chapter, the basic definitions and concepts of the surface EMG signal processing methods have been examined. The surface EMG signal interpretations such as relative intensity of muscle activity, muscle activation intervals, and muscle fatigue were covered in Section 5.2. The methods used to estimate the muscle activation intervals will be discussed in Chapter 8. The first step of the signal processing, sampling and A/D conversion was introduced. Section 5.4 has described common methods of the surface EMG signal quantification during non-dynamic and dynamic contractions respectively. Normalization methods by using various anchors, such as maximum voluntary contraction, reference voluntary contraction, and averaging peak value, have been examined. The surface EMG quantification

and normalization are necessary steps during the signal pre-processing, which is applied and completed before any further signal processing methods that are used in the following chapters of this thesis. Providing relevant information with respect to the frequency content, such as the motor unit firing rate, the main spectral estimation algorithms including the power spectrum and the power spectral density were presented in Section 5.6. One of spectrum estimation methods, the power spectral density, will be used to assess the simulation model presented in Chapter 7 by the calculation and comparison of the PSD of both simulated and real surface EMG signals.

Chapter 6 Surface EMG Collection during Dynamic Movement

6.1 Overview

In this chapter, a gait experiment used to investigate the muscle activity during dynamic movement is presented. During the gait experiment, three main signals, surface EMG, foot switches, and body movement, were measured by using the Noraxon EMG & Sensor System (Telemetry 2400T), Noraxon Multi-Mode Foot Switch Sensor (Multimode Footswitch) and Vicon Motion Analysis System (Vicon Peak's System). The data, the surface EMG signals and foot switches, recorded from the experiment are used to demonstrate the validity of the simulated surface EMG signals produced by the simulation model and to assess the potential of the novel algorithm to detect muscle activation intervals. The body movement data has not been analysed thoroughly for this thesis but will be investigated further in future studies.

The experimental design, setting and measurement are described in this chapter. Section 6.2 introduces the ethics application, which is a first and essential step prior to undertaking the experiment. Participants' recruitment is detailed in Section 6.3. Measurement such as sensors, acquisition system, software, and signal pre-processing methods are examined in Section 6.4. Section 6.5 discusses the management of the experiment in more detail, for example, pilot work, project schedule, data collection timetable, and methods used to prevent the provocation of discomfort or distress in participants. In addition, the items such as data protection are also shown in this chapter.

6.2 Ethics Approvals

All experiments involving human subjects require an approval of appropriate Ethics Committees. Two ethics approvals were obtained from the Human Experimentation Safety and Ethics Committee of the Institute of Sound and Vibration Research (ISVR), University of Southampton, and from the Ethics Committee of the School of Health Professions and Rehabilitation Sciences (SoHPRS), University of Southampton.

All materials included in the ethics application and the gait experiment, for example, Participant Information Sheet, Participant Consent Forms, and copies of the Ethics Approvals granted by the two ethics committees are shown in Appendices IV and V.

6.3 Participants Recruitment

6.3.1 Sample Size and Recruitment

The total number of healthy subjects required for this research was twenty (20). It took 90 minutes to accomplish a trial for each subject, and hence twenty was considered sufficient to demonstrate principles and to be practical within the project timescale.

University students and staff were recruited for convenience and availability. Participants taking part in this research were entirely voluntary. The participants were recruited by the use of a recruitment poster. The contact details of researchers, such as email address and telephone number, were shown in the poster. The participants who responded were contacted by the author who was able to explain the project thoroughly and provide information sheets and a reply slip by email. Appointments were made for those participants who were interested in taking part in the research, and who met the requirement that they had no history of leg, ankle, or foot injury affecting normal walking and were aged between 18 and 65 years old.

All information that was collected about participants during the course of the research was kept strictly confidential. Any information about the participants that may be used in the research reports or publications will have the name and address of the participants removed so that the participants cannot be recognised.

6.3.2 Setting

The study took place in the Biomechanics Laboratory at the School of Health Professions & Rehabilitation Sciences, University of Southampton. Three main signals were recorded from healthy subjects during normal

walking. Using the Noraxon EMG & Sensor System, surface EMG signals were collected from three muscles of the lower limb: tibialis anterior, gastrocnemius medialis and gastrocnemius lateral. Foot switches indicate the heel-down and toe-off events and were recorded using the Noraxon Multi-Mode Foot Switch Sensor. In addition, lower limb movements were captured by an array of video cameras of the Vicon Motion Analysis System. This movement data was visualized but not analysed in parallel with the surface EMG data; that will form the basis of a future study.

6.4 Measurement and Instrumentation

6.4.1 Participants Information

The participants who were interested in taking part in the research were contacted by the author who was able to answer any questions the participant might have and arranged a visit to the Biomechanics Laboratory if the participants so wished.

On arrival at the Biomechanics Laboratory the participant was shown the equipment used in the experiment and given all information about the procedure of the test. If the participant was happy to continue, he/she was required to sign a consent form. The participant was still free to withdraw at any time, and without giving a reason, even though he/she had signed the consent form. The participant was asked to wear shorts in order to attach surface electrodes and reflective markers easily.

After the preparation of the skin, the surface EMG electrodes, reflective markers, and foot pressure sensors were attached and all sensors were connected to the recording instruments. The participant was asked to walk normally as usual on a treadmill while the author recorded the surface EMG,

foot pressure signals, and the body movements. The participant was allowed to have a rest and the test could be stopped at any time if participant became tired. Three segments of data were recorded for each participant under the same conditions. The length of each data segment was 10 seconds. The total amount of time for the test including the preparation and data recording was between 60 and 90 minutes.

6.4.2 Signal Measurement

Three main signals, the surface EMG, foot contact, and lower limb movement, were recorded for this study. The configuration of the instruments and measurement environment are displayed in Figure 6-1. The surface EMG signals were collected from three muscles, tibialis anterior, gastrocnemius medialis, and gastrocnemius lateral, by using the Noraxon EMG & Sensor System. The Noraxon System provides a set of surface EMG products containing data analysis and acquisition software and an elaborate 32-channel telemetry system. A configuration for this experiment includes an eight-channel telemetric EMG system combined with a portable laptop hosting the MyoResearch XP software that has specific automated features.

In order to obtain a good electrode-skin contact, proper skin preparation, such as shaving hair, cleaning with alcohol swab and abrading with sand paper may be necessary. After skin preparation, the participant was positioned in the recommended starting posture. The locations of the surface EMG electrode were marked on the skin of the participant. Then, Noraxon dual-electrodes were attached on the marked placement of the target muscles. The surface EMG signals were recorded by the use of three channels of Noraxon transmitter.

Foot contact data was collected by using the Noraxon Multi-mode Foot Switch System. The pressure sensors were placed under the big toe and the heel of the participant, and the heel-down and toe-off signals were measured when the participant walks on the treadmill. The lower limb movement was captured by the Vicon Motion Analysis System, a three-dimensional optical motion capture device. Reflective markers were placed at specific and easily identified anatomical locations on the leg, i.e. thigh, knee, ankle, heel and toe. The 3-D movement of the reflective markers was recorded by an array of high-resolution cameras.

SURFACE EMG COLLECTION DURING DYNAMIC MOVEMENT

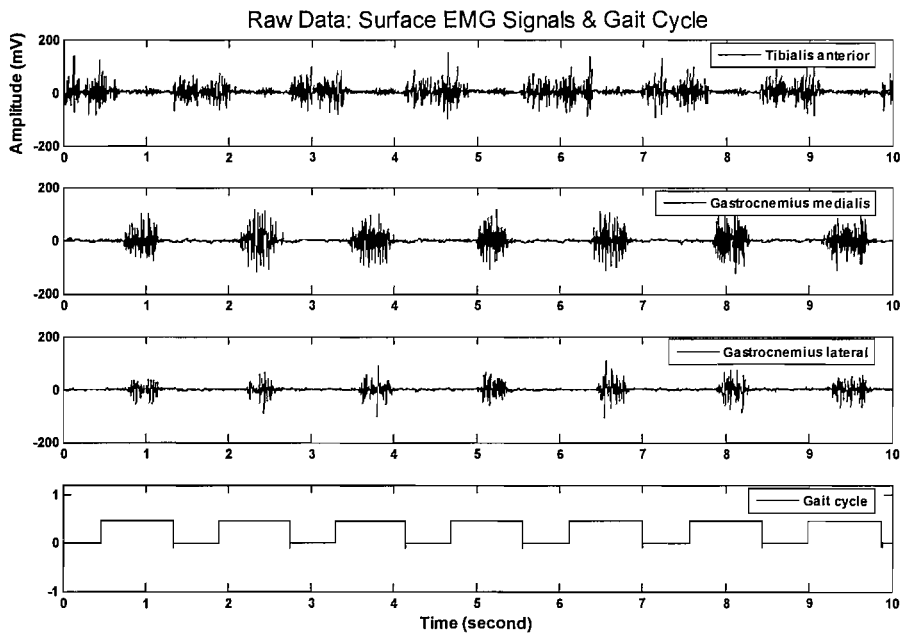


(a)

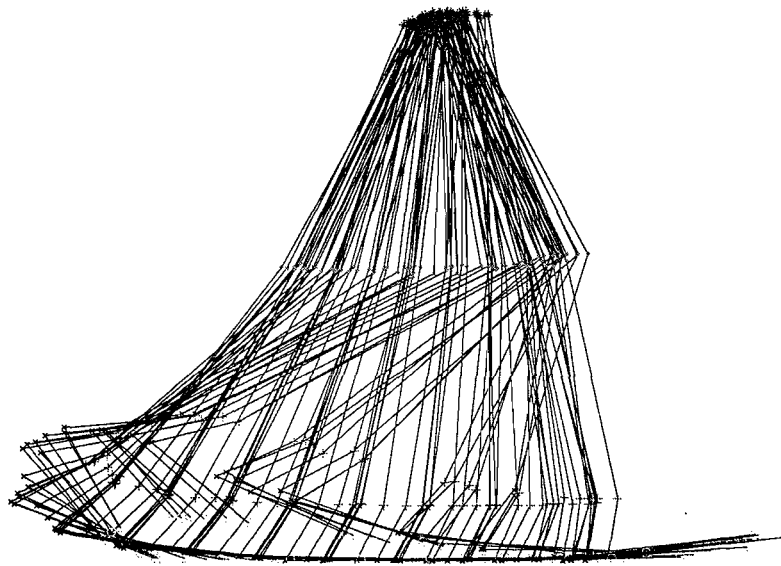


(b)

SURFACE EMG COLLECTION DURING DYNAMIC MOVEMENT



(c)



(d)

Figure 6-1 The experimental setup and data recorded.

(a) The configuration of instruments and measurement environment. Instruments include the Noraxon EMG & Sensor System, the Noraxon Multi-Mode Foot Switch System, the BioDex Rehabilitation Treadmill and the Vicon Motion Analysis System.

(b) The signal recording conducted in the laboratory.

(c) A sample of the recording of the surface EMG signals from three muscles, tibialis anterior, gastrocnemius medialis, and gastrocnemius lateral, and the recording of the foot switches.

(d) The recording of the lower limb movement during walking displayed by the Vicon Motion Analysis System. The reflective markers on the hip, knee, ankle, heel and toe are displayed by the symbol * . + x o, respectively.

6.4.3 Instrumentation

Instruments used in the experiment and their accessories are shown in Figures 6-2, 6-3 and 6-4.

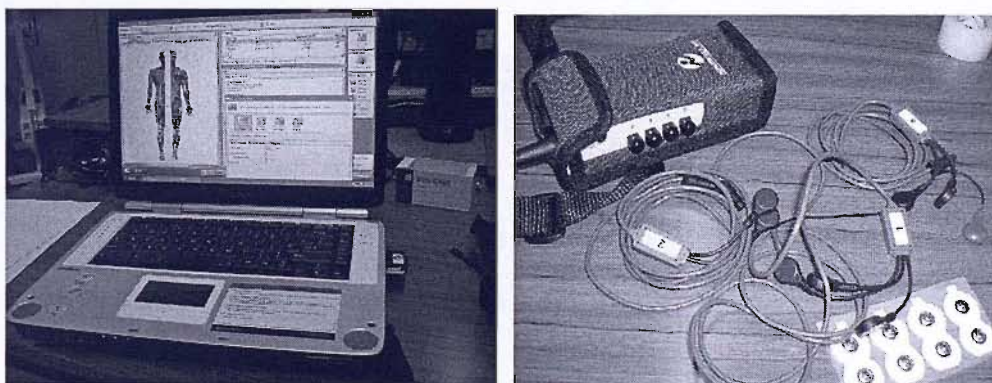


Figure 6-2 The Noraxon EMG & Sensor System and its accessories.

Eight-channel telemetric system consists of a transmitter accommodating eight channels of any combination of the surface EMG and a variety of analogue signals, and eight active electrode leads using a Noraxon's patented signal processing technology to provide consistent and reliable data. Data acquisition, analysis, and reporting can be efficiently executed by the MyoResearch XP software. The software has ability to generate ASCII file from the raw surface EMG data, hence, the signal can be exported to mathematical or statistical software, such as MATLAB, EXCEL, for further analysis.



Figure 6-3 The Noraxon Multi-Mode Foot Switch System

The Noraxon Multi-Mode Foot Switch System. Depicting the gait cycle, the heel-down and toe-off signals are measured by the Noraxon Multi-Mode Foot Switch System. It is easy to connect the Foot Switch System with the transmitter of the Noraxon EMG & Sensor System. As a result, the surface EMG signals recorded from three muscles and foot switches collected from the pressure sensors attaching to heel and toe can be displayed synchronously on the screen of the laptop by the connection of five channels of the transmitter.



Figure 6-4 The Vicon Motion Analysis System and the BioDex Rehabilitation Treadmill.

(a) The lower limbs movement during walking can be recorded by the Vicon Motion System, a three-dimensional optical motion capture device. It is designed to capture the 3D movement of specialised reflective markers by an array of video cameras. A typical configuration of the Vicon Motion System comprises a number of high-resolution cameras, a number of reflective markers attached to a subject in well-defined positions, a data station controlling the cameras and sending data to the workstation computer, and particular software such as Polygon. For this experiment, in order to capture the lower limbs movement, markers

should be placed at specific and easily identified anatomical locations on the legs, for example, thigh, knee, ankle, heel, and toe.

(b) The BioDex Rehabilitation Treadmill. The treadmill is considered as a trial platform in order to achieve a desired length data. It is easy to set up different lengths of data.

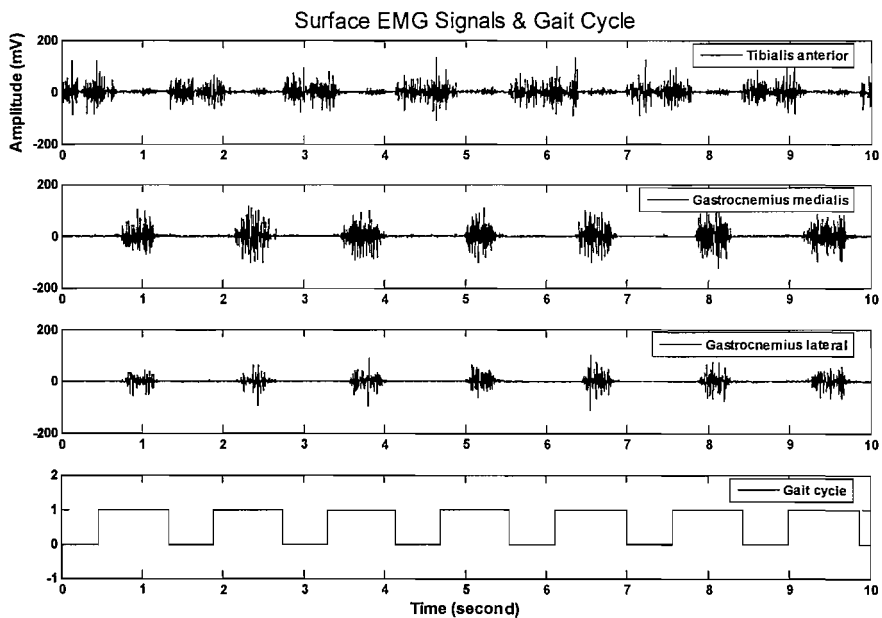
6.5 Management of the Experiment

Pilot work was completed before the main study. The author asked two or three colleagues to attend the pilot work and collected the surface EMG signal, the movement signal and the foot contact from them, in order to become familiar with the equipment and methods used for collecting and analysing the data. The procedure of the test and the method used for processing the data was then clarified and finalised. The full experiment started at 06 June 2005. Twenty volunteers attended this study, eight females and twelve males. Data collection time per participant was 90 minutes. Hence, the total data collection time was approximately 30 hours. In order to prevent discomfort, such as fatigue or distress in participants, they were allowed to rest between tests if they became fatigued. Moreover, the trial could be stopped at any time if the participants asked. The data recorded from the trials are held at the University of Southampton in the line with the policy for postgraduate study.

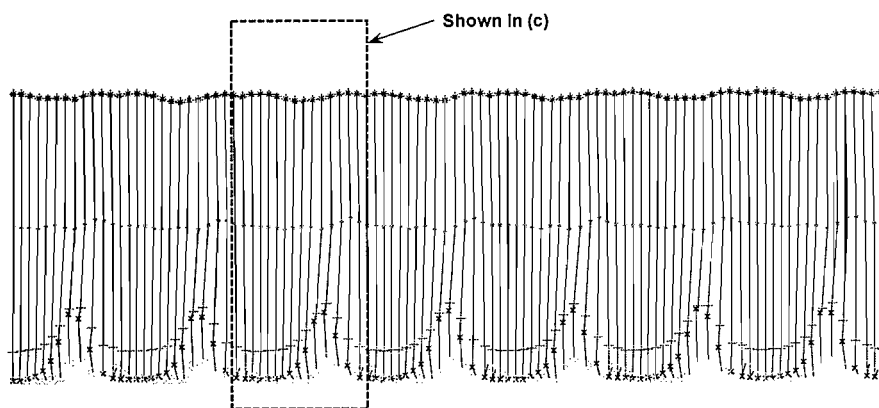
6.6 Results Analysis

The default sampling frequency of the MyoResearch XP software built into the Noraxon EMG and Sensor System is 1500 Hz or 3000 Hz. The raw surface EMG signals and foot switches can be exported as ASCII files by the software. Hence, it is easy to export the raw data to mathematical or statistical software, such as MATLAB or EXCEL, for further analysis. The data recorded from the experiment were stored as ASCII files and displayed

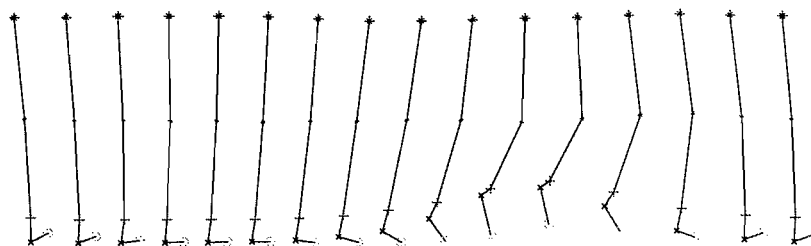
in the EXCEL. The surface EMG signals, foot switches and body movement data are shown in Figure 6-5. The further signal processing, such as filtering, integrating and spectrum analysis, is completed in next chapters. Both the simulation model originated from Chapter 7 and the algorithm to detect the muscle activation intervals derived from Chapter 8 are generated and examined on the basis of these data recorded from the gait experiment. At this stage, the surface EMG signals and foot switches are used to assess the feasibility of the model as well as to prove the validity of the algorithm. The body movement data recorded by the Vicon Motion System has not been processed, but was used for visualising the gait cycle patterns and for cross-checking signal timings. The analysis of the body movement data will be the main part of the future work.



(a)



(b)



(c)

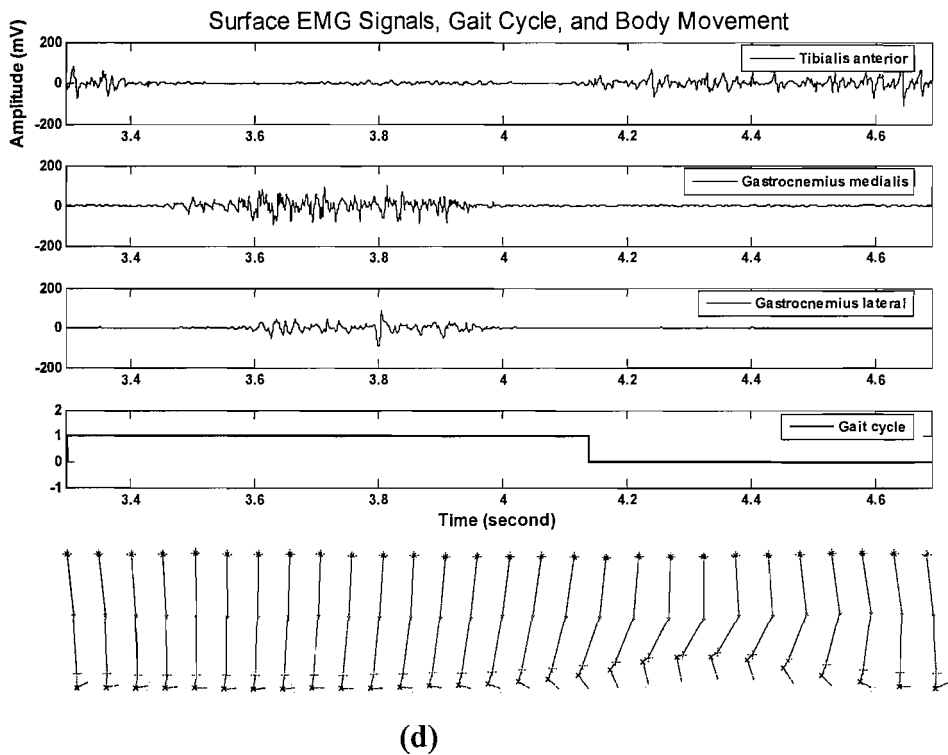


Figure 6-5 The processed surface EMG signals, gait cycle, and body movement.

(a) The surface EMG signals and foot switches. The length of data is 10 seconds. In this case, a bandpass filter (8 -500 Hz) is used to reduce the movement artefacts and high frequency components of the surface EMG signals; the appropriate signal processing methods are used to eliminate the noise contained in the foot switches in order to obtain the smooth foot switches.

(b) A series of the recording of the lower limb movement during the gait cycle.

*(c) A sample of the recording of the lower limb movement during walking. The reflective markers on the hip, knee, ankle, heel and toe are displayed by the symbol * . + x o, respectively.*

(d) The surface EMG signals and the lower limb movement during one gait cycle.

6.7 Summary

The gait experiment has been addressed in this chapter. All information of the gait experiment, for example, the ethics approvals, participants

recruitment, instrument setting and data measurement, have been described. The three main signals, the surface EMG signal, foot switch signals and body movement data have been recorded in the experiment. The surface EMG signal and foot switch data, are used to assess the simulation model in Chapter 7 and to examine the algorithm to detect the muscle activity in Chapter 8. The body movement will be processed in future studies.

Chapter 7 Surface EMG Simulation Modelling

7.1 Overview

The purpose of this chapter is to produce a simulation model of the surface EMG signal for the analysis of muscle activity during the gait cycle. A multiple-layer structure of the model is shown. The method to generate the surface EMG signal from the model is chiefly described at the beginning of this chapter. Section 7.5 and Section 7.6 present the detailed algorithms to simulate the single fibre action potential, motor unit action potential, and voluntary contraction respectively. The surface EMG simulation during the gait cycle is described as well. In addition, simulation results including the single fibre action potential, motor unit action potential, surface EMG during voluntary contraction and surface EMG during the gait cycle are displayed

in Section 7.8. Comparison between the simulated signals and real signals recorded from gait experiment is discussed in Section 7.9.

7.2 Surface EMG Simulation Models: Properties and Applications

New methods or algorithms for processing the surface EMG signal need to be assessed by comparing actual and known values of parameters with the values obtained using the new method; hence, it is necessary to create a simulation model that produces the surface EMG signal containing known values of key parameters. In this study, in order to explore the muscle activity during walking, a simulation model of the surface EMG signal during the gait cycle is essential and valuable tool to examine novel signal processing techniques.

A wide range of models has been presented over recent decades by many research groups (*Dimitrov, G V and Dimitrova, N A, 1998; Duchene, J and Hogrel, J Y, 2000; Farina, D et al., 2004; Farina, D and Merletti, R, 2001; Helal, J N and Bouissou, P, 1992; Lowery, M M et al., 2002; Merletti, R et al., 1999a; Merletti, R et al., 1999b; Nandedkar, S D and Stalberg, E, 1983; Nandedkar, S D, Stalberg, E V, and Sanders, D B, 1985; Roeleveld, K et al., 1997; Stashuk, D W, 1993; Stegeman, D F et al., 2000*). Some of the models aimed to simulate the single fibre action potential (*Nandedkar, S D and Stalberg, E, 1983*), or voluntary and elicited muscle contractions (*Duchene, J and Hogrel, J Y, 2000; Merletti, R et al., 1999a; Merletti, R et al., 1999b; Nandedkar, S D and Stalberg, E, 1983*). The characteristics of the surface EMG signal detected by the electrodes depend on anatomical, physiological and experimental system parameters. Other simulation models (*Farina, D et al., 2004; Farina, D and Merletti, R, 2001; Roeleveld, K et al., 1997*) are used to test the influence of various parameters such as on the surface EMG

signals, together with a description of the effect of an anisotropic homogeneous medium, interpretation of the influence of internal bone (Lowery, M M *et al.*, 2002), and illustration of the effect of the detection system (Stegeman, D F *et al.*, 2000), for example, the influence of the electrode shape and size (Dimitrov, G V and Dimitrova, N A, 1998; Helal, J N and Bouissou, P, 1992).

Despite the large number of works on the subject of surface EMG simulation, few researchers have attempted to explore the relationship between the surface EMG and the phases of the gait cycle, and to model the surface EMG signal based upon those different phases. In this study, we describe a novel method to produce a model of the surface EMG signal during the gait cycle, which contains the characteristics of the surface EMG, such as the fibre distribution, motor unit type, location and recruitment, tissue anisotropy, electrode configuration and phases of the gait cycle.

7.3 A Multiple-layer Model of Surface EMG

To simulate the surface EMG signal during the gait cycle, the first task is to choose several muscle groups as targets in the model. The surface EMG signal might be very different on the basis of various muscle groups, because different muscles contains different compositions of motor units that are composed of different sizes and numbers of muscle fibres. In the model, values of parameters that represent the above characteristics can be changed to describe different muscles. Because the tibialis anterior and gastrocnemius muscle groups in the lower limb have an important responsibility to maintain the body balance and support the movement in walking, they are selected as target muscles for the model. Most of the recent models for limb muscles (Roeleveld, K *et al.*, 1997) are described as a

cylindrical volume conductor composed of anisotropic media which are representative of skin, fat and muscle tissue. The multiple-layer structure is shown in Figure 7-1.

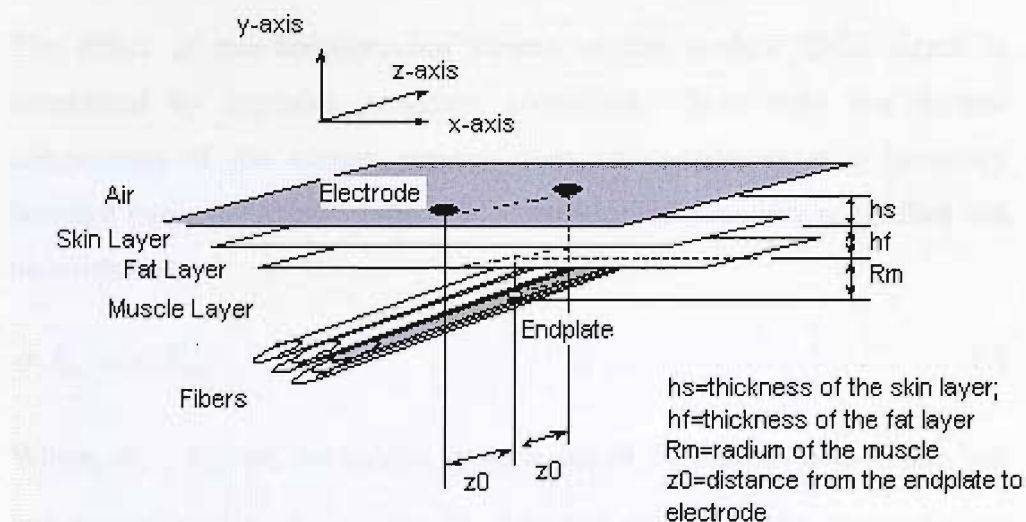


Figure 7-1 The multiple-layer model comprising muscle, fat and skin layers.

In this simulation model, z-axis is the axial direction (the direction of the muscle fibres); the centre of the muscle is assumed as the zero point of the coordinate system (coordinate (0,0,0)).

7.4 Method to Generate the Surface EMG Signal from the Model

The model is based on the single fibre action potential generation, which depends on the fibre conduction velocity. The motor unit action potential is then estimated by summation of all fibre activities assuming that they have a uniformly parallel distribution in each motor unit. The surface EMG of muscle voluntary contraction is calculated by grouping the motor unit action potentials on the basis of their different sizes, positions, recruitment periods and sequences. The surface EMG during a gait cycle is simulated by fixing

the values of motor unit action potential trains in accordance with features of the gait phases. In addition, the characteristics of the acquisition system, such as location and configuration of the electrodes, sampling frequency and signal to noise ratio (SNR), are also taken into account.

The effect of non-homogeneous tissues on the surface EMG signal is considered by imposing boundary conditions. These state that normal components of the current density must be continuous at a boundary between two conducting media. The expression of boundary conditions can be written as:

$$\sigma_1 E_{n1} = \sigma_2 E_{n2} \tag{7.1}$$

Where, E_{n1} , E_{n2} are the normal components of the electric field in the first and second media; σ_1 , σ_2 are the first and second media conductivities (*Landau, L D and Lifshitz, E M, 1984; Lowery, M M et al., 2002; Ohanian, H C, 1988*).

Let us now analyse the individual elements of the simulation model. Table 7-1 lists the values of the parameters used in this simulation model.

Table 7-1 The parameters of the simulation model.

PARAMETERS	VALUES	COMMENTS	REFERENCE
Muscle axial conductivity	$\sigma_z = 0.328 \text{ S.m}^{-1}$	The conductivity of a structure, especially the ability of a nerve to transmit a wave of excitation.	(Andreassen, S and Rosenfalck, A, 1981)
Muscle radial conductivity	$\sigma_y = 0.063 \text{ S.m}^{-1}$	--	(Andreassen, S and Rosenfalck, A, 1981)
Intracellular conductivity	$\sigma_1 = 1.010 \text{ S.m}^{-1}$	--	(Andreassen, S and Rosenfalck, A, 1981)
Skin conductivity	$\sigma_s = 4.55 \times 10^{-4} \text{ S.m}^{-1}$	--	(Gabriel, C, Gabriel, S, and Corthout, E, 1996)
Fat conductivity	$\sigma_f = 0.0379 \text{ S.m}^{-1}$	--	(Gabriel, C, Gabriel, S, and Corthout, E, 1996)
Conduction velocity	$v = 4 \text{ m.s}^{-1}$	The depolarisation of the muscle fibre produces the action potential, and this change in transmembrane potential, travels along the muscle fibre at a velocity in the range from 1 ms^{-1} to 5 ms^{-1} .	(Cram, J R, Kasman, G S, and Holtz, J, 1998) (Duchene, J and Hogrel, J Y, 2000)
Muscle radius R	Tibialis anterior: $R_t = 20 \text{ mm}$ Gastrocnemius medialis: $R_g = 30 \text{ mm}$	The muscles can be described as a cylindrical volume conductor in the model, the size of muscle is defined by the parameter of muscle radius.	(Perry, J, 1992)
Thickness of fat and skin	$h_{\text{fat}} = 3 \text{ mm}$, $h_{\text{skin}} = 1 \text{ mm}$	The cylindrical volume conductor in the model is composed of anisotropic media that is representative of skin and fat. The thickness of skin and fat that have an influence on the	--

		simulated signal are chosen based upon the health adults.	
Fibre diameter d	Tibialis anterior: dt = 57 μ m Gastrocnemius medialis: dg = 54 μ m	With regard to a given motor unit, the diameters of the muscle fibres have little difference. Such a result, the simulation assumes all fibres contained within a muscle have a constant diameter.	(Perry, J, 1992)
Muscle fibre length	Mean value: LM = 100 mm; Length variation: Gaussian distribution: SD = 1 mm, Mean = 0;	Muscle fibre length might effect the travelling time of the action potential produced at the endplate. It can be considered by two values, mean value and variation.	(McComas, A J, 1996)
Fibre endplate position	At the axial direction: Gaussian distribution: Mean = 0, SD = 1 mm. At the radial direction: Uniform distribution: range within ± 1 motor unit radius	Fibre endplate position has an influence on the distance between the observation point and the location that action potential might be produced and starts to propagate along the fibre. The fibre endplate position at the axial direction is assumed to have a Gaussian distribution and its position at the radial direction is considered as a uniform distribution.	(Duchene, J and Hogrel, J Y, 2000)
Motor unit size - Tibialis anterior - Gastrocnemius medialis	Circle shape, Poisson distribution: range 5-10 mm, ambda = 6 mm; range 5-10 mm, ambda = 8 mm.	Motor unit recruitment territories are imagined as the small, overlapping circles on cross section of muscle. The size of motor unit and the composition of muscle fibres it contained are determined by the function of muscle. The muscles in the lower limb are adapted for weighting bearing, locomotion and maintaining the posture. All of these functions	(Cram, J R, Kasman, G S, and Holtz, J, 1998)

		need much more strength and stability than the requirement of hand muscles. Hence, the motor units situated in the lower limbs have a larger size of cross-sectional area and contain a greater size of muscle fibres.	
Motor unit recruitment sequence	From small size (diameter = 5 mm) to large size (diameter = 10 mm)	When muscle is activated, motor unit recruitment abides by the size principle. The smaller motor units are recruited at the beginning of the muscle contraction occurrence, subsequently, the larger motor units are activated, which play an important role in increasing the amplitude of the surface EMG signal.	--
Motor unit position	Uniform distribution: range within ± 1 muscle radius	In the model, the position of motor unit determines the position of muscle fibre.	--
Motor unit firing rates - Tibialis anterior - Gastrocnemius medialis	Range from 8 Hz to 90 Hz. Steady voluntary contraction: Poisson distribution, range 8-35 Hz, $\lambda = 12$ Hz; Poisson distribution, range 8-40 Hz, $\lambda = 12$ Hz.	Generally, the maximum firing frequency of motor units is generated at the beginning of a maximal contraction, at rates from 70 Hz to 90 Hz. Then, motor units modulate their firing frequency from the very high frequency to steady firing frequency of 8-30 Hz. Because of the effect of mechanical fatigue, the maximum firing frequency continues to decline to 8-15 Hz. In addition, the firing frequency will remain an appropriate value for ensuring a fused contraction.	(Cram, J R, Kasman, G S, and Holtz, J, 1998; McComas, A J, 1996)
Motor unit	Uniform	In voluntary contraction,	--

starting time	distribution: range from 0 to 1/mean firing rate	the activities of motor units are considered as random with no synchronization process and therefore the starting times of motor unit activation are not identical. In the model, the starting time of motor unit activation can be computed by the parameters both mean of firing rate and the number of motor units contained in a given muscle.	
Gait cycle period	Period = 1.03 ± 0.08s	Walking is composed of a repetitious sequence of limb functions both moving the body forward and maintaining body stability. A single sequence of these functions accomplished by one limb is defined a gait cycle.	<i>(Brown, B H, 1999)</i>
Muscle activation timing Tibialis anterior Gastrocnemius medialis	<p>Mean value: on-time = 58%, off-time = 9%, stronger contraction time = 95%;</p> <p>Time variation: Gaussian distribution, mean = 0, SD = ± 5 %.</p> <p>Mean value: on-time = 9%, off-time = 50%, stronger contraction time = 38%;</p> <p>Time variation: Gaussian distribution, mean = 0, SD = ± 5 %.</p>	Segments in a gait cycle are described as occurring at specific percentages of the cycle. Dividing by the period of a gait cycle might normalize the timing of muscle activity.	<i>(Gage, J R, 1991; Perry, J, 1992)</i>

7.5 Single Fibre Action Potential Simulation

7.5.1 Muscle Fibre Characteristics and Distribution

It is essential to understand the fibre characteristics and distribution in order to simulate its action potential. This model originates from the single fibre action potential, which is calculated by the conduction velocity. Muscles are composed of several thousand muscle fibres, which run parallel to the central axis of the muscle and the skin surface. In this model, the distribution of the fibre in each motor unit is defined by two parameters: the distribution of the fibre endplate positions, and the distribution of the fibre lengths. The fibre endplate position at the axial direction is assumed to have a Gaussian distribution with mean = 0 and SD = 1 mm. The fibre endplate position at the radial direction is described as a uniform distribution in the range of ± 1 motor unit radius; the mean value of the fibre length is assumed to be 100 mm, the fibre length variation is a Gaussian distribution with mean = 0 and SD = 1 mm. With regard to a given motor unit, the diameters of the muscle fibres have little difference (*Duchene, J and Hogrel, J Y, 2000; Martin, T P et al., 1988*). As a result, the simulation assumes all fibres in a muscle have a constant diameter (default value: the fibre diameter of the tibialis anterior muscle is 57 μm ; the fibre diameter of the gastrocnemius medialis muscle is 54 μm (*Perry, J, 1992*)).

7.5.2 Method to Simulate Single Fibre Action Potential

The depolarisation of the muscle fibre produces the action potential, and this change in transmembrane potential, travels along the muscle fibre at a velocity in the range from 1 ms^{-1} to 5 ms^{-1} , with amplitude of approximately

100 mV (*Brown, B H, 1999*). The single fibre action potential can be simulated by using Dimitrov' assumption. Dimitrov and Dimitrova (*Dimitrov, G V and Dimitrova, N A, 1998*) indicated that a muscle fibre can be described as a polarized shell. The assumption of two stacks of double-layer disks can be used to simulate the fibre excitation, thus, the single fibre action potential $V(x, y, z)$ at an observation point (x, y, z) can be expressed as the following equations (*Dimitrov, G V and Dimitrova, N A, 1998*):

$$V(x, y, z) = -\frac{\sigma_i}{4\pi\sigma_m} \int_{s_1} ds \int_{-\infty}^{\infty} \frac{\partial e_i(z)}{\partial z} \cdot \frac{\partial(1/r)}{\partial z} dz \quad 7.2$$

$$e_i(z) = 96z^3 e^{-z} - 90 \quad 7.3$$

Where, $e_i(z)$ is the intracellular potential of the fibre (mv); z is the axial direction, in mm (*Rosenfalck, P, 1969*); s is the fibre section; σ_i is the intracellular conductivity (default value is 1.010 s.m^{-1} (*Andreassen, S and Rosenfalck, A, 1981*)); σ_m is the muscle conductivity,

$$\sigma_m = \sqrt{\sigma_y \cdot \sigma_z} \quad 7.4$$

Where, σ_y is the muscle radial conductivity (default value is 0.063 s.m^{-1}) and σ_z is the muscle axial conductivity (default value is 0.328 s.m^{-1}) (*Andreassen, S and Rosenfalck, A, 1981*). r is the distance between the fibre sections and the observation point.

Applying Green's theorem, the single fibre action potential can be written as the following equation (*Dimitrov, G V and Dimitrova, N A, 1998*),

$$V(x, y, z) = -\frac{\sigma_i}{4\pi\sigma_m} \left[\int_{s_1} \frac{\partial e_i(z)}{\partial z} \cdot \frac{1}{r} \cdot ds + \int_{s_2} ds \int_{-\infty}^{\infty} \frac{\partial^2 e_i(z)}{\partial^2 z} \cdot \frac{1}{r} \cdot dz - \int_{s_2} \frac{\partial e_i(z)}{\partial z} \cdot \frac{1}{r} \cdot ds \right] \quad 7.5$$

Then,

$$V(x, y, z) = H_1 \cdot \left[\frac{\partial e_i(z)}{\partial z} \cdot \frac{1}{r} \Big|_{s_1} + \int_{-\infty}^{\infty} \frac{\partial^2 e_i(z)}{\partial z^2} \cdot \frac{1}{r} \cdot dz - \frac{\partial e_i(z)}{\partial z} \cdot \frac{1}{r} \Big|_{s_2} \right] \quad 7.6$$

Where S_1 and S_2 are the fibre sections at the fibre ends, S is the fibre section.

$$H_1 = \frac{\sigma_i}{4\pi\sigma_m} \cdot \frac{\pi d^2 \sigma_i}{4} \quad 7.7$$

Where, d is the fibre diameter.

The middle term of equation 7.6 can be calculated by a convolution between the second derivative of $e_i(z)$ and the function H_1/r ; the two other terms of the equation 7.6 can be computed by integrating the second derivative of $e_i(z)$ along the fibre, and then multiplied by the value of the function H_1/r at the fibre ends. Therefore, the whole equation 7.6 can be calculated by using only the second derivative of $e_i(z)$.

In addition, there is a straight relation between space (z) and time (t) on the basis of the conduction velocity (v), $z = v \cdot t$. The distribution of the intracellular potential $e_i(z)$ along the fibre can be expressed by the time t ,

$$e_i(t) = 96(vt)^3 e^{-vt} - 90 \quad 7.8$$

7.6 Motor Unit Action Potential and Voluntary Contraction Simulation

7.6.1 The Motor Unit Distribution

The surface EMG represents the activation of the motor units, which are the basic level of the muscle nerve system and have a great deal of branches and

innervates the muscle fibres contained within the motor unit. “...All the varied reflex and voluntary contractions of a muscle are achieved by different combinations of active motor units. ...” (*McComas, A J, 1996*). Therefore, the shape and power range of the surface EMGs are influenced by the parameters of the recruitment and distribution of the motor units contained within the muscle.

The parameters of the distribution of motor units include two major elements: size and position of the motor unit. The size of motor unit is determined by the function of the muscle and the characteristics of individuals. There is a large variation for the muscles of different functions and also many differences for the same muscle between healthy individuals. For a given muscle, the average size of the motor units can be estimated by dividing the total number of muscle fibres by the number of the motor axons. For example, the tibialis anterior having a 13.5 cm² cross section contains 445 motor units, and there are about 610 fibres within each motor unit; the gastrocnemius medialis muscle having a 28 cm² cross section contains 579 motor units, and there are about 1784 fibres within each motor unit (*Perry, J, 1992*). Moreover, the action potential of the motor unit that is close to the surface of the skin has a greater contribution to the surface EMG signal than the action potential of the motor unit that nears to the centre of the muscle (*Cram, J R, Kasman, G S, and Holtz, J, 1998*).

7.6.2 Principles of the Motor Unit Recruitment

The parameters of the recruitment of the motor unit include also two elements: impulse firing rates and sequence of motor units. There are considerable ranges of the contraction times for motor units to contract and relax in most human muscles. In general, the contraction time of a twitch, which is the interval between the onset of the tension and the peak tension, is used as a parameter that expresses the activity of the motor units. For human

muscles, the range of contraction times of the motor units is between 20 ms and 140 ms (*McComas, A J, 1996*). There is a relatively long contraction time in the human limb muscles because of the presence of a substantial slow-twitch motor unit population in the limb muscles. For example, the contraction time of the motor units contained within the tibialis anterior muscle is 81 ± 7.4 ms; the contraction time of the motor units of the gastrocnemius muscle is 118 ± 6.5 ms (*McComas, A J, 1996*).

In addition, the motor units have various thresholds for recruitment; some motor units can be activated during weak contraction, the others are only involved in the forceful contraction. Based upon the research of Adrian and Bronk (*Adrian, E D and Bronk, D W, 1929*), the force of the muscle contraction can be increased by raising the firing frequency and by calling additional motor units into activity (recruiting the motor units). DeLuca and colleagues stated that the different size muscles have various ways to increase the muscle force, small and distal muscles depend on increases in the firing rate for development of large forces, on the contrary, large and proximal muscles rely on recruiting additional motor units (see *Tanji, J and Kato, M, 1972*). There is agreement among investigators that the lowest frequency at which motor units can discharge steadily is from 8 Hz to 12 Hz. The lower frequencies can only be generated by repetitive voluntary contractions of a muscle (*Adrian, E D and Bronk, D W, 1929; McComas, A J, 1996*). It is difficult to determine the maximum firing frequency, because the considerable overlaps of motor unit territories make impossible to recognize the firing pattern of an individual motor unit in any region of a muscle. Generally, the maximum firing frequency of motor units is generated at the beginning of a maximal contraction (*McComas, A J, 1996*), at rates from 70 Hz to 90 Hz (*Tanji, J and Kato, M, 1972*), then, motor units modulate their firing frequency from very high frequencies to steady firing frequencies of 8 - 30 Hz. Because of the effect of mechanical fatigue, the firing frequency continues to decline to 8 - 15 Hz. In addition, the firing frequency may

remain an appropriate value for ensuring a stable contraction, for example, the mean firing frequency of the soleus is 11 Hz, the mean firing frequency of the biceps brachii is approximately 30 Hz (*Adrian, E D and Bronk, D W, 1929*).

Henneman and colleagues (*Henneman, E, Somjen, G, and Carpenter, D O, 1965*) found that an order of the motor unit recruitment only changes when the motor task is modified and the order of the motor unit recruitment remains fixed when the same motor task is undertaken in exactly the same way. Smaller motor units have lower thresholds than larger motor units. In a steady contraction, the small motor units are recruited before the large ones.

Increasing the firing rate of motor units and recruiting the additional motor units are very effective ways of increasing the force of muscle contraction. However, beyond a certain optimal firing frequency, for example, 60 Hz, no further increase in force can be generated, even though the firing frequency continues to increase. The recruitment is a more important way to bring contractile force closer to the maximum possible because some motor units can develop up to 100 times as much tension as others within the same muscle (*McComas, A J, 1996*). In addition, there is an important relationship between the firing rate and the recruitment. The recruitment of additional motor units is always accompanied with a transient drop in the firing rates of those motor units in order to ensure a smooth increase in contractile force rather than abrupt (*Broman, H, DeLuca, C J, and Mambrito, B, 1985*).

7.6.3 Method to Simulate Motor Unit Action Potential

The motor unit action potential is calculated by summation of all the single fibre action potentials in the time domain. The parameters, such as the length of the fibres, position of the fibre endplate, number of the muscle fibres and

recruitment territories of the motor unit are basic variables for computing the motor unit action potential. All parameters' values of muscle fibres and their distribution used to estimate the motor unit action potential are given in Table 7-1. Each muscle fibre action potential at the observation point can be calculated by the equation 7.2 on the basis of the various values of parameters. Our model assumes that all fibres in a muscle have a constant diameter and run uniformly parallel to the central axis of muscle and skin surface (*Duchene, J and Hogrel, J Y, 2000*). The number of muscle fibres comprised by each motor unit may be enumerated by the value equal to the area of the motor unit divided by the area of the muscle fibre. The motor unit action potential can be expressed as:

$$V_{mu} = \sum_{i=1}^{N_f} V_{f_i} \tag{7.9}$$

Where, V_{f_i} is each single fibre action potential contained within a given motor unit. N_f is the number of muscle fibres.

The motor units recruitment territories are assumed as small and overlapping circles. The territories of the motor units have cross-sectional diameters of 5-10 mm, with 10 to 25 units overlapping with each other (*Burke, R E et al., 1973; Cram, J R, Kasman, G S, and Holtz, J, 1998; McComas, A J, 1996*). The diameters of motor units are assumed to be a Poisson distribution (*Duchene, J and Hogrel, J Y, 2000*). For example, the diameters of motor units of tibialis anterior muscle are defined as a Poisson distribution with the range from 5 mm to 10 mm and mean value is 6 mm. The distribution of motor units in the section of tibialis anterior muscle is also shown in the Figure 7-6.

7.6.4 Method to Simulate Motor Unit Action Potential Trains and Voluntary Contraction

The different types of muscle activities are caused by the various actions of the motor units contained within the muscle. The surface EMG signal is determined by motor unit action potential trains that are constituted by an asynchronous series of motor unit action potentials that vary in amplitude and duration. The activities of the motor units can generally be described by parameters such as size, position, starting-time and firing rate as well as sequence of activation. For a given muscle, each motor unit action potential train can be estimated by firing rate, starting timing and the motor unit action potential that is calculated by summation all single fibre action potentials within this motor unit. In this model, the range of the firing rate between 8 Hz and 90 Hz is divided into two parts, high firing rate and low firing rate. High firing rate occurs at the beginning of muscle maximal contraction, which has a uniform distribution between 70 Hz and 90 Hz. Low firing rate happens at the muscle steady voluntary contraction, which is abided by a Poisson distribution with the range from 8 Hz to 40 Hz, mean value equals to 12 Hz.

In voluntary contraction, the activities of motor units are considered as random with no synchronization process and therefore the starting times of motor unit activation are not identical. The order of motor unit activation is decided by their sizes and is described by a general criterion that the motor units having a small size are activated earlier than the large motor units. Therefore, the motor unit that has a smaller diameter may be recruited firstly; then the motor unit with a larger diameter may be activated subsequently. The starting time of motor unit activation can be computed by the parameters both mean of firing rate and number of motor units contained in a given muscle. The starting time of each motor unit activation can be expressed as the equation:

$$t_{start_ti} = n \cdot \Delta t_{int} = n \cdot \frac{1}{N_{mu} \cdot fr} \quad 7.10$$

Where, $n = 1, 2, \dots, N_{mu}$; N_{mu} is the number of motor units within a given muscle; fr is the mean of firing rate, default value $\frac{1}{fr} = 85$ ms.

The relation of motor unit action potential trains (V_{muts}) and single motor unit action potential train (V_{mui}) can be illustrated by the array format:

$$V_{muts} = \begin{bmatrix} V_{mut1}(t_{start_ti1}, fr_1, V_{mu1}) \\ V_{mut2}(t_{start_ti2}, fr_2, V_{mu2}) \\ \cdot \\ \cdot \\ V_{muti}(t_{start_tii}, fr_i, V_{mui}) \\ \cdot \\ \cdot \\ V_{mutn}(t_{start_tin}, fr_n, V_{mun}) \end{bmatrix} \quad 7.11$$

Where, V_{mui} can be obtained by the equation 7.9; fr_i is the firing rate that obeys the Poisson distribution. For instance, the firing rate of motor unit within the muscle, tibialis anterior, has a Poisson distribution with a range from 8 Hz to 35 Hz and mean value 12 Hz when it is in the steady voluntary contraction. As a result, the simulated surface EMG signal during voluntary contraction is the summation of all motor unit action potential trains in the time domain.

7.7 Surface EMG Simulation during the Gait Cycle

7.7.1 Parameters of the Gait Cycle

“...During walking, muscles are sequentially activated in response to the stance and swing demands which are imposed on the limb...” (*Gage, J R, 1991*). Analysing the timing of muscle activation relative to the gait cycle can determine whether a muscle or muscle group is behaving appropriately or pathologically. In our model, using the timing value of the muscle’s activation mainly simulates the activities of the tibialis anterior and gastrocnemius medialis muscles during the gait cycle.

The timing of the tibialis anterior activation starts at approximately 58% of the gait cycle and ends at approximately 9% of the gait cycle, and has the two more strength contractions at approximately 70% (flexor) and 98% (extensor) of the gait cycle. The timing of the gastrocnemius medialis muscle activation starts at approximately 9% of the gait cycle and ends at approximately 50% (extensor) of the gait cycle, and arrives a peak value at approximately 38% of the gait cycle (*Gage, J R, 1991; Perry, J, 1992*). The timings of muscle activation and the intensity of muscle contraction of the tibialis anterior and gastrocnemius medialis defined in this model are shown in Figure 7-2.

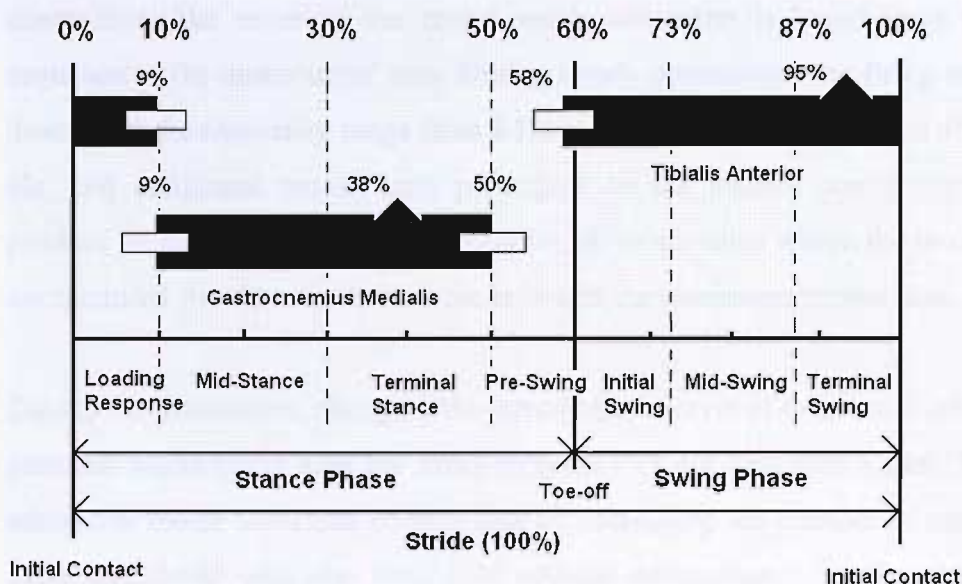


Figure 7-2 The timing of muscle activation and locations of muscle maximum contraction during the different gait phases.

The onset and cessation points of the muscle activation are described by the percentage of the gait cycle. For the tibialis anterior muscle, the onset and cessation points of muscle activation are 58% and 9% of a gait cycle; a larger force contraction occurs at approximately 95% of a gait cycle. For the gastrocnemius medialis muscle, the onset and cessation points of muscle activation are 9% and 50% of a gait cycle, a maximum force contraction occurs at approximately 38% of a gait cycle. The white boxes at the beginning and the end of each bar represent the standard deviation, value is $\pm 5\%$.

7.7.2 Method to Generate the Simulated Surface EMG Signal during the Gait Cycle

During a gait cycle, muscle activity such as voluntary contraction and relaxation are alternately brought into being by activating or discharging the motor units and modulating the firing rates. In this simulation model, increasing the firing rates of the motor units is the main mechanism to increase the muscle activity at the starting time of muscle contraction; the muscle force will continue to increase by recruiting additional motor units during steady contraction. At the same time, the firing rates have a related drop so that the muscle force increases smoothly. At the beginning of muscle

contraction, the order of the motor unit's activation is based upon the sequence of the motor units' size. During steady contraction, the firing rates descend to the frequency range from 8 Hz to 40 Hz, with a mean value of 12 Hz, and additional motor units participate to the muscle contraction to produce an increase in activity. In addition, all motor units within the muscle are recruited simultaneously in order to obtain the maximum contraction.

During this simulation, changing the inter-pulse-interval of motor unit action potential trains might alter the firing frequency of the simulated signal. The additional motor units can be recruited by increasing the number of motor units associated with the timing of muscle contraction. In the model presented here approximately 400 motor units, each containing 612 muscle fibres, are synchronously activated to produce the maximum contraction.

7.8 Simulation Results

In this section, simulation results including a single fibre action potential, a motor unit action potential, motor unit distributions, motor unit action potential trains, surface EMG signals during a gait cycle and surface EMG signals during several gait cycles are shown by using MATLAB™, a high-level technical computing language and interactive environment.

7.8.1 Simulated Single Fibre Action Potential

A single fibre action potential of the simulated activity of the tibialis anterior muscle is shown in Figure 7-3. The fibre diameter and length are assumed respectively to be 57 μm and 100 mm. The fibre endplate is assumed to be in the origin of the axis (coordinates $[0,0,0]$). The position of the electrode is described by the coordinates $[0, R_m+h_{\text{fat}}+h_{\text{skin}}, 10 \text{ mm}]$, where, $R_m = 20 \text{ mm}$,

$h_{fat} = 3 \text{ mm}$, $h_{skin} = 1 \text{ mm}$; the center of the muscle is the origin of the coordinate system (0,0,0).

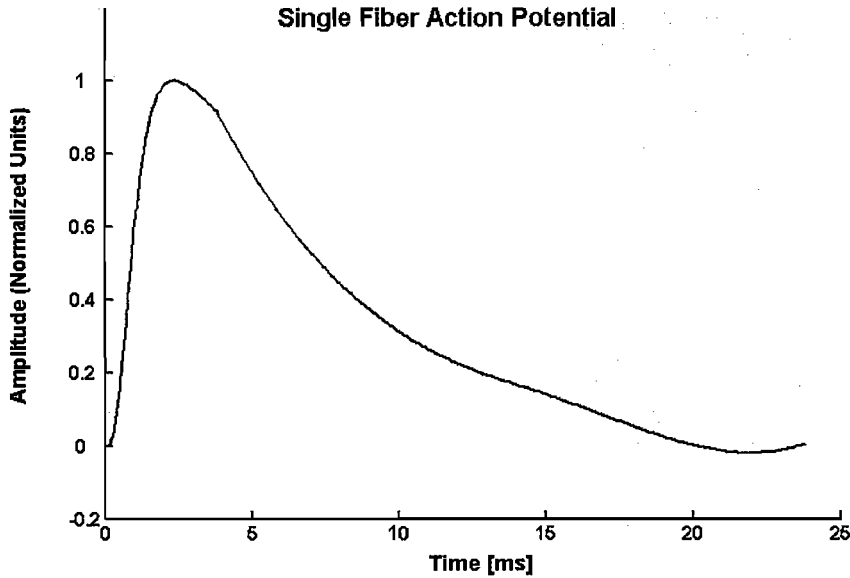


Figure 7-3 *Single fibre action potential of the tibialis anterior muscle.*

The amplitude values shown in y-axis are normalized to the maximum value of amplitude.

7.8.2 Simulated Motor Unit Action Potential

The motor unit action potential can be simulated by summation of all of the single fibre action potentials in the time domain. A simulated motor unit action potential of the tibialis anterior muscle is shown in Figure 7-4. In this case, the motor unit includes 612 muscle fibres, which run parallel to the surface skin. The endplates of muscle fibres in the axial direction are assumed to have Gaussian distribution with zero mean value and $SD = 1 \text{ mm}$. The fibre endplates in the radial direction have a uniform distribution in the range of ± 1 motor unit radius. The fibre length variation has a Gaussian distribution with zero mean value and $SD = 1 \text{ mm}$.

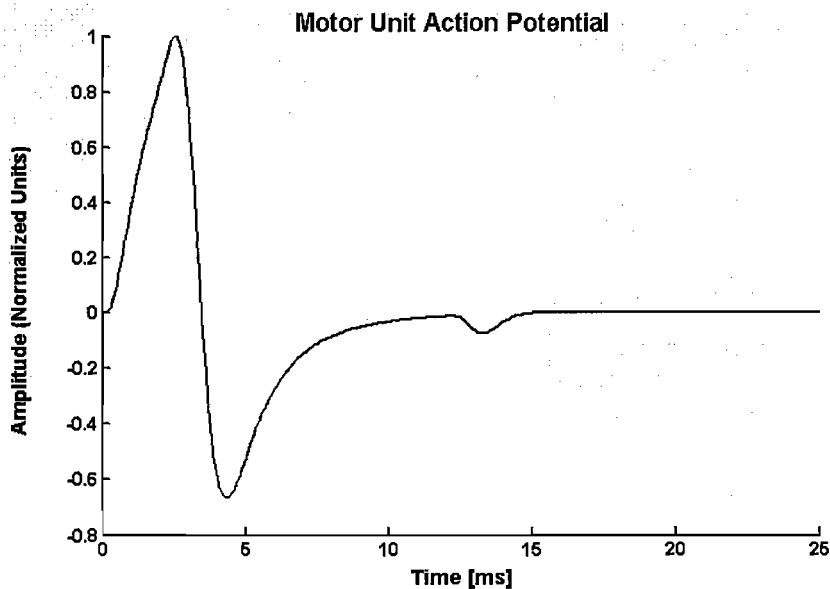


Figure 7-4 Motor unit action potential of the tibialis anterior muscle.

The amplitude values shown in y-axis are normalized to the maximum value of amplitude.

7.8.3 Simulated Surface EMG during Voluntary Muscle Contraction

The surface EMG represents the activities of the motor units. Different combinations of active motor units determine the various muscle activities such as reflex and voluntary contractions. The shape and energy range of the surface EMG are influenced by the parameters of recruitment and distribution of the motor units contained within the muscle.

For instance, the effects of the motor units' parameters on their action potentials are illustrated in Figures 7-5. Figure 7-5(b) shows six motor unit action potential trains of length 1000 ms each, which are related to the distributions of the six motor units given in Figure 7-5(a) having different sizes, positions, starting-times of contraction, and firing rates.

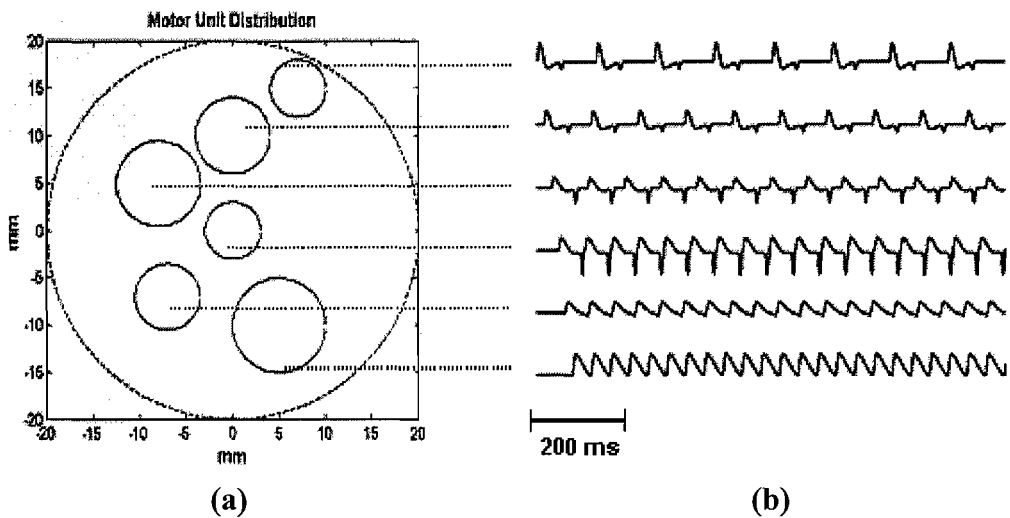


Figure 7-5 *The influence of the motor unit distribution and features of recruitment on the its potential.*

(a) Six motor unit distributions within the muscle. The positions are (7,15,0), (0,10,0), (-8,5,0), (0,0,0), (-7,-7,0) and (5,-10,0); the diameters are 6 mm, 8 mm, 9 mm, 6 mm, 7 mm and 10 mm; firing rates are 8 Hz, 10 Hz, 13 Hz, 17 Hz, 20 Hz and 25 Hz; the starting times are 0 ms, 15 ms, 30 ms, 35 ms, 50 ms and 65 ms.

(b) Motor unit action potentials based upon the different parameters of motor units.

Motor unit action potential trains and the distribution of their positions and firing rates within the muscle in voluntary contraction are shown in Figure 7-6. In this model, the number of motor units is 400. The diameters of the motor units is assumed to be a Poisson distribution with a range from 5 mm to 10 mm, lambda is 6 mm. The position of the motor units is considered to be a uniform distribution with a range of between ± 1 muscle radius. The number of motor units and the size of a given muscle determine the overlapping. The motor unit firing rates of the tibialis anterior in the voluntary contraction is assumed as a Poisson distribution with the range from 8 Hz to 40 Hz, mean value is 12 Hz. The small motor units are recruited before large ones. The interval of recruitment is a uniform distribution within the value $1/\text{mean firing rate}$.

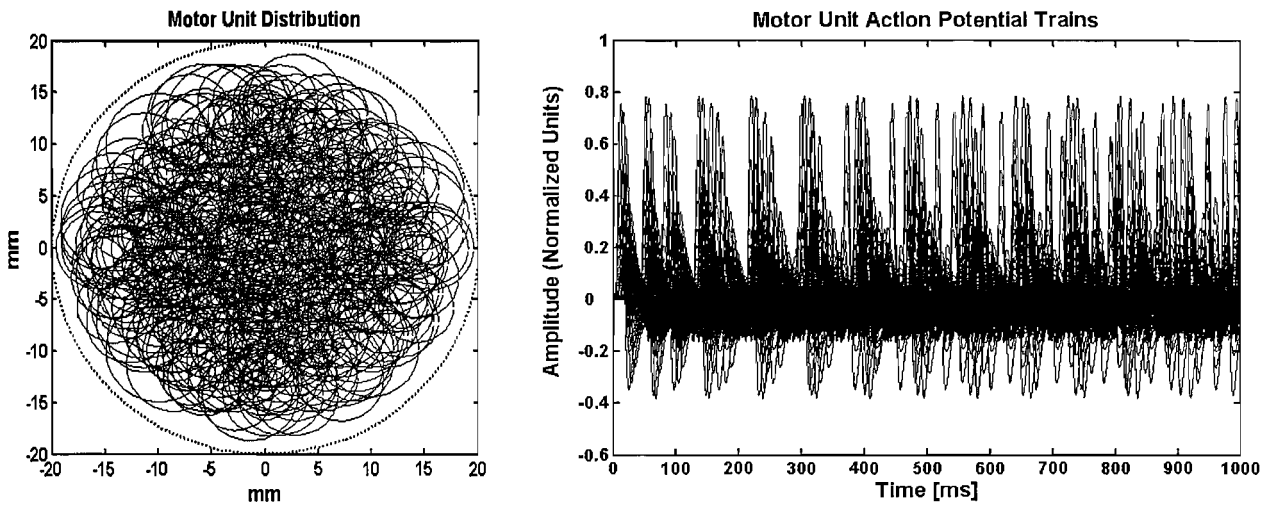


Figure 7-6 *The motor unit action potential trains of the tibialis anterior muscle.*

(a) *Motor unit distribution in the tibialis anterior muscle.*

(b) *Motor unit action potential trains.*

The amplitude values shown in y-axis are normalized to the maximum value of amplitude.

Figure 7-7 shows the simulated surface EMG signal of the tibialis anterior muscle in voluntary contraction and its power spectral density. The surface EMG is computed by summation of 400 motor unit action potential trains in the time domain. The frequency content of the simulated surface EMG signals is from 8 Hz to 150 Hz, mainly concentrated in the range of 10 - 30 Hz.

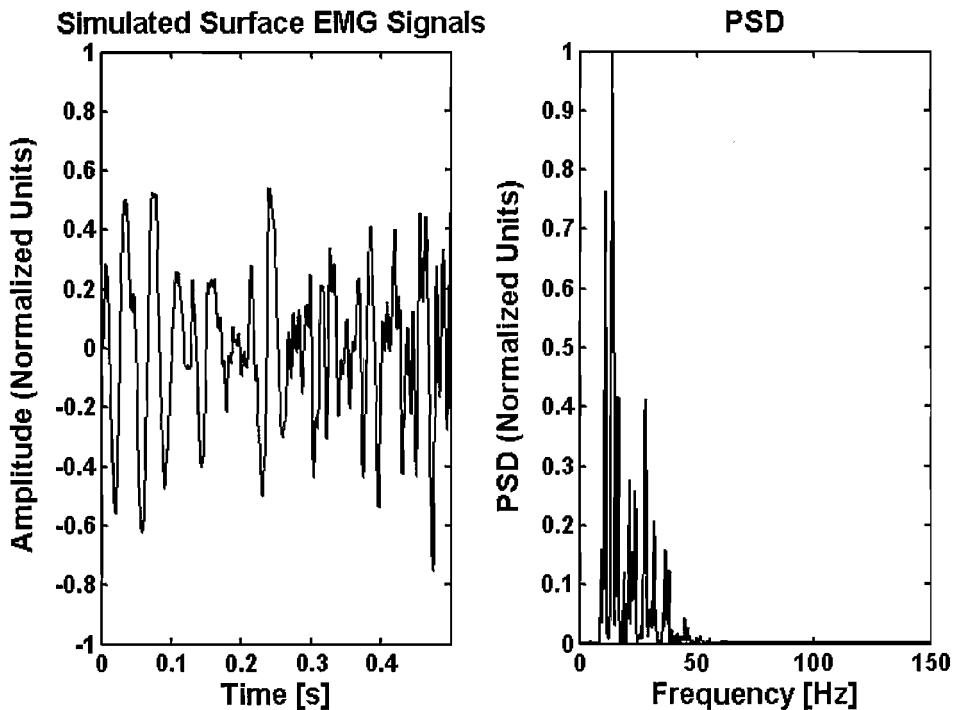


Figure 7-7 The simulation EMG signal of the tibialis anterior muscle in voluntary contraction and corresponding power spectral density (400 motor units).

The amplitude values shown in y-axis are normalized to the maximum value of amplitude.

7.8.4 Simulated Surface EMG during the Gait Cycle

The simulated surface EMG signals, assuming collection from the tibialis anterior and gastrocnemius medialis muscles during the gait cycle are illustrated in Figure 7-8. The time axis (x-axis) of the simulated surface signals is normalized to a gait cycle that is defined by two consecutive heel-down signals. The tibialis anterior muscle is activated between 58% and 9% of the gait cycle, the stronger contraction occurs at approximately 95%; the gastrocnemius medialis is activated between 9% and 50% of the gait cycle, the stronger contraction occurs at approximately 38%; for the each gait cycle, there is $\pm 5\%$ standard deviation at the timing of muscle activation. The

intensity of the muscle contraction is simulated by the summation of the different motor unit action potential trains, which is calculated by changing the number and firing rate of the motor unit recruitment. The details are explained in the method of model generation. The simulated surface EMG signal during the gait cycle is given in Figure 7-8.

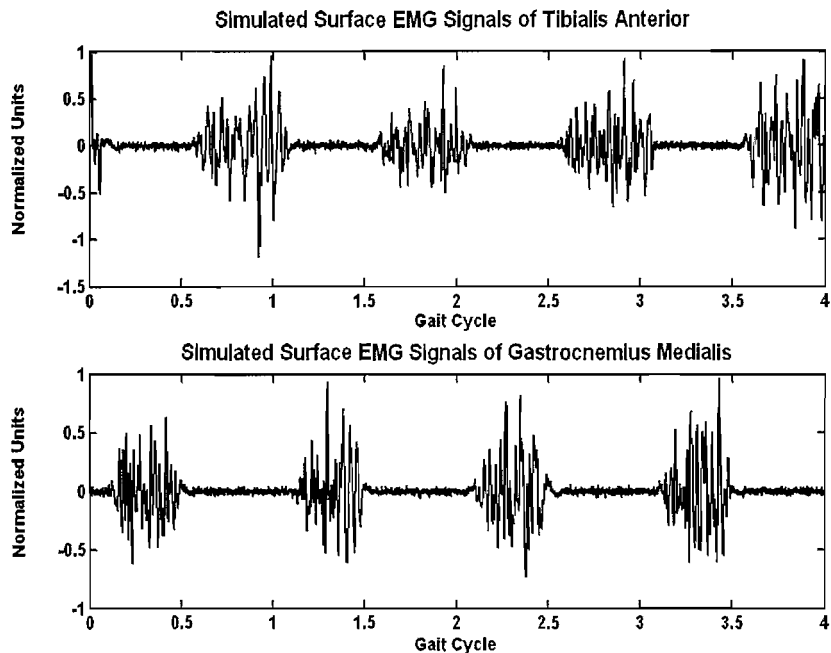
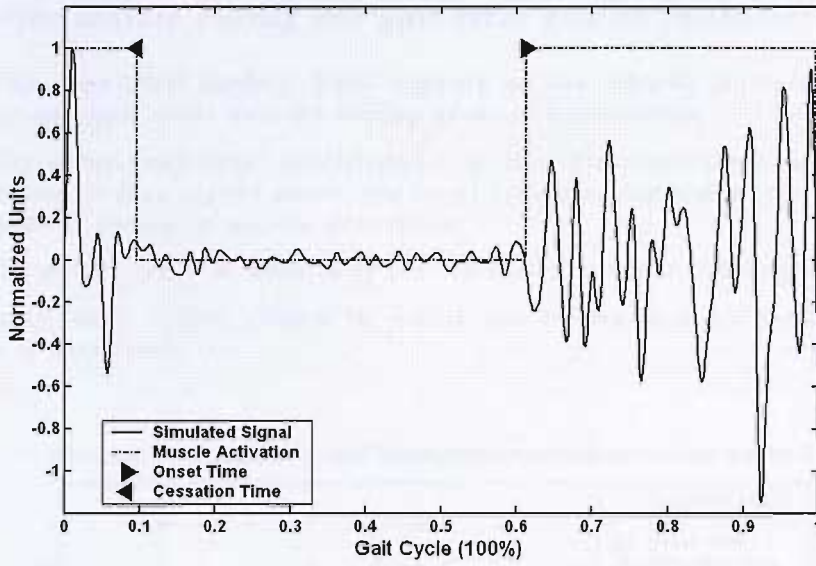


Figure 7-8 The simulated surface EMG signals of the tibialis anterior and gastrocnemius medialis muscles during the gait cycle, including four cycles.

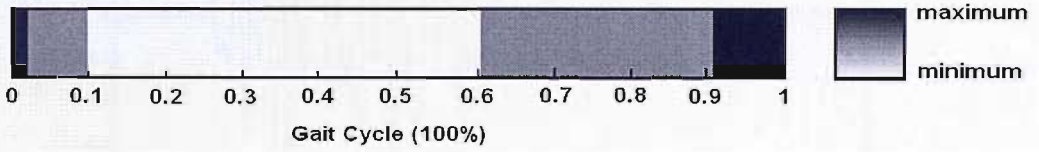
In this case, SNR = 20 dB. The amplitude values shown in y-axis are normalized to the maximum value of amplitude.

In order to analyse and assess the simulated surface EMG signal during gait cycle, a segment of simulated data such as a gait cycle is selected and its timing of muscle activation (onset and cessation time) and power spectral density are calculated. The simulated surface EMG signal during one gait cycle and its characteristics are shown in Figure 7-9 (Tibialis anterior) and Figure 7-10 (Gastrocnemius medialis).

Simulated Surface EMG Signal of Tibialis Anterior during One Gait Cycle

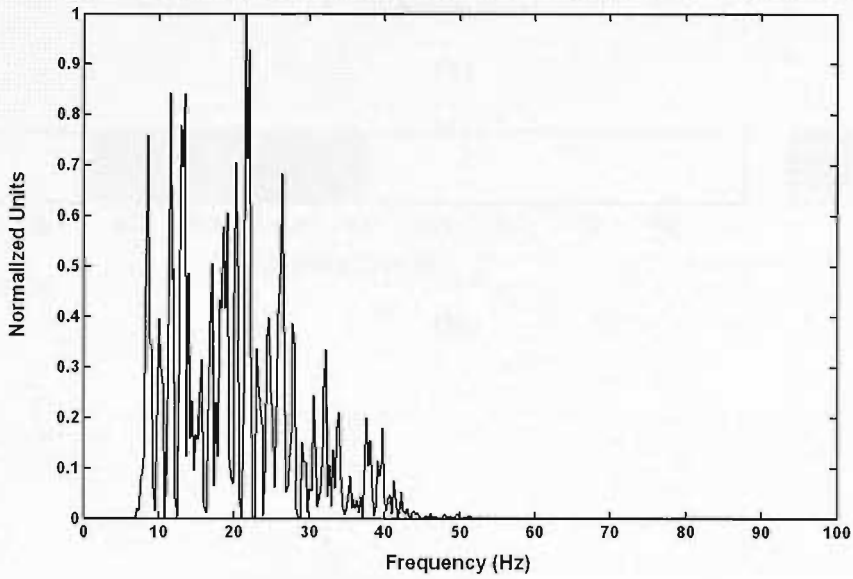


(a)



(b)

Power Spectral Density of Simulated Surface EMG Signal of Tibialis Anterior Muscle



(c)

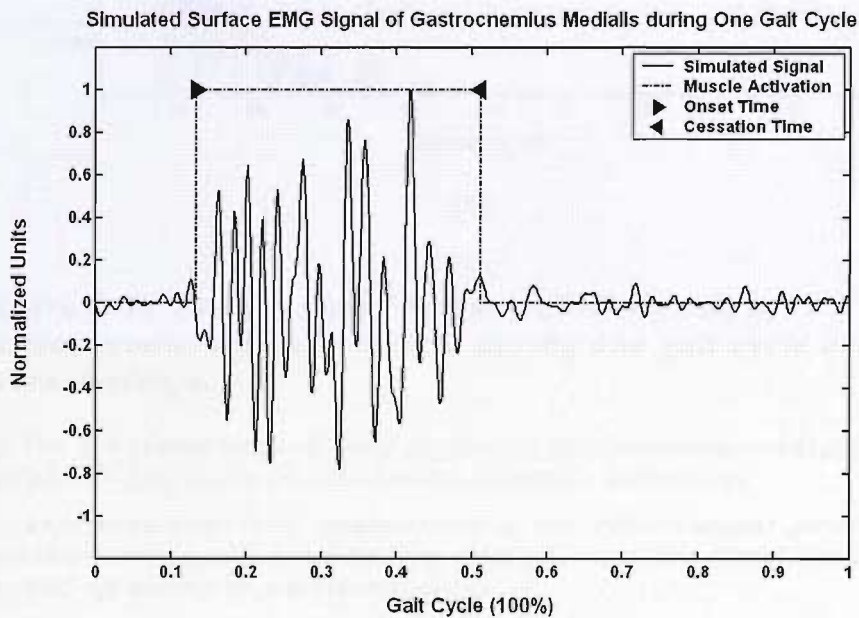
Figure 7-9 *The simulated surface EMG signals of tibialis anterior muscle during one gait cycle and its characteristics.*

(a) *The simulated surface EMG signals of the tibialis anterior muscle during one gait cycle and the timing of muscle activation.*

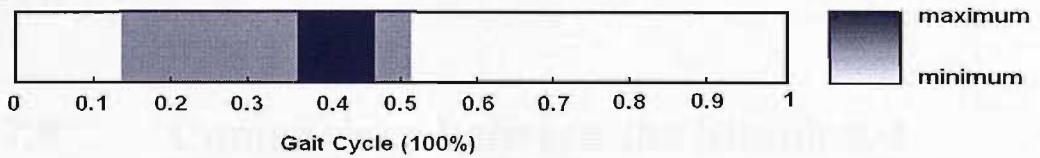
(b) *The three-gray-level quantization of the instantaneous power of the simulated surface signal shows the localization of the signal peak and the on- and-off timing of muscle activation.*

(c) *The power spectral density of the simulated surface EMG signal.*

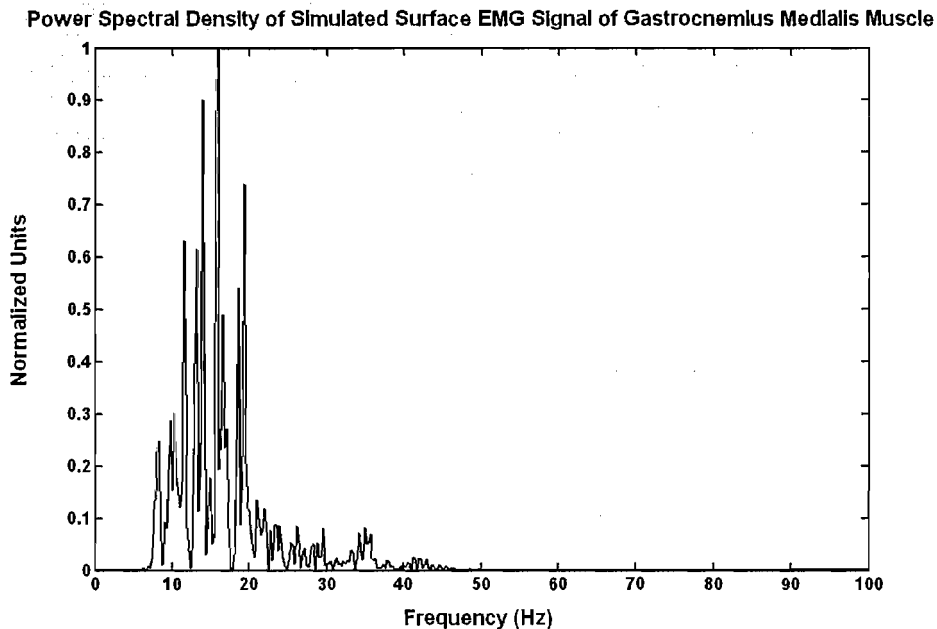
The amplitude values shown in y-axis are normalized to the maximum value of amplitude.



(a)



(b)



(c)

Figure 7-10 The simulated surface EMG signals of gastrocnemius medialis muscle during one gait cycle and its characteristics.

(a) The simulated surface EMG signals of gastrocnemius medialis muscle during one gait cycle and the timing of muscle activation.

(b) The three-gray-level quantization of the instantaneous power of the simulated surface signal shows the localization of the signal peak and the on- and-off timing of muscle activation.

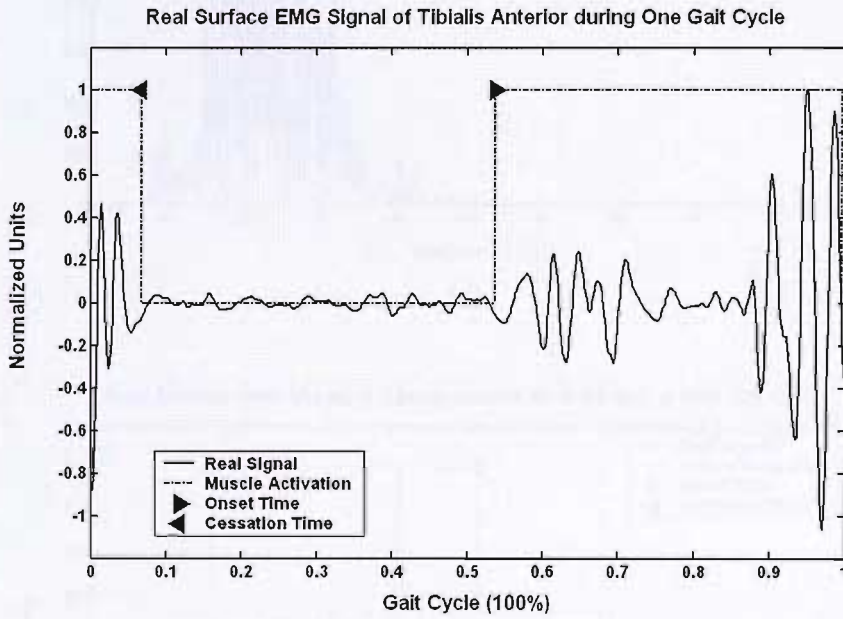
(c) The power spectral density of the simulated surface EMG signal.

The amplitude values shown in y-axis are normalized to the maximum value of amplitude.

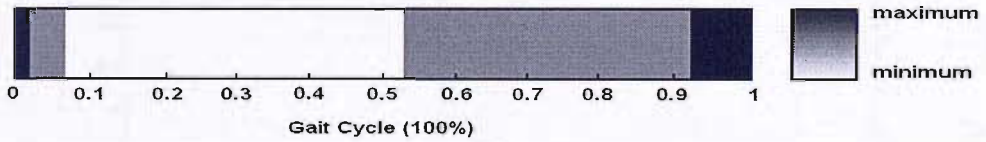
7.9 Comparison between the Simulated Surface EMG and Real Surface EMG Recorded from Gait Experiments

The surface EMG signals of tibialis anterior and gastrocnemius medialis muscles collected by the gait experiment, the timing and intensity of muscle activation and power spectral density, are shown in Figure 7-11. Comparing the real surface EMG signals with simulated surface EMG signals on the

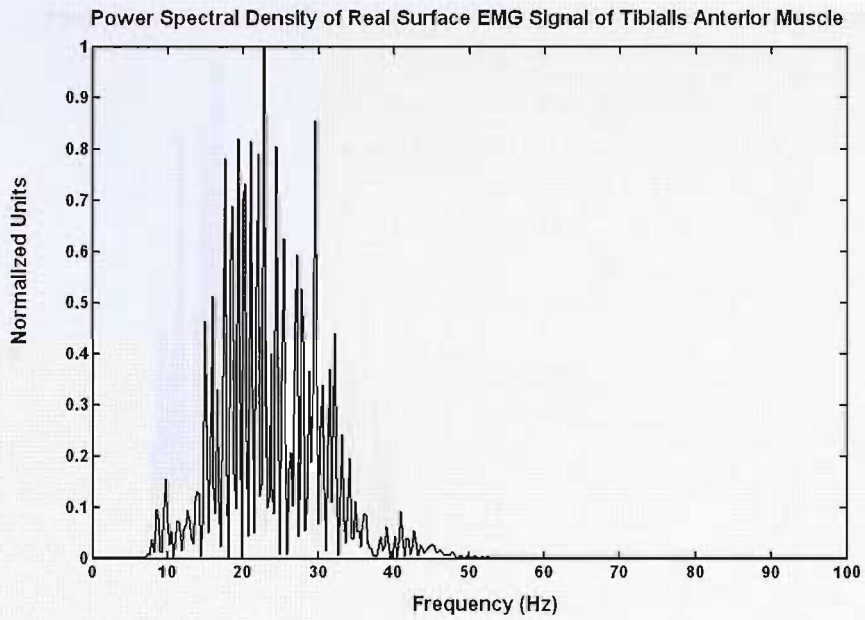
features of the timing of muscle activation and power spectral density of the signals, the results are presented in Table 7-2. These illustrate that the simulated signals can reproduce surface EMG signals due to various motor unit action potential trains determined by the special anatomical conditions and detect system parameters.



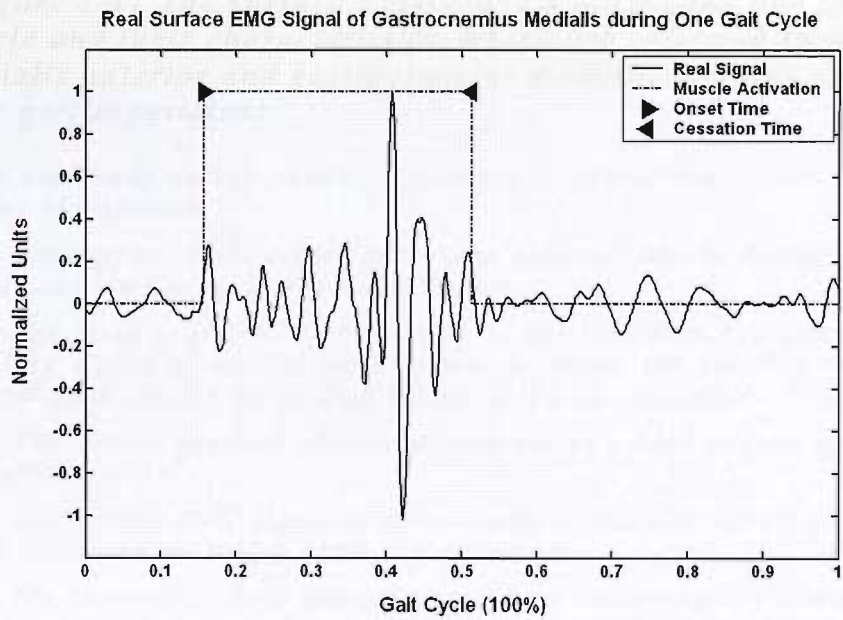
(a)



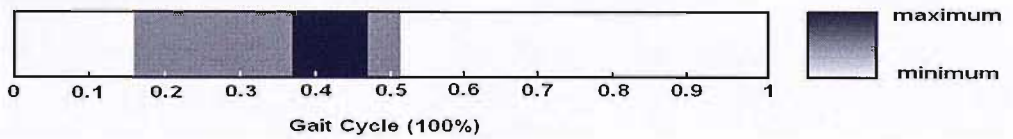
(b)



(c)



(d)



(e)

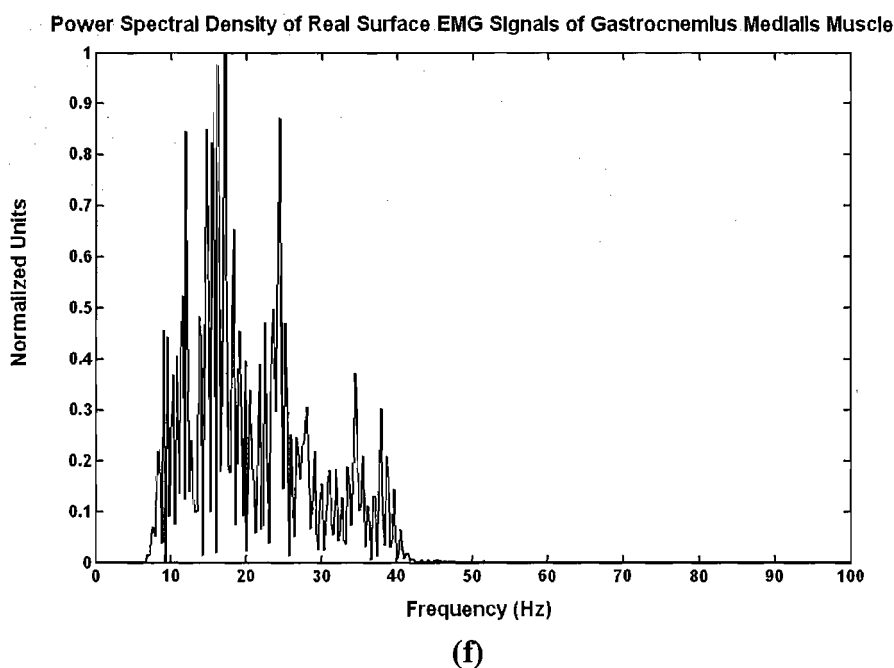


Figure 7-11 The surface EMG signals during the one gait cycle and their characteristics, which are collected from the tibialis anterior and gastrocnemius medialis muscles during the gait experiment.

The amplitude values shown in y-axis are normalized to the maximum value of amplitude.

(a) The surface EMG signal of tibialis anterior muscle during one gait cycle and the timing of muscle activation.

(b) The three-gray-level quantization of the instantaneous power of the surface signal of tibialis anterior muscle shows the localization of the signal peak and the on- and-off timing of muscle activation.

(c) The power spectral density of the surface EMG signal of tibialis anterior muscle.

(d) The surface EMG signal of gastrocnemius medialis muscle during one gait cycle and the timing of muscle activation.

(e) The three-gray-level quantization of the instantaneous power of the surface signal of gastrocnemius medialis muscle shows the localization of the signal peak and the on- and-off timing of muscle activation.

(f) The power spectral density of the surface EMG signal of gastrocnemius medialis muscle.

Table 7-2 *The characteristics of the simulated surface EMG signals and the real surface EMG signals collected during the gait experiment.*

MUSCLES		TIMING OF MUSCLE ACTIVATION						PSD
		Onset		Offset		Stronger Contraction		
		Mean %	SD %	Mean %	SD %	Mean %	SD %	Range Hz
Simulated surface EMG signals (SNR = 10 dB)	<i>Tibialis anterior</i>	60.5	2.1	6.5	2.4	92.1	2.0	<i>Range from 8 – 50 Hz, focus on 15 – 25 Hz</i>
	<i>Gastrocnemius medialis</i>	12.7	1.2	48.5	1.0	36.5	3.6	<i>Range from 8 – 50 Hz, focus on 10 – 20 Hz</i>
Real surface EMG signals	<i>Tibialis anterior</i>	58.1	4.0	6.5	2.2	95.6	2.1	<i>Range from 8 – 50 Hz, focus on 15 – 25 Hz</i>
	<i>Gastrocnemius medialis</i>	11.6	2.1	50.2	2.8	41.8	4.6	<i>Range from 8 – 50 Hz, focus on 10 – 20 Hz</i>

7.10 Discussion of the Simulation Model

A simple approach to present this model, suitable for analysis of the surface EMG signals, is to compare the features of simulated surface signals with the parameters of the real signals in time domain. For example, the onset and cessation time of muscle activation and the power of signals displaying the various activities of muscle contraction during a gait cycle. The simulated and real surface EMG signals of tibialis anterior and gastrocnemius medialis muscles and their characteristics, such as the timing and intensity of muscle activation in time domain, are respectively given in Figure 7-9 (a) (b),

Figure 7-10 (a) (b), and Figure 7-11(a) (b) (d) (e). In contrast to the above-mentioned temporal method, the approach to transform the surface EMG into its frequency representation where the various frequency and amplitude can be used to describe the EMG is efficient to interpret the features of the surface EMG. In the current study, we applied power spectral density method to extract frequency components and their power distributions from the surface EMG signal. The power spectral density of the simulated and real surface EMG signals of tibialis anterior and gastrocnemius medialis are respectively shown in Figure 7-9 (c), Figure 7-10 (c), and Figure 7-11 (c) (f).

In the model, the influence of the electrode size and shape is not considered; the position of electrode, which is modelled as point electrode, is introduced as this has a more important effect for estimating the surface EMG signals than electrodes' size. Previous studies have reported only minor differences in the recorded waveform when electrode size is changed, and these minor differences disappear with increasing distance between the electrode and muscle fibre (*Fuglevand, A J et al., 1992*).

In the current status, the simulation model only produces the surface EMG during the normal adult gait cycle, but it has potential in helping to assess the algorithms or methods that are used to analyse the surface EMG signals. Due to its existing modular parameters that can be modified and altered to suit by the different requirements, this model is intended to decide the novel algorithms that are utilized to process pathological surface EMG signals during abnormal walking.

7.11 Summary

In this chapter, an approach for modelling the generation of the surface EMG signals during the gait cycle was proposed. Important features of the

model, such as, the multiple-layer volume conductor, anatomical conditions, electrode positions, muscle fibres distribution, motor unit recruitment and firing frequency, and gait phases, have been discussed detailed. Section 7.8.3 demonstrated that the motor unit action potential trains could be changed according to the specific anatomical conditions and acquisition system parameters. The simulation results, for example, the single fibre action potential, the motor unit action potential, the motor unit action potential trains, the surface EMG of the voluntary contraction, and the surface EMG signals during the gait cycle have been shown in the section 7.8, respectively. By comparing the simulated signals with the real data recorded from the gait experiment, Section 7.9 illustrated that the simulated signals are able to reproduce the surface EMG signals by modulating the parameters on the basis of the anatomical conditions and detection system configuration.

© 2012, published by Elsevier, a subsidiary of the copyright owner. All rights reserved. No part of this publication may be reproduced, stored in a retrieval system, or transmitted, in any form or by any means, electronic, mechanical, photocopying, recording, or by any information storage or retrieval system, without the prior written permission of the copyright owner.

Chapter 8 Estimation of Muscle Activation Timing based upon Surface EMG Analysis

8.1 Overview

The aim of this chapter is to develop a new algorithm to detect the timing of muscle activation and overcome shortcomings of approaches proposed previously. The methods used to detect the muscle activation intervals, for example, traditional visual determination, algorithms with a fixed threshold, statistical methods with a double-threshold, and the generalized likelihood ratio test method, are introduced in Section 8.3, respectively. After providing a brief description of different methods, their features, especially limitations, are examined based upon simulated surface EMG signals. A novel algorithm with a power-threshold is then presented. Derivation of the algorithm, selection of basic parameters, post processing and a description of the algorithm output are set forth in more detail in Section 8.4. Section 8.6 examines the algorithm by application to both the simulated surface EMG

signals produced by the model described in Chapter 7 and the real data recorded from the gait experiment presented in Chapter 6. Comparison with other methods is also addressed. It is evident that the algorithm is very useful in overcoming some of the weaknesses related to the approaches proposed previously. The performance also illustrates that the algorithm is more suitable for analysing muscle activity during dynamic movement.

8.2 Introduction to Detection of Muscle Activation Intervals

In clinical research, the detection of characteristics of the surface EMG between normal and pathological subjects is widely used to assess the physiological processes of muscle activities. Those physiological processes stimulate muscles to generate force, movement and achieve the necessary functions of everyday life. The information extracted from the surface EMG signal can be taken advantage of in several different applications. For instance, it might be useful to explore the biomechanics and motor control of the muscular skeletal system during various movements.

More recently, the estimation of the timing of muscle activation during movement has become an important issue in surface EMG signal processing (*Micera, S et al., 2001*). Although some differences exist in the methods mentioned, a fundamental approach that is used to estimate muscle activation intervals is the detection of onset and cessation of muscle activation. The evaluation of the timing of muscle action is shown in different applications; for example, it could be employed to highlight the features of the normal gait of children or could be of value during the treatment of pathological gait of children with cerebral palsy. However, there are no standard approaches to estimate such parameters (*Hodges, P W and Bui, B H, 1996*). Many methods and algorithms to address this issue are

proposed in the literature, and their performances vary considerably. Those approaches include the so-called single-threshold method, the double-threshold algorithm, the generalized likelihood ratio test method, and the approach based-upon wavelet transforms.

The single-threshold method (*Thexton, A J, 1996*) is based upon a comparison of the rectified raw surface EMG signal and fixed threshold. The double-threshold algorithm (*Bonato, P, D'Alessio, T, and Knaflitz, M, 1998*) is applied to whitened data with the possibility of setting the probabilities of false-alarm and correct detection. The generalized likelihood ratio test method (*Micera, S et al., 2001; van Putten Jr, J D, 1999*) is an algorithm used to analyse abrupt changes of time-varying linear systems. The results produced from this algorithm are similar to the single-threshold and double-threshold methods. The continuous wavelet transform (*Merlo, A, Farina, D, and Merletti, R, 2003*) has been used to investigate the single motor unit action potential and detects the on-off muscle action.

The characteristics of traditional and recent approaches for the detection of the timing of muscle activation are illustrated by applying these algorithms to the simulated surface EMG signal. The properties and limitations of the approaches mentioned are illustrated in this chapter. In order to overcome the limitations of some methods, a novel algorithm that is called the power-threshold algorithm is presented. This algorithm could be advantageous in detecting the onset and cessation timing of muscle activation, especially for gait analysis. The onset and cessation timings of muscle activation are estimated by comparison of the power of raw surface EMG within the observation window with the threshold. The timing of maximum contraction occurs when the value of the power of the raw surface EMG signal within the observation window attains the maximum value. As a result, the standard deviation of the timing of muscle activation is lower than 20 ms when this algorithm is used to analyse the simulated surface EMG signal with a SNR

greater than 3 dB. In addition, it is lower than 25 ms when the algorithm is used to process the real data recorded from the gait experiment.

8.3 Approaches and Algorithms Used in Present Clinical Research

The failure in detecting the onset and cessation timing might lead to the possibility of achieving an incorrect insight into the motor control and muscle activity. For many years the detection of the timing of muscle contraction has been determined by traditional methods, for example, visual inspection carried out by experts or a fixed threshold performed by computer. In the recent past some more advanced approaches have been introduced in the clinical application.

8.3.1 Visual Determination and its Limitations

In the traditional approaches to determine the on-off timing of muscle action, visual determination is widely used by clinicians and researchers based upon their skill and experience. Clinicians attempt to indicate all onset and cessation times and abrupt changes along the recorded surface EMG signal. In general, the visual determination method can supply highly accurate detection of the onset time and can identify any abrupt spikes in the course of the entire recorded surface EMG signal. However, the limitations of visual determination are also apparent and unavoidable. This method strongly depends on the expertise of clinicians; hence, the limitations of poor reproducibility and high subjectivity are inevitable. Furthermore, this method is carried out off-line and is very time-consuming.

8.3.2 Methods with a Fixed Threshold

8.3.2.1 Fixed Threshold Algorithm

The single-threshold algorithm detection, and other methods based upon a fixed threshold, are computer-based determination of the timing of muscle activation and can overcome the limitations of traditional visual determination approaches. A computerized analysis of features of EMG signals has been first shown in animal studies in order to illustrate the central nervous system activity related to peripheral muscle discharge (*Neafsey, E J, Hull, C D, and Buchwald, N A, 1978*). Generally, the methods based upon a fixed threshold involve identification of the onset and cessation points of muscle activity. Comparing the raw surface EMG signal with a fixed threshold chosen by the operator, the sample is considered as a valid sample when the amplitude of sample exceeds the threshold. The time when the first sample of a block of valid samples occurs is the onset point of muscle contraction; the time when the last sample happens is the cessation point. The baseline level is determined by standard deviation of the raw surface EMG signal (*Micera, S et al., 2001; Thexton, A J, 1996*). The flowchart of this method with a fixed threshold is shown in Figure 8-1.

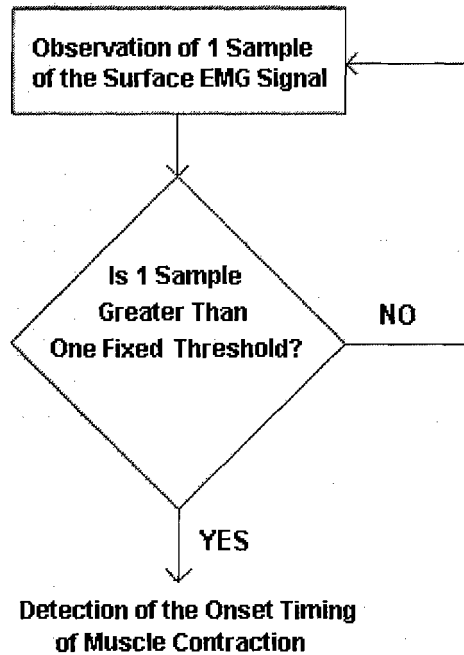


Figure 8-1 Flowchart of the algorithm with a fixed threshold.

8.3.2.2 Limitations of the Single-threshold Algorithm

Let us show a typical single threshold algorithm (Merlo, A, Farina, D, and Merletti, R, 2003; Micera, S et al., 2001; Thexton, A J, 1996) used to detect the timing of muscle activation, and illustrate its limitations.

In this single threshold algorithm, the threshold is calculated from the mean value and standard deviation of background noise. Any amplitude of EMG signal more than the selected threshold is taken to represent the desired signal. The threshold can be expressed as the equation:

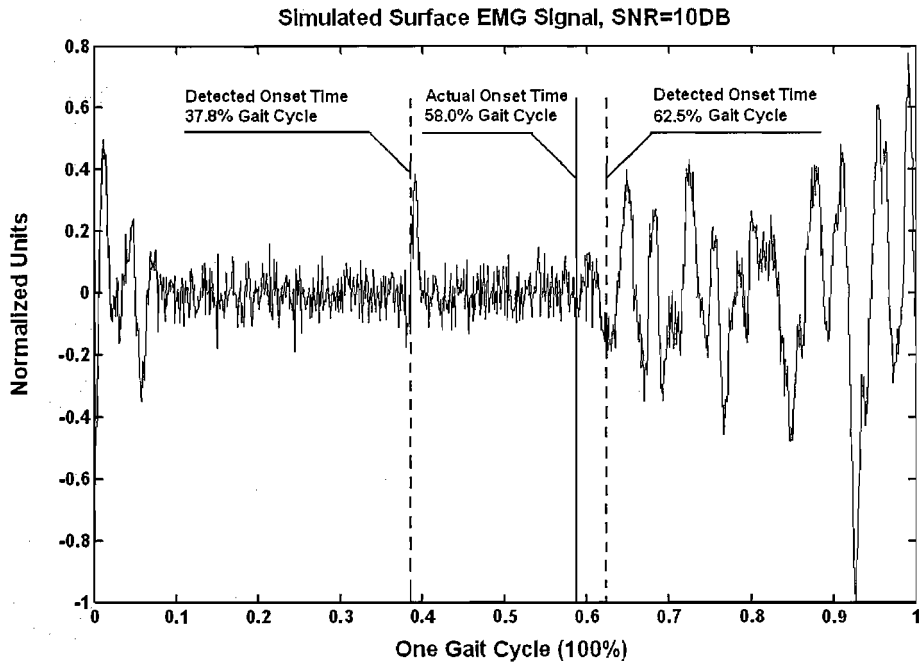
$$T_h = \mu_n + \gamma \cdot \sigma_n \quad 8.1$$

Where, T_h is the fixed threshold to assess the surface EMG signal, μ_n is the mean value of the background noise, σ_n is standard deviation of the background noise, $\gamma = [1...3]$, typical values for γ are $\gamma = 2$ or $\gamma = 3$. The

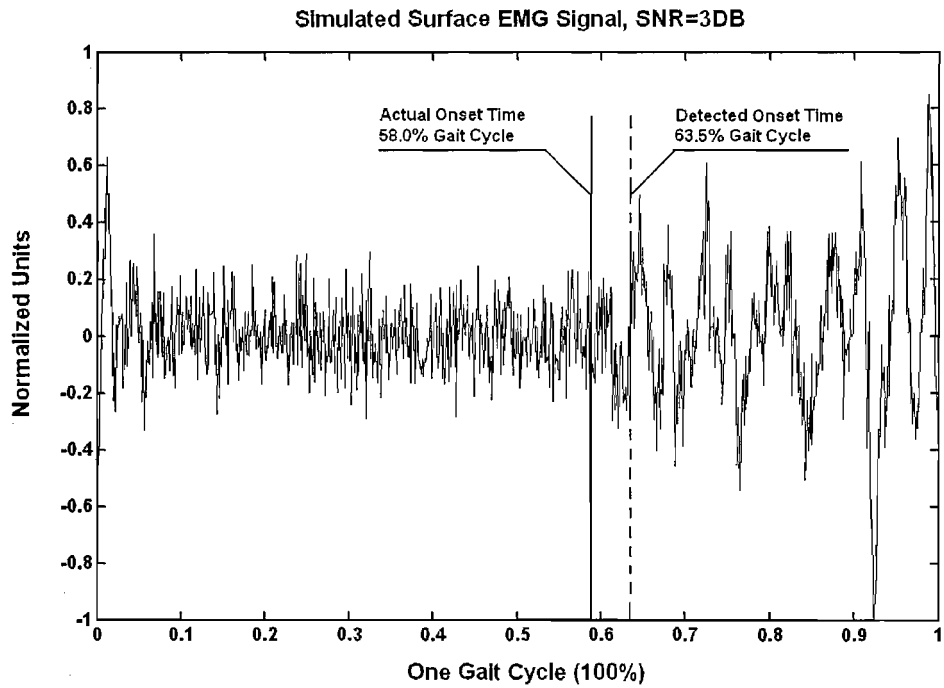
value of γ can be changed by the operator to suit different requirements such as different SNR values.

In this algorithm, the surface EMG signal containing the desired signal and background noise is firstly full-wave rectified. The data is then separated into two parts with respect to the fixed threshold value. The two parts are composed of a series of samples whose values lie above the threshold and a series of samples whose values lie below. A series of samples whose values exceed the threshold are the desired signals, which represent muscle activation.

The single threshold algorithm strongly depends upon the chosen threshold value, and the value of threshold crucially influences on the results of the timing of muscle activation. Generally, the number of standard deviation (σ_n) changes between $1\sigma_n$ and $3\sigma_n$ from the baseline activity level. When the threshold value is set to $1\sigma_n$, the error due to a large spike is quite high (see Figure 8-2), however, when the threshold value is set to $3\sigma_n$, the error due to a small difference between the signals representing the muscle activation or muscle rest could dramatically increase (see Figure 8-2). Another factor that might affect the performance of the algorithm is the signal-to-noise ratio of the raw surface EMG signal. The error could increase when a signal-to-noise ratio decreases. The simulated surface EMG signal of tibialis anterior during a gait cycle is used to assess the algorithm in this case. The limitations of the single threshold algorithm are shown in Figure 8-2.



(a)



(b)

Figure 8-2 Errors produced by using the fixed threshold algorithm.

The correct onset timing is 58.0% gait cycle. In this case, the threshold is calculated by the mean value and standard deviation of background noise.

(a) Error due to a large spike during the muscle relaxation. Detected onset times along the simulated surface EMG signal (SNR = 10 dB) are respectively 37.8% gait cycle based upon the large spike that occurs on the rest of muscle, and 62.5% gait cycle because of the influence of the background noise.

(b) Error due to a low value of signal-to-noise ratio. The simulated surface EMG signal with SNR = 3 dB. Detected onset time is 63.5 % gait cycle. Comparison of the detected onset time in Figure 8-2(a) and the detected onset time in Figure 8-2 (b); the results show that the bias of detected onset time is increased based upon the decreasing signal-to-noise ratio.

8.3.3 Statistical Method: Double-threshold Algorithm

8.3.3.1 Double-threshold Algorithm

A statistical algorithm, the double-threshold algorithm (Bonato, P, D'Alessio, T, and Knaflitz, M, 1998), has been introduced to overcome the limitations of the more traditional methods, visual determination and fixed threshold algorithm. The behaviour of the double-threshold algorithm is fixed by three parameters: the first threshold η , the second threshold n_0 , and the length of the observation window m . Their values are selected to jointly minimize the value of false-alarm probability ($P_{false-alarm}$) and maximize detection probability ($P_{detection}$) on the basis of specific SNR (Bonato, P, D'Alessio, T, and Knaflitz, M, 1998). For the algorithm, it is essential to obtain a series of whitened data that is generated by applying a whitening filter to the surface EMG signal. For the whitened data, with a setting of the false-alarm probability at 5 %, the bias of the estimates of the onset and cessation timing is smaller than 10 ms, and the standard deviation is lower than 15 ms (Bonato, P, D'Alessio, T, and Knaflitz, M, 1998).

The whole process of derivation of the double-threshold algorithm is established on the foundation that the simulated surface EMG signal might be considered as a zero-mean, Gaussian distribution corrupted by independent zero-mean Gaussian additive noise. Abiding by the algorithm requirement, the simulated signals are firstly filtered by the whitening filter. An auxiliary time series is then established by summing the squared values of two successive samples. If at least n_0 samples (second threshold) within the observation window m are above the first threshold η , the signal is taken to represent the desired signal and the muscle activation is acknowledged. A flowchart of the double-threshold algorithm is shown in Figure 8-3.

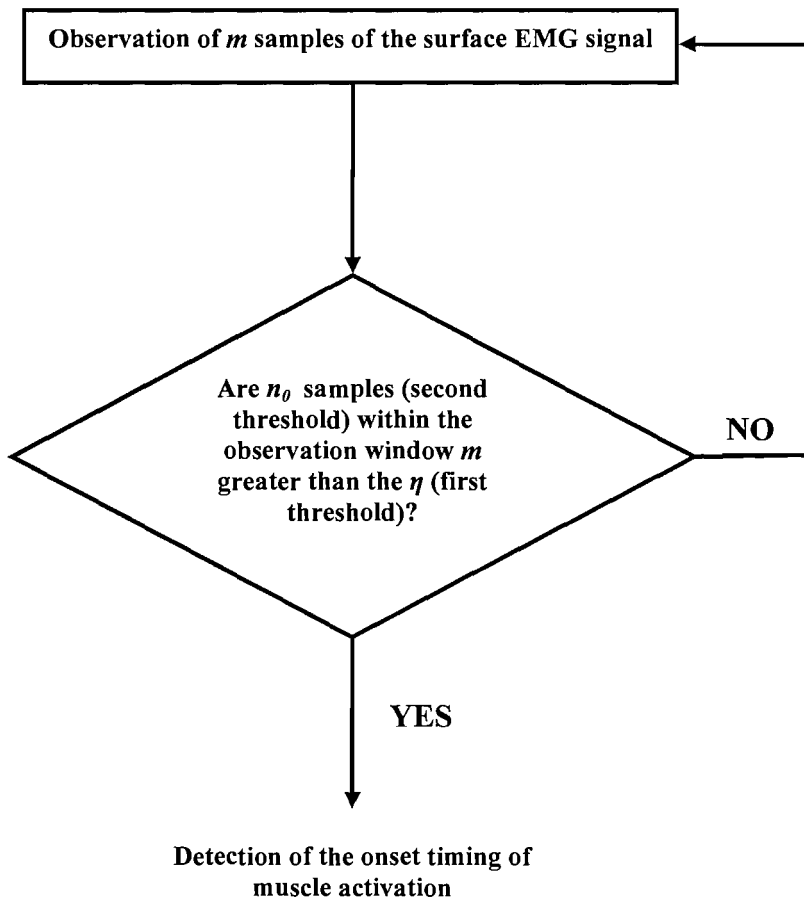


Figure 8-3 Flowchart of the double-threshold algorithm.

Using the observation window (m) to detect the whitened data presenting the surface EMG signal, the onset timing of muscle activation is detected when at least n_0 samples exceed a chosen threshold η .

8.3.3.2 Derivation of the Double-threshold Algorithm

Equation 8.2 shows the probability $P_{n_0}(n \geq n_0; m)$ that at least n_0 samples out of m exceed the first threshold η , derived by considering a repetition of Bernoulli trials. P is the probability that a single sample exceeds the threshold.

$$P_{n_0}(n \geq n_0; m) = \sum_{r=n_0}^m \binom{m}{r} P^r (1-P)^{m-r} \quad 8.2$$

Equation 8.3 presents the probability $P_\eta = P[x > \eta, s(t) = n(t)]$ that a specific noise sample crosses the first threshold η .

$$P_\eta = P[x > \eta, s(t) = n(t)] = e^{-\eta / (2\sigma_n^2)} \quad 8.3$$

Equation 8.4 shows the probability $P_{dr} = P[x > \eta, x(t) = s(t) + n(t)]$ that the r th sample crosses the first threshold η .

$$P_{dr} = P[x > \eta, x(t) = s(t) + n(t)] = e^{-\eta / \left[2\sigma_n^2 \left(1 + 10^{(SNR/10)} \right) \right]} \quad 8.4$$

Where, $SNR = 10 \log_{10} \left(\frac{\sigma_s^2}{\sigma_n^2} \right)$; $s(t)$ is the whitened EMG signals without noise; $n(t)$ is whitened noise signals; $x(t)$ is simulated whitened EMG signals with noise, $x(t) = s(t) + n(t)$.

The probability of false-alarm ($P_{false-alarm}$) is the probability that the noise samples are incorrectly considered as signal samples, and is achieved from the equation 8.2 by setting $P = P_\eta$, as shown by

$$P_{false\text{-}alarm} = \sum_{r=n_0}^m \binom{m}{r} P_{\eta}^r (1 - P_{\eta})^{m-r} \quad 8.5$$

Similarly, the probability of detection ($P_{detection}$) is the probability that signal samples are correctly interpreted, and is obtained from the equation 8.2 by setting $P = P_{dr}$, as given by

$$P_{detection} = \sum_{r=n_0}^m \binom{m}{r} P_{dr}^r (1 - P_{dr})^{m-r} \quad 8.6$$

After setting the desired values of $P_{false\text{-}alarm}$ (0.05) and $P_{detection}$ (0.95), the length of the observation window m and the second threshold n_0 are requested. The feature of the double-threshold algorithm is described by its receiver operating characteristic (ROC) curves (*Bonato, P, D'Alessio, T, and Knaflitz, M, 1998*), which interpret the relationship between $P_{false\text{-}alarm}$ and $P_{detection}$ based upon different values of SNR, n_0 , and m . By reference to ROC curves, the length of observation window m is chosen as 5 samples at a sampling frequency of 1000 Hz and the second threshold n_0 is equal to 1 to maximize $P_{detection}$ and minimize $P_{false\text{-}alarm}$. The last step is the calculation of the first threshold η . Given $P_{false\text{-}alarm}$, the equation 8.5 is solved with respect to P_{η} . By solving equation 8.3 with respect to η , the first threshold can be obtained.

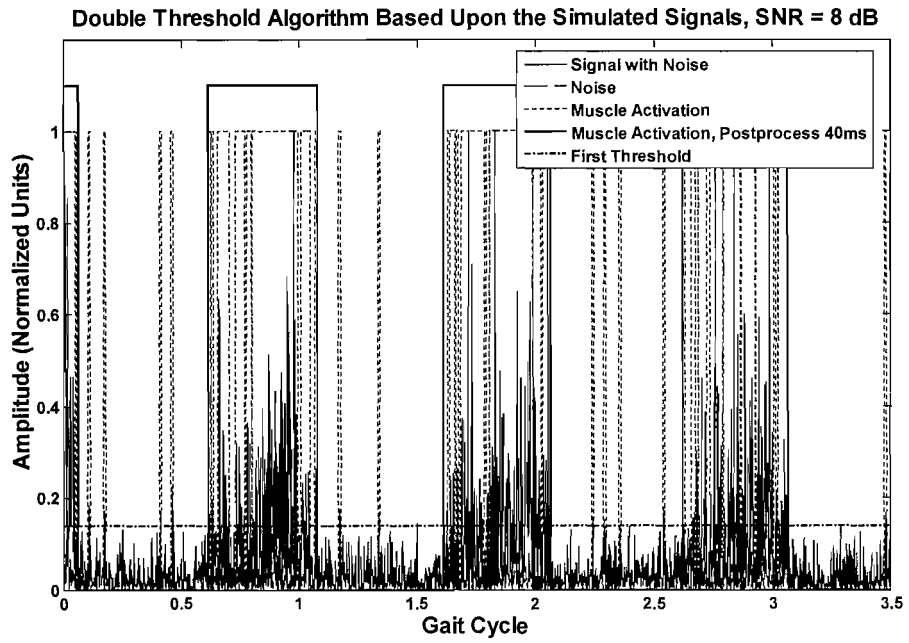
In the post-processor procedure, the transitions which last for less than 40 ms are considered as 'no muscle activation' (*Bogey, R A, Barnes, L A, and Perry, J, 1992; Bonato, P, D'Alessio, T, and Knaflitz, M, 1998*).

8.3.3.3 Performance of the Double-threshold Algorithm Applied to Phenomenologically Simulated Surface EMG Signals

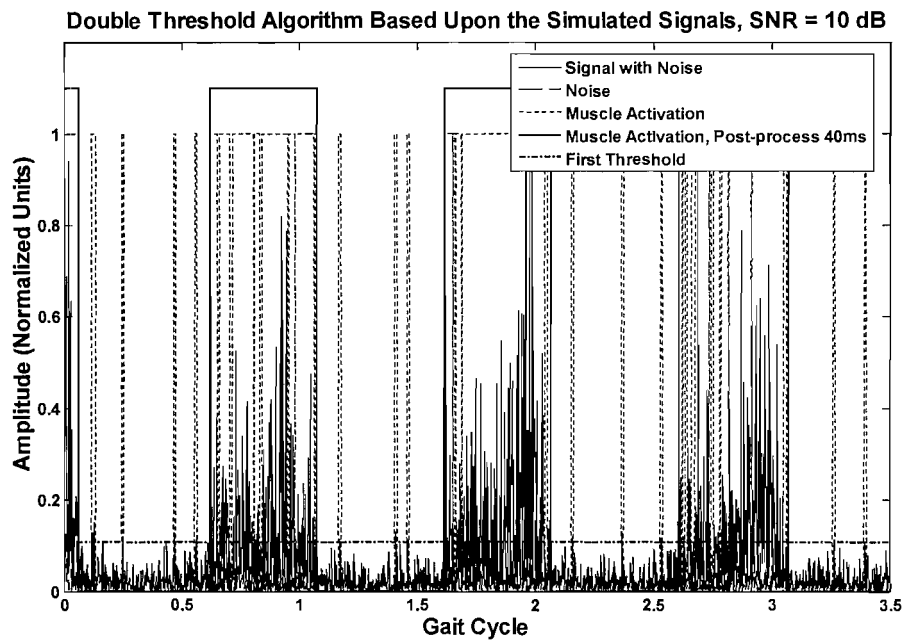
The double-threshold algorithm is derived on the basis of the phenomenologically simulated EMG signal. In order to assess this algorithm, a series of phenomenologically simulated surface EMG signals during the

gait cycle were generated from the phenomenological simulation model. In the phenomenological model, the surface EMG signal of the voluntary contraction is assumed as a stochastic signal with a zero-mean, Gaussian distribution plus an independent zero-mean, Gaussian, additive noise signal. The surface EMG signals during the gait cycle are then produced by adapting the amplitude of the data to suit the muscle activation intervals.

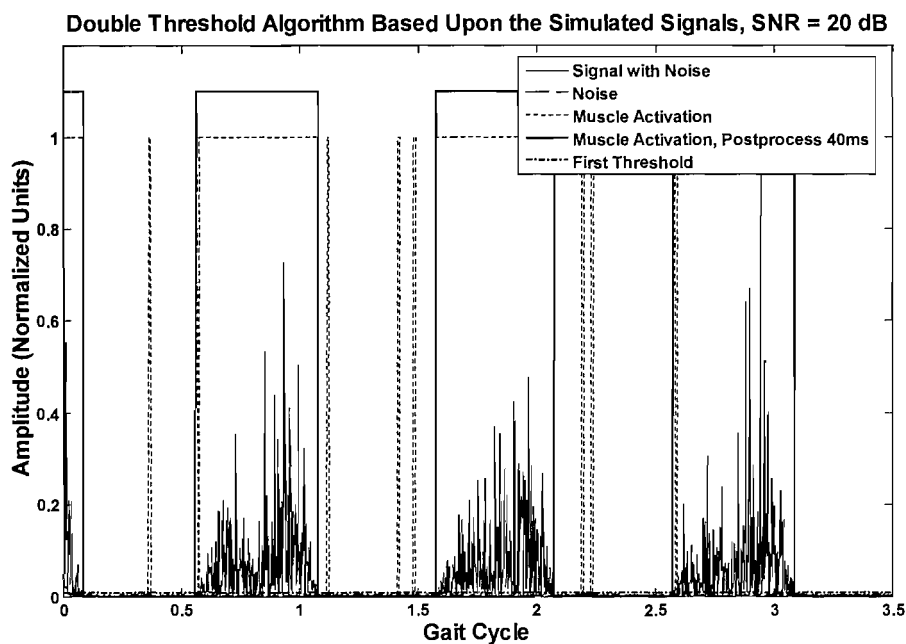
The results of the double-threshold algorithm applied to simulated surface EMG signals with different signal-to-noise ratios (SNR = 8 dB, 10 dB and 20 dB) during the gait cycle produced by the phenomenological model described above are illustrated in Figure 8-4 and Table 8-1. For the simulated surface EMG signal with signal-to-noise ratio greater than 3 dB, the bias of onset and cessation timing of muscle activation is less than 15 ms, and the standard deviation is smaller than 15 ms (when SNR = 3 dB, the standard deviation increases up to 59.7). The performance of the algorithm shows that the double-threshold algorithm may be suitable for detection of on-off timing of muscle activation of the simulated EMG signal with SNR > 3 dB that is generated from the phenomenological model.



(a)



(b)



(c)

Figure 8-4 The performance of the double-threshold algorithm applied to the simulated surface EMG signal produced by the phenomenological model.

The simulated surface EMG signal, added noise (SNR = 8 dB, 10 dB, and 20 dB), the first threshold of double-threshold algorithm, onset and cessation timing before the post-processing, and onset and cessation timing after the post-processing, are presented. In this case, $m = 5$, $n = 1$; $P_{\text{false-alarm}} = 0.05$, $P_{\text{detection}} = 0.95$; all transitions lasting more than 40 ms are considered as a valid activation in the post-processor (See Section 8.4.4). The amplitude values shown in y-axis are normalized to the maximum value of amplitude.

Table 8-1 Bias and standard deviation of the onset and cessation timing of muscle activation produced by the double-threshold algorithm applied to the simulated surface EMG signals during the gait cycle, which are originated from the phenomenological model.

		Onset Timing				Cessation Timing			
		Bias ms			SD ms	Bias ms			SD ms
		1 st gc	2 nd gc	3 rd gc		1 st gc	2 nd gc	3 rd gc	
SNR	3 dB	40.0	30.0	-68.0	59.7	34.0	-63.0	29.0	54.6
	6 dB	-9.0	6.0	3.0	7.9	-4.0	3.0	1.0	3.6
	8 dB	-1.6	-4.6	6.3	5.7	10.0	-5.0	-4.0	8.4
	10 dB	4.0	2.0	-6.0	5.3	4.0	-5.0	3.0	4.9
	20 dB	-10.0	6.0	4.0	8.7	0	-5.0	5.0	5.0

1st gc indicates the first, 2nd gc indicates the second, 3rd gc indicates the third cycle of the gait cycles, respectively; SD is the standard deviation of three gait cycles.

The performance of the double-threshold algorithm applied to the simulated signal with the different signal-to noise ratio (SNR = 3 dB, 6 dB, 8 dB, 10 dB, 20 dB) shows that the algorithm may be satisfactory to analyse the simulated EMG signal originated from the phenomenological model. For the simulated EMG signal with the signal-to-noise ratio more than 3 dB, the bias of the estimates of the onset and cessation timing is smaller than 15 ms, and the standard deviation is lower than 15 ms. In this case, $P_{false-alarm} = 0.05$, $P_{detection} = 0.95$.

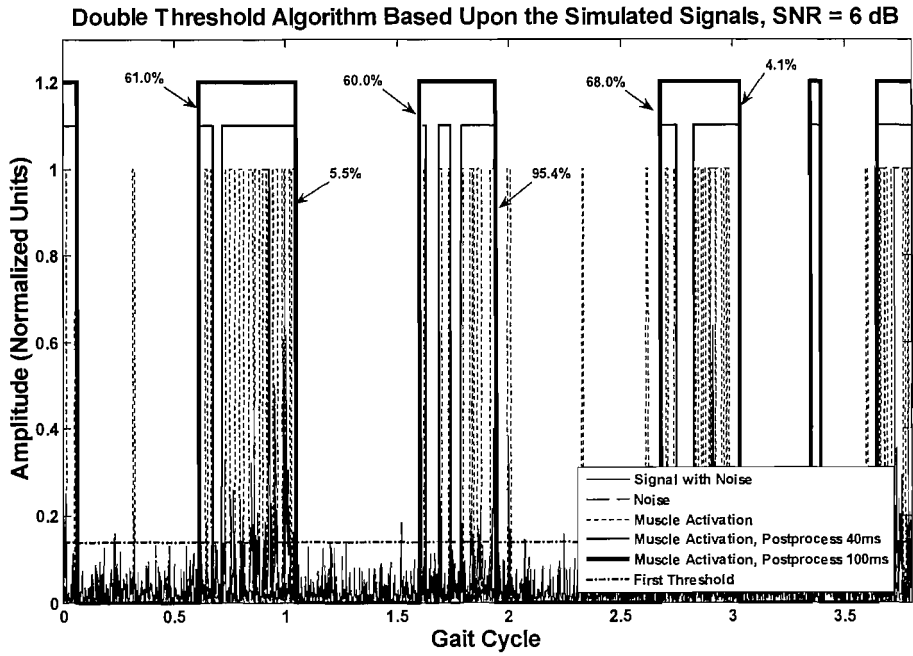
8.3.3.4 Limitations of the Double-threshold Algorithm

The assumption that the surface EMG signal is a stochastic signal is not necessarily valid for proper interpretation of the real surface EMG signal, or for fairly assessing the threshold algorithm. In this section, the algorithm is applied to the analysis of the simulated surface EMG signal produced by the model on the basis of the physical structure of the muscle, which is presented in Chapter 7, rather than a phenomenological model.

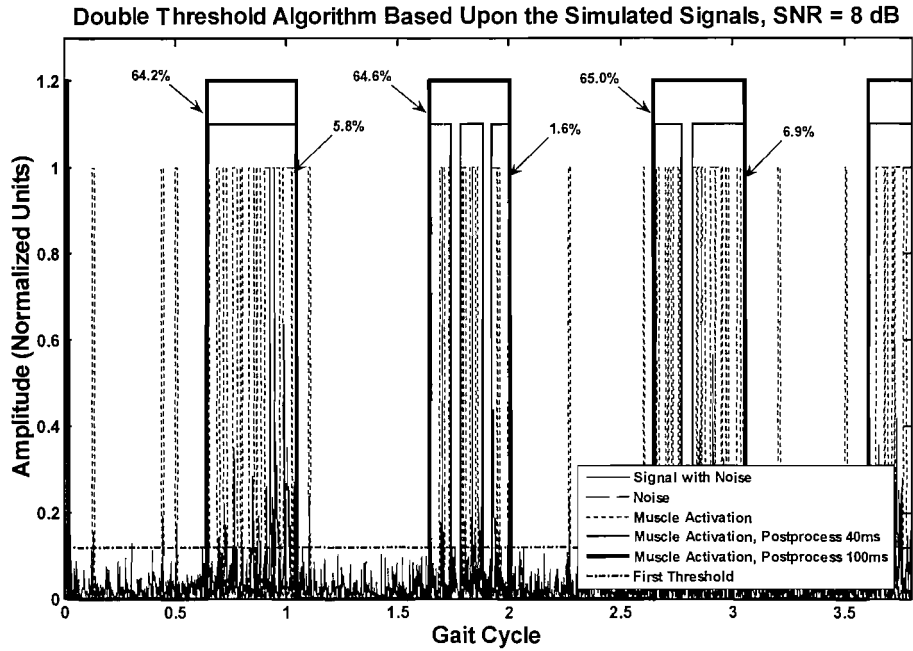
The results of the double-threshold algorithm on the simulated surface EMG signals during the gait cycle produced by the physically-based model are shown in Figure 8-5 and Table 8-2. Larger errors are produced by using this

algorithm. For example, the algorithm presents worse results for the analysis of the simulated surface EMG signals with SNR 6 dB and 8 dB. Standard deviations of onset and cessation timing are 40.8 ms and 69.6 ms for detecting the simulated signal with SNR = 6 dB; and 36.1 ms and 31.9 ms for analysing the simulated signal with SNR = 8 dB. However, the results reported previously for the simulated data produced by the phenomenological model showed the bias of onset and cessation timing is smaller than 10 ms, and the standard deviation is lower than 15 ms.

The results of the estimate of bias and standard deviation of the onset and cessation timing of muscle activation are given in Table 8-2. The bias of timing changes from 0 ms (detected timing is equal to the actual timing of the model) up to -116 ms (detected timing is earlier than the actual timing); the range of standard deviation of timing is between 32 ms and 70 ms. However, for gait analysis, the bias of on-off timing of muscle activation is usually required to be smaller than 30 ms (*Bogey, R A et al., 2000*). Hence, the on-off timings produced by the double-threshold algorithm are not accurate enough to characterize muscle activation intervals. It is evident that the double-threshold algorithm is not suitable for detecting the timing of the simulated surface EMG signal originated from the physically-based model.



(a)



(b)

Figure 8-5 Errors produced by using the double-threshold algorithm to detect the timing of muscle activation for the

simulated surface EMG signals produced by the physically-based model.

In this case, the correct onset timing is 61% of a gait cycle; the correct cessation timing is 7% of a gait cycle. SNR=6 dB and 8 dB. The amplitude values shown in y-axis are normalized to the maximum value of amplitude.

(a) SNR=6 dB. The onset timings of muscle activation are 61.0% GC, 60.0% GC, and 68.0% GC; the cessation timings of muscle activation are 5.5% GC, 95.4% GC, and 4.1% GC. The standard deviation of the onset timing is 40.8 ms; the standard deviation of cessation timing is 69.6 ms..

(b) SNR=8 dB. The onset timings of muscle activation are 64.2% GC, 64.6% GC, and 65.0% GC; the cessation timings of muscle activation are 5.8% GC, 1.6% GC, and 6.9% GC. The standard deviation of the onset timing is 36.1 ms; the standard deviation of cessation timing is 31.9 ms.

Table 8-2 Bias and standard deviation of the onset and cessation timing produced by the double-threshold algorithm applied to the simulated signals generated by the physically-based model.

		Onset Timing				Cessation Timing			
		Bias ms			SD ms	Bias ms			SD ms
		1 st gc	2 nd gc	3 rd gc		1 st gc	2 nd gc	3 rd gc	
SNR	6 dB	0	-10.0	70.0	40.8	-15.0	-116.0	-29.0	69.6
	8dB	32.0	36.0	40.0	36.1	-12.0	-54.0	-1.0	31.9

8.3.4 Other Methods Used in Clinical Research

The traditional methods appear to not be reliable enough to estimate the value of muscle activation intervals. In order to overcome the shortcomings of the traditional methods for clinical application, researchers have used various approaches to estimate the value of this parameter. Recently, EMG onset detection using the maximum likelihood method (*Stylianou, A P, Luchies, C W, and Insana, M F, 2003*) and muscle activity detection based upon the identification of single motor unit action potentials from the surface EMG signal with using the continuous wavelet transform (*Merlo, A, Farina, D, and Merletti, R, 2003*) have been developed. The maximum likelihood method is derived on the basis that the surface EMG signal is considered as

a Gaussian distribution. It leads to a similar result that is brought about from the double-threshold algorithm. The resultant bias of the onset timing estimate is smaller than 40 ms and the standard deviation is lower than 30 ms in the analysis of the simulated signals with signal-to-noise ratio as low as 2 dB by using the algorithm based upon the identification of single motor unit action potentials produced by the use of the continuous wavelet transform (Merlo, A, Farina, D, and Merletti, R, 2003). It is generally accepted that a timing of muscle activation smaller than 30 ms during the analysis of the gait cycle is not an occurrence of muscle activation (Bogey, R A, Barnes, L A, and Perry, J, 1992), a timing greater than 30 ms is considered as a valid muscle activity. Therefore, in order to detect an accurate timing of the muscle activity during walking, the bias of the timing is required to be smaller than 30 ms. Whereas the bias of the timing generated from the continuous wavelet transform is up to 40 ms when it is used to detect the signal with the signal-to-noise ratio more than 2 dB. Hence, the approach based upon the continuous wavelet transform might not suffice for detecting the timing of muscle activation in the gait analysis.

8.4 A Novel Algorithm to Detect the Muscle Activation Timing

8.4.1 Overview of the Algorithm

To overcome the limitations of previously introduced approaches, a novel method, named the *power-threshold algorithm*, is proposed in this section. The power-threshold algorithm is applied to detect the timing of muscle activation, and is specially developed for gait analysis. The algorithm operates on the raw surface EMG signal and is assessed by simulated EMG signals produced by the physically-based model introduced previously. The basic detector parameters comprise the length of the observation window (w), initial threshold (th_0), threshold coefficient (λ), and final threshold (th).

In the following, the mathematical derivation of the power-threshold algorithm and the optimal selection of its parameters are described first and discussed. Then, an additional post-processor of the detection is illustrated to eliminate erroneous transitions due to the nature of the simulated signal. The performance of the algorithm is presented in terms of bias and standard deviation of the estimates of the timing of simulated surface EMG signal during dynamic movement. Finally, comparing previously developed methods and the power-threshold algorithm, the advantages of the latter is outlined. The algorithm is designed for a complete real-time implementation and may be employed in clinical routine activity. The performance of the algorithm on the real surface EMG signals recorded from the gait experiment is also shown in this section.

8.4.2 Derivation of the Algorithm

The simulated signal $x(t)$ consists of the pure surface EMG signal $s(t)$ which is the summation of motor unit action potential trains modulated by the muscle activity during dynamic movement, and additional noise $n(t)$ which is created by an independent zero-mean Gaussian distribution. Equations 8.7, 8.8, and 8.9 express the simulated signal, the variance of the simulated signal (signal $s(t)$ and noise $n(t)$ both present), and the variance of the noise signal (only noise present).

$$x(t) = s(t) + n(t) \tag{8.7}$$

$$\sigma_x^2 = \frac{1}{N-1} \sum_{i=0}^{N-1} (x_i - \mu_x)^2 \tag{8.8}$$

$$\sigma_n^2 = \frac{1}{N-1} \sum_{i=0}^{N-1} (n_i - \mu_n)^2 \tag{8.9}$$

Where, N is the length of the signal; μ_x is the mean of $x(t)$; μ_n is the mean of $n(t)$.

In the algorithm, the muscle activity may be considered as a valid action when the power of the surface EMG signal exceeds the power threshold set by the algorithm. The behaviour of the power-threshold algorithm is fixed by the values of the parameters and their values are selected to jointly minimize the value of standard deviation of timing of muscle activation. The selection of parameters' values is shown in Section 8.4.3.

The length of the observation window is determined by the desired time resolution that is generally smaller than 10 ms and by the standard deviation of the timing of muscle activation. The initial threshold is calculated by using the length of the observation window multiplied by the power of noise σ_n^2 presented in the simulated signals. The threshold coefficient is applied varying its value from one to three in steps of 0.2, in order to assess the performance of this algorithm on simulated signals. The suitable value of the threshold coefficient is chosen to calculate the final threshold (see Table 8-3). The final threshold is described by the equation:

$$th = \lambda \cdot th_0 \tag{8.10}$$

($\lambda=1.2, 1.4, 1.6 \dots 2.8, 3.0$)

The on-off timing of muscle activation is estimated by comparison of the power of the surface EMG signals within the observation window with the value of the final threshold. The power of surface EMG signals exceeding the final threshold is considered as a valid muscle activity. All transitions lasting more than 30 ms are considered as valid muscle activations, and a distance between two consecutive valid activations smaller than 100 ms is considered to belong to the same contraction and is merged.

A flowchart of the algorithm based upon the calculation of power of surface EMG signal for analysing the timing of muscle activation is shown in Figure 8-6.

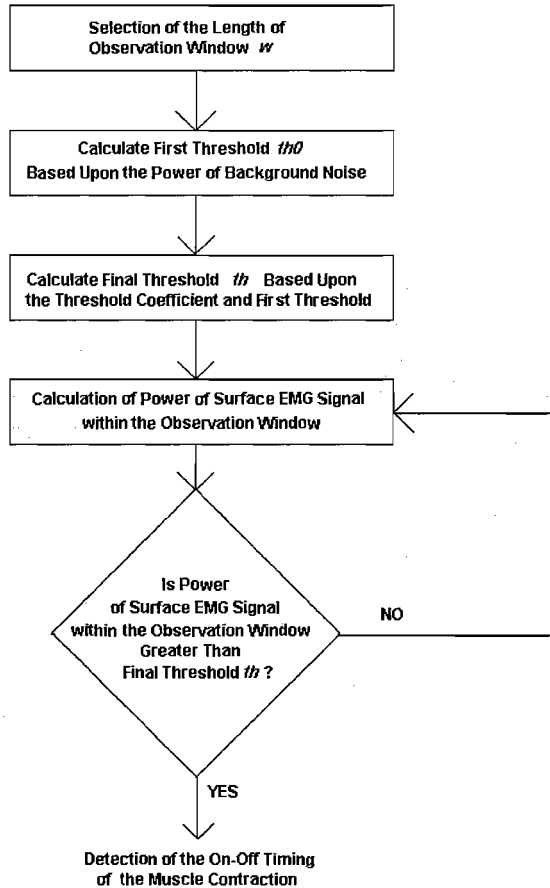


Figure 8-6 Flowchart of the power-threshold algorithm to detect the on-off timing of muscle contraction.

8.4.3 Selection of the Basic Parameters of the Algorithm

Tuning the algorithm parameters may alter its behaviour and their values may be chosen by computation of the standard deviation of the timing of muscle activation based upon the various SNRs and the time resolution.

8.4.3.1 Determination of the Length of the Observation Window

The simulated surface EMG signal is sampled at 1000 Hz in our model. Therefore, if the desired time resolution is smaller than 20 ms, the length of the observation window must not more than 20 samples. Increasing the length of the observation window will reduce the time resolution. The acceptable time resolution is smaller than 10 ms during dynamic movement and thus the length of the observation window should be less than 10 samples in analysis of the muscle activity during the gait cycle. A brief guideline for the selection of the length of the observation window is given by study of the relationship between the detection accuracy and the length of the observation window presented by Table 8-3. A valid length of the observation window is necessary to improve the detection accuracy and to be compatible with an acceptable time resolution while other parameters are maintained. In Table 8-3 the length of the observation window is considered as a variable, while the threshold coefficient and signal-to-noise ratio are kept constant. The length of the observation window is chosen from 1 to 10 samples. It is evident that, for a fixed SNR and λ , the corresponding value of standard deviation changes as the length of the observation window alters. The probability of detection increases as the length of observation window increases. Moreover, the value of standard deviation may begin to increase when the length of the observation window is greater than eight samples. The minimum value of standard deviation, and hence the maximum detection accuracy, occurs when the length of the observation window is 7-9 samples. As a result, the length of the observation window is considered as 8 samples in this study.

8.4.3.2 Calculation of the Initial Threshold

The initial threshold is determined by the noise power and the length of the observation window. The noise power depends on the noise within the simulated surface EMG signal. For the simulated surface EMG signal, the

noise power can be obtained directly by solving the equation 8.9. It also corresponds to two parameters, the SNR and the signal power, and can be calculated by solving equation 8.11 with respect to the signal power obtained from the equation 8.8. For the real surface EMG signal, the noise power can be estimated by calculating the variance of the background noise, which can be recorded from the muscle during relaxation.

$$\sigma_n^2 = \frac{\sigma_x^2}{10^{SNR/10}} \quad 8.11$$

Moreover, the particular value of the length of the observation window w is selected from Table 8-3, and the initial threshold is then described by the following equation 8.12:

$$th_0 = w \cdot \sigma_n^2 = w \cdot \frac{1}{N-1} \sum_{i=0}^{N-1} (n_i - \mu_n)^2 \quad 8.12$$

8.4.3.3 Calculation of the Final Threshold

The final threshold is determined by both the value of threshold coefficient and the initial threshold. The effect of the threshold coefficient on the result of this algorithm is presented by the standard deviations of the timing of muscle activation reported by Table 8-3. In this case, the threshold coefficient λ is set from one to three in steps of 0.2, $\lambda = 1.2, 1.4, 1.6 \dots 2.8, 3.0$, so that we can choose the best performance of the timing detection by comparing the values of standard deviation based upon the different values of threshold coefficient λ that correspond to the fixed signal-to-noise ratio (SNR = 8 dB, 10 dB and 20 dB) and the particular the length of the observation window. The final threshold is expressed by the equation 8.9.

The relationship between these three parameters, the final threshold, the threshold coefficient, and the length of the observation window, is given in Figure 8-7. It is evident that the final threshold increases as λ increases from

1.2 to 3 when a specific value of w is selected. In fact, the error due to a spike during the relaxation of the muscle is quite high when the final threshold is set to a small value, while the error due to a small difference between the signals of the relaxation and voluntary contraction of the muscle becomes greater when the final threshold is set to a high value. In this case, the value of the final threshold can be chosen with regard to the standard deviation of the timing. The results shown in Table 8-3 depict that the best value of the standard deviation of the timing occurs when the threshold coefficient is set to the range between 1.6 and 2.0.

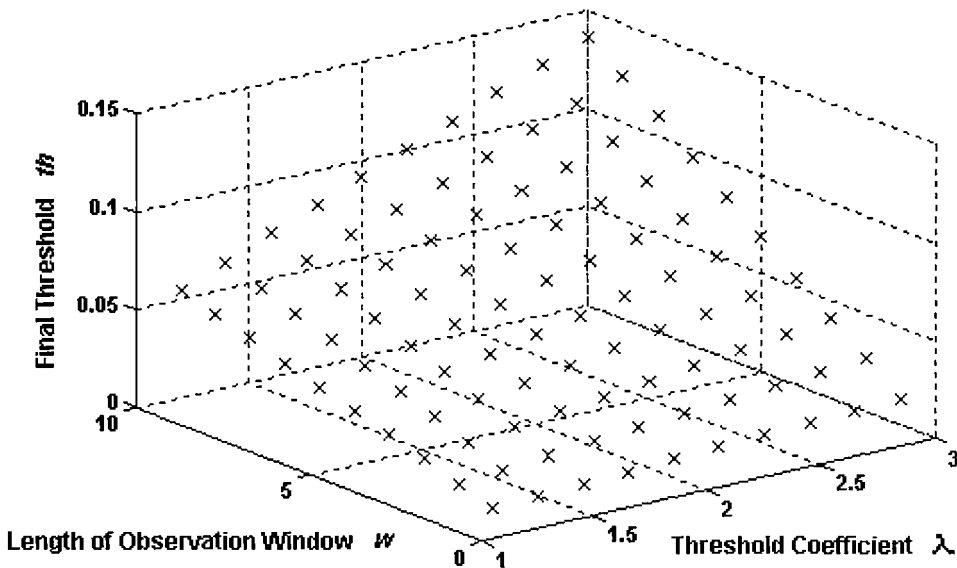


Figure 8-7 The relationship between the final threshold, the length of the observation window and the threshold coefficient. In this case, the fixed signal-to-noise of the simulated EMG signals is 8 dB.

To summarize, the proposed procedure consists of the following steps. First the length of the observation window is set to the range from 1 to 10 samples. The threshold coefficient is set from one to three at the steps of 0.2, $\lambda = 1.2, 1.4, 1.6 \dots 2.8, 3.0$. Second, choosing the particular values of w and λ to achieve the best value of standard deviation of the timing when SNR is fixed. The behaviour of the parameters is depicted in Table 8-3. Third, the

initial threshold is obtained by solving the noise power that corresponds to SNR and signal power or by estimating the variance of the background noise in practice. Finally, the final threshold is calculated by multiplying the initial threshold by the threshold coefficient. Table 8-3 presents the family of standard deviations of the timing obtained for the different values of the length of the observation window, the threshold coefficient and SNR. It is evident that the acceptable standard deviation of the timing may be achieved given the selected values of w and λ for different values of SNR. The results given by Table 8-3 show that the desired standard deviation of the timing that is smaller than 7 ms occurs as $w = [7,8,9]$ and $\lambda = [1.6,1.8,2.0]$. For the simulated surface EMG signal with different SNR 8 dB, 10 dB and 20 dB, the performance of the algorithm with the particular values of parameters $w = 8$ and $\lambda = 1.8$ is also shown in Figure 8-8.

Table 8-3 The standard deviation of the timing of muscle activation for different lengths of the observation window (w) and different threshold coefficients (λ) based upon the simulated surface EMG signal of a fixed signal-to-noise ratio.

In this case, the length of observation window is smaller than 10 ms, $w = 1, 2, 3 \dots 10$; threshold coefficient λ from one to three in steps of 0.2, $\lambda = 1.2, 1.4, 1.6 \dots 2.8, 3.0$; signal-to-noise ratio equal to 8 dB, 10 dB, and 20 dB.

(i) The standard deviation of the timing of muscle activation for the simulated signals with signal-to-noise equal to 8 dB. The length of observation window w and the threshold coefficient λ resulting in the lower standard deviation (≤ 7 ms) are highlighted.

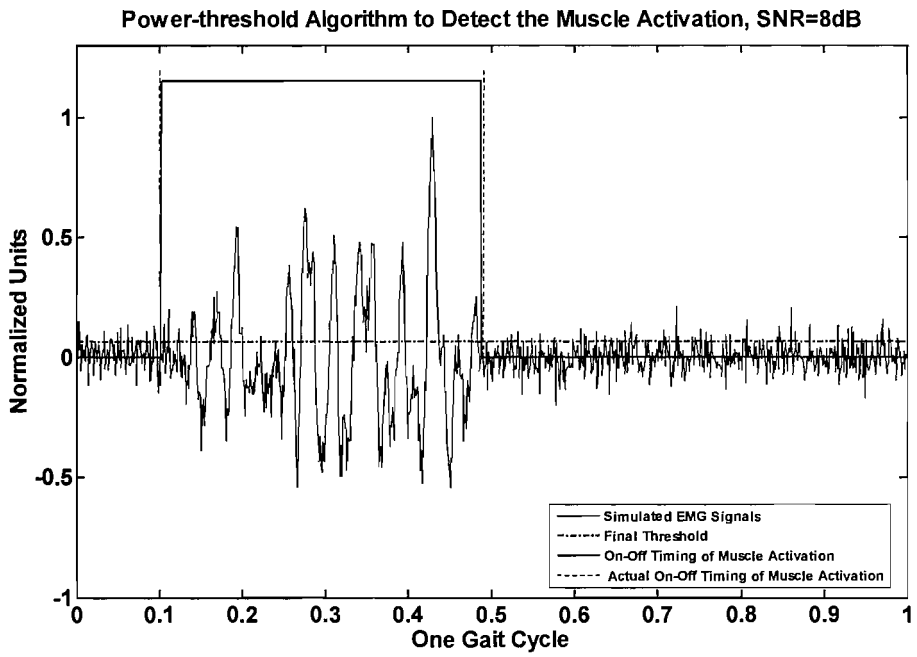
The Standard Deviation, SNR = 8 dB												
ms												
		Threshold Coefficient λ										
		1.2	1.4	1.6	1.8	2.0	2.2	2.4	2.6	2.8	3.0	
Length of observation window w (samples)	1	--	--	--	--	--	--	--	--	--	--	--
	2	--	--	--	--	--	--	--	--	--	--	7
	3	--	--	--	--	--	--	--	9	9	9	9
	4	--	--	6	6	7	7	7	19	19	19	19
	5	--	--	6	7	7	17	17	17	17	17	17
	6	--	8	6	18	18	18	18	18	18	18	21
	7	--	6	6	6	6	6	6	23	23	23	23
	8	8	8	3	3	3	19	19	19	19	19	19
	9	3	3	3	15	15	19	19	19	19	19	19
	10	6	15	15	15	15	15	15	15	15	15	20

(ii) The standard deviation of the timing of muscle activation for the simulated signals with signal-to-noise equal to 10 dB. The length of observation window w and the threshold coefficient λ resulting in the lower standard deviation (≤ 7 ms) are highlighted.

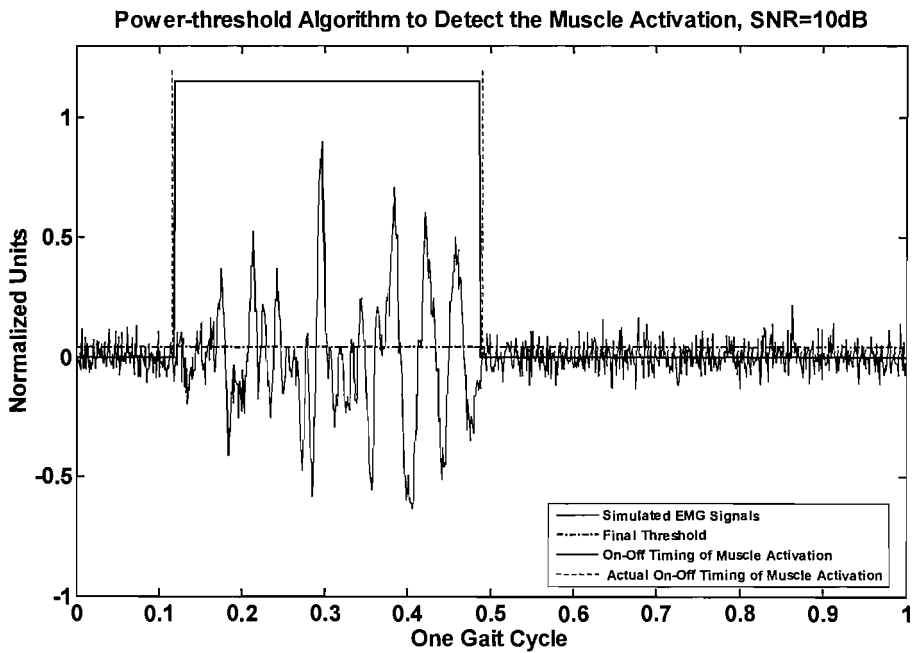
The Standard Deviation, SNR = 10 dB ms											
		Threshold Coefficient λ									
		1.2	1.4	1.6	1.8	2.0	2.2	2.4	2.6	2.8	3.0
Length of observation window w (samples)	1	--	--	--	--	--	--	--	--	--	--
	2	--	--	--	--	--	67	18	5	5	6
	3	--	--	--	50	36	6	6	9	9	9
	4	--	--	--	5	5	5	5	9	9	9
	5	--	28	5	5	5	5	7	7	7	27
	6	--	23	6	6	6	6	6	10	10	10
	7	--	5	5	5	5	5	5	5	5	5
	8	--	3	3	3	7	7	7	7	7	27
	9	--	8	8	7	7	7	7	7	7	30
	10	--	3	3	7	7	7	27	27	27	27

(iii) The standard deviation of the timing of muscle activation for the simulated signals with signal-to-noise equal to 20 dB. The length of observation window w and the threshold coefficient λ resulting in the lower standard deviation (≤ 7 ms) are highlighted.

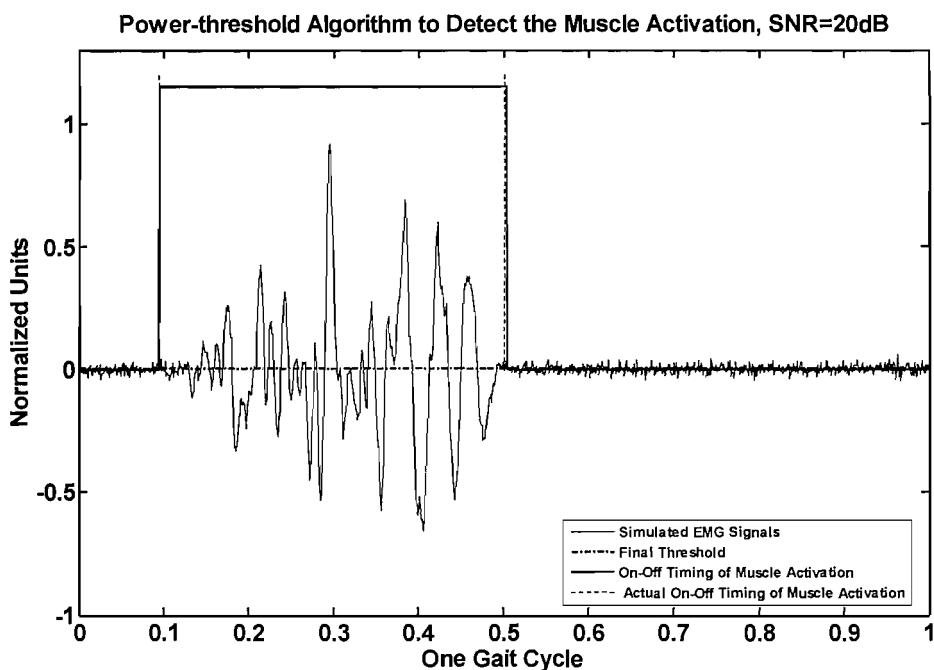
The Standard Deviation, SNR = 20 dB ms											
		Threshold Coefficient λ									
		1.2	1.4	1.6	1.8	2.0	2.2	2.4	2.6	2.8	3.0
Length of observation window w (samples)	1	--	--	--	--	--	--	--	--	--	--
	2	--	--	--	--	--	--	51	51	27	27
	3	--	--	--	--	--	14	14	5	7	7
	4	--	--	--	18	22	22	8	8	8	20
	5	--	--	--	7	7	7	7	7	7	20
	6	--	--	17	17	5	7	7	7	7	7
	7	--	--	--	5	4	6	6	10	10	21
	8	--	14	2	2	6	6	6	18	18	18
	9	--	19	5	4	4	18	18	18	18	18
	10	--	3	2	2	2	7	23	23	23	23



(a)



(b)



(c)

Figure 8-8 The performance of the algorithm with the length of observation window $w = 8$ and the threshold coefficient $\lambda = 1.8$, in the processing of the simulated EMG signals with signal-to-noise ratio (a) 8 dB, (b) 10 dB and (c) 20 dB.

The actual on-off timing of muscle activation produced by the physically-based model is shown by the dashed line, the on-off timing of muscle activation detected by the algorithm is displayed by rectangular window plotted by the bold line, and final threshold are depicted by the dash-dot line as well. A post processor is applied. All transitions lasting more than 30 ms are considered as valid muscle activations and a distance between two consecutive valid activations smaller than 100 ms is considered to belong to the same contraction and merged. The amplitude values shown in y-axis are normalized to the maximum value of amplitude.

8.4.4 The Post Processor

Due to the characteristics of the surface EMG signal and the size of the observation window, the output of the algorithm may be affected by erroneous transitions that may bring about a reduced performance. Figure 8-9(e) illustrates this clearly and shows the timing of muscle activation during a gait cycle in the case of the parameters $w = 8$, $\lambda = 1.8$. The rectangular

functions depicted by the dashed line present the muscle activation intervals. The binary output switches from zero to one at the time instant that corresponds to the start point of the observation window. The output of zero shows that the summation of the signal power within the observation window is lower than the final threshold; the output of one shows that the summation of the signal power exceeds the final threshold. The erroneous transitions of the output occur because the samples contained by the observation window are very small numbers. Moreover, the time resolution requires that the size of the observation window is not larger than 10 samples. Therefore, it is essential to apply a post processor to correct all transitions and obtain a reliable estimate of the muscle activation intervals.

Different applications might require a different time resolution that determines the length of observation window. Hence, different post processor approaches would be used for the different applications in order to eliminate the erroneous transitions. In general, muscle activation smaller than 30 ms has no influence on controlling the movement during gait (*Bogey, R A, Barnes, L A, and Perry, J, 1992; Bonato, P, D'Alessio, T, and Knaflitz, M, 1998*). In this case, for our simulated signals, all transitions less than 30 ms are rejected and considered as an invalid muscle contraction. At the same time, when the distance between two consecutive transitions is lower than 100 ms, they are considered as belonging to the same contraction and merged. Figure 8-9 (a) (e) (f) (g) illustrates the effect of the post processor. The muscle activation interval of the simulated surface EMG signal during a gait cycle that is detected by the algorithm depicted by the rectangular window plotted by the dashed line, and the actual on-off timing of muscle activation presented by the solid line are shown in Figure 8-9(g). It is evident that the erroneous transitions are rejected and muscle activation intervals are detected correctly. The result illustrates that the post processor may discard the erroneous transitions and recognizes valid on-off timing of muscle activity.

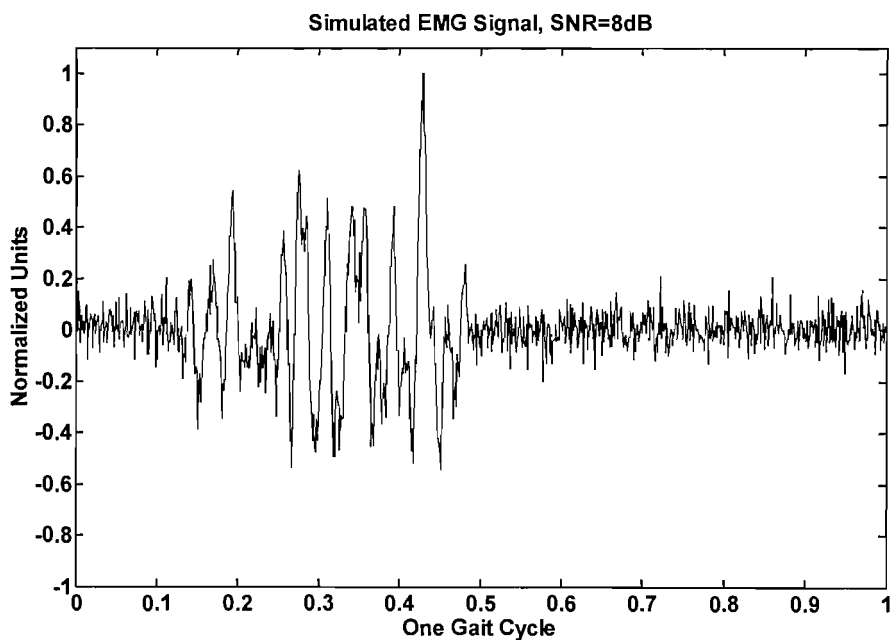
8.4.5 Output of the Algorithm

The complete algorithm used to detect the simulated surface EMG signal is summarized below:

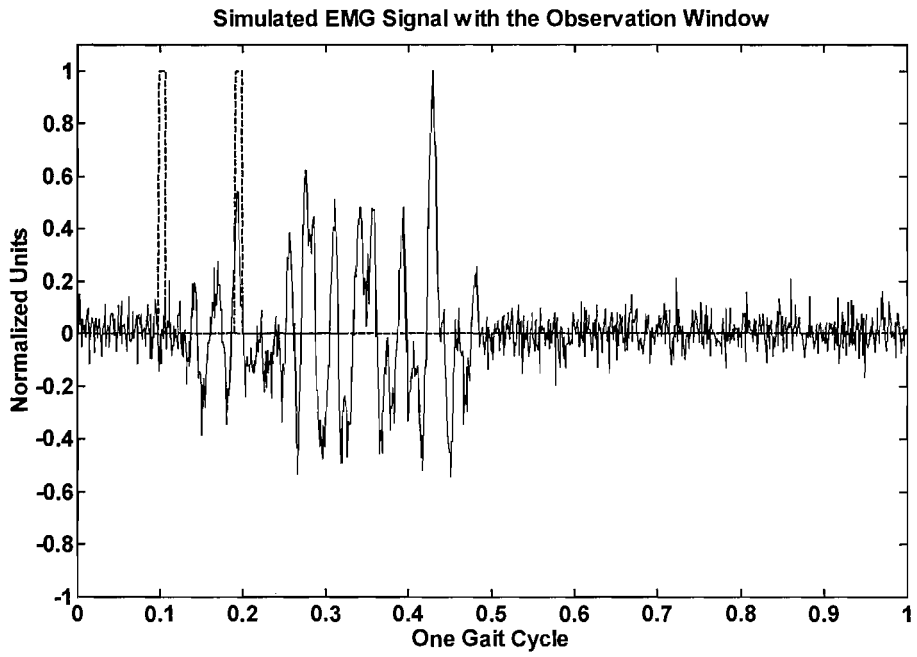
- (1) Selection of the length of the observation window, $w = 8$ is chosen in order to achieve the best performance of detection (see Table 8-3).
- (2) Calculation of the initial threshold, th_0 .

$$th_0 = w \cdot \sigma_n^2 = w \cdot \frac{1}{N-1} \sum_{i=0}^{N-1} (n_i - \mu_n)^2$$

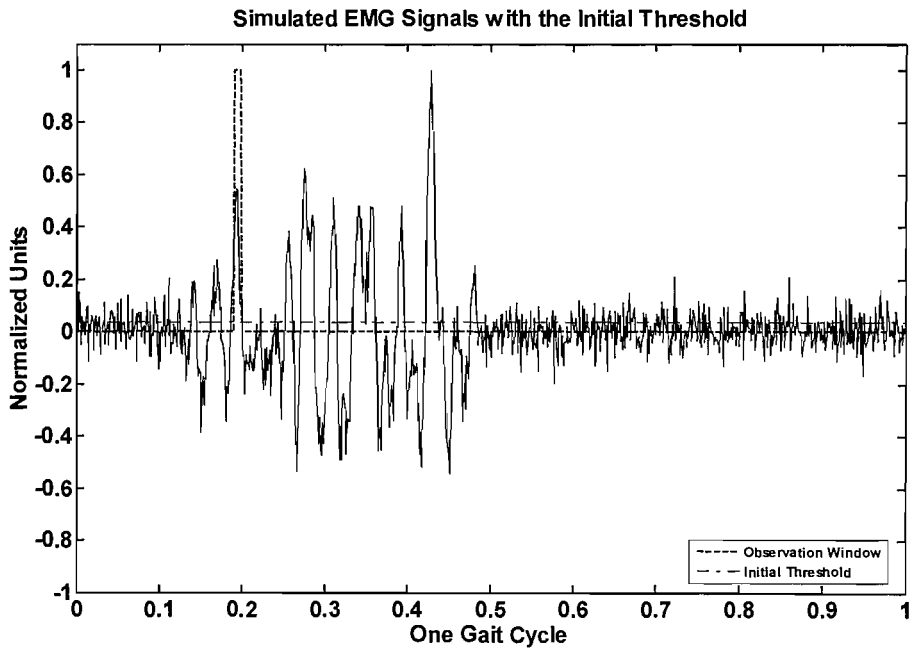
- (3) Selection of the threshold coefficient λ , in this case, $\lambda = 1.8$.
 - (4) Calculation of the final threshold th , $th = \lambda \cdot th_0$.
 - (5) Comparison between the power of the simulated surface EMG signal contained within the observation window and the final threshold.
 - (6) Using the postprocessor to eliminate the erroneous transitions.
- The whole process of the algorithm is presented in Figure 8-9



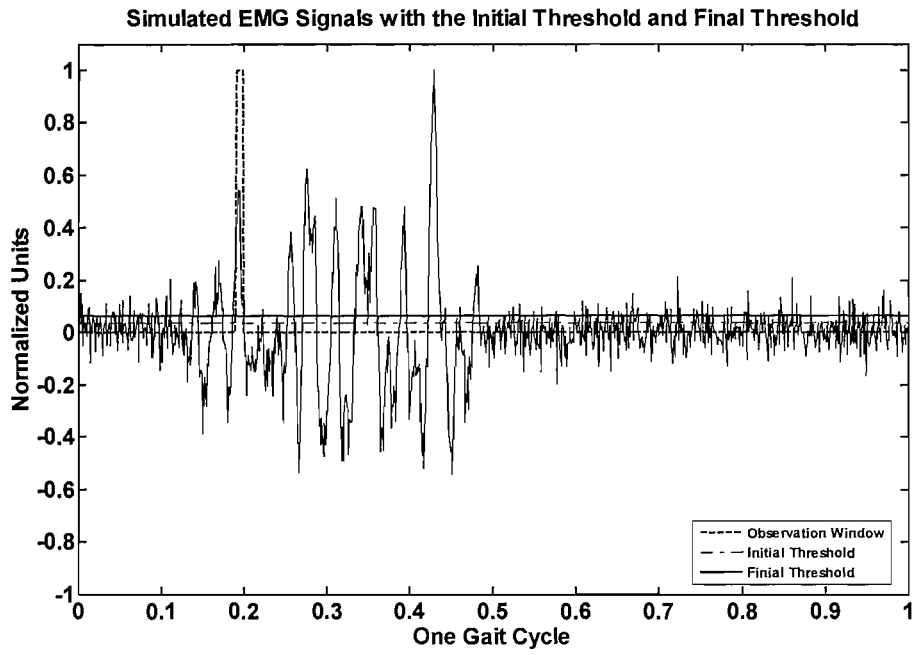
(a)



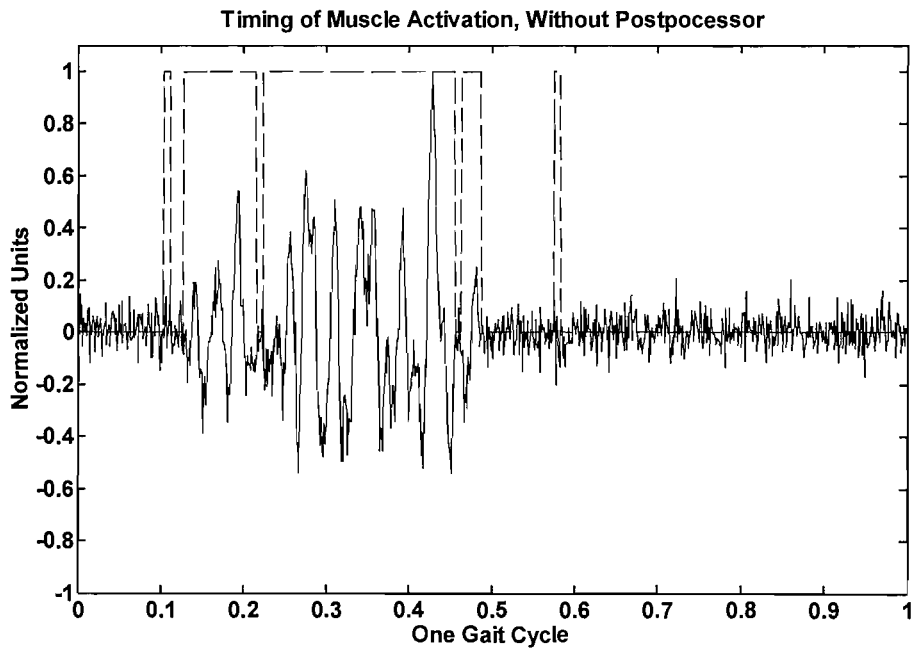
(b)



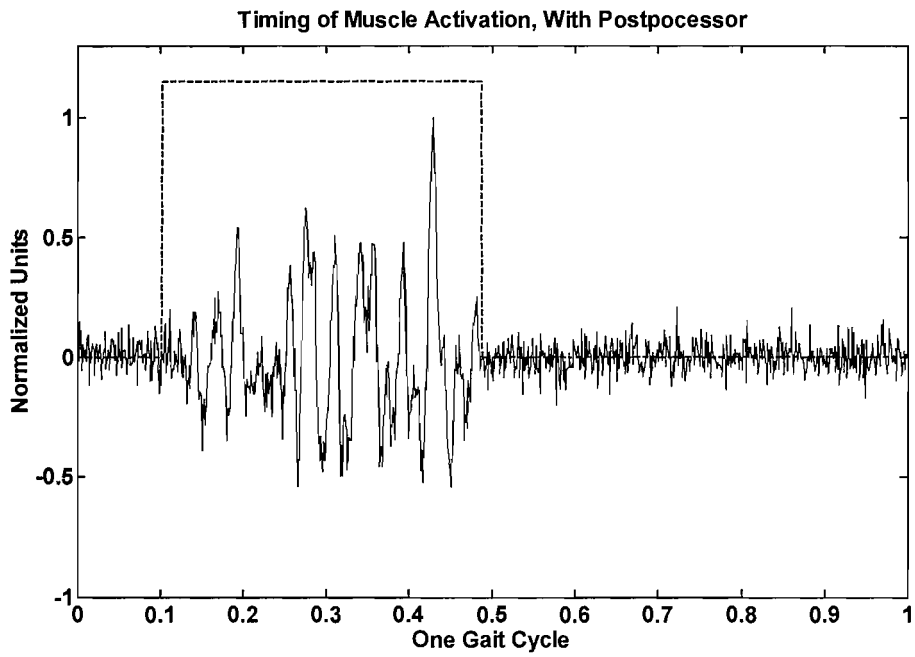
(c)



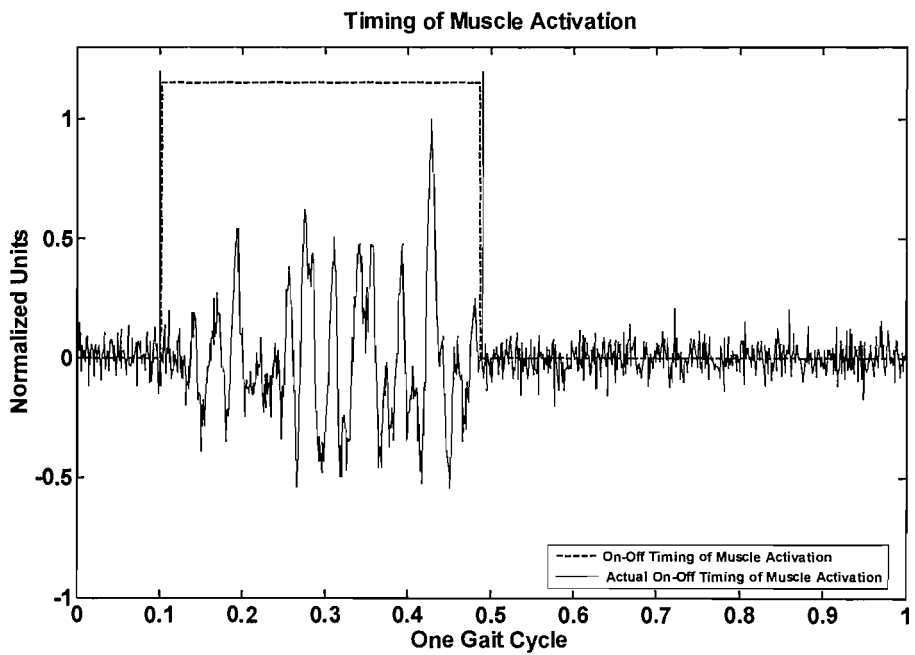
(d)



(e)



(f)



(g)

Figure 8-9 The complete algorithm.

- (a) A simulated surface EMG signal during a gait cycle, SNR=8 dB.
 - (b) The signal and observation windows. In this case, the length of observation windows that are depicted by rectangular windows plotted by the dashed line is 8 samples.
 - (c) The signal, the observation window and the initial threshold. The initial threshold presented by the dash-dot line is obtained by calculation of the power of the noise contained within the observation window.
 - (d) The signal, the observation window, the initial threshold and the final threshold. The initial threshold and final threshold are respectively depicted by the dash-dot line and the bold solid line. The final threshold is calculated by multiplying the initial threshold by the threshold coefficient. In this case, the threshold coefficient $\lambda = 1.8$.
 - (e) The on-off timing of muscle activation without a post processor. The muscle activation intervals are shown by the rectangular windows plotted by the dashed line.
 - (f) The on-off timing of muscle activation with a post processor. In this case, all transitions less than 30 ms are assumed as an invalid muscle activity and the distant between two consecutive transitions lower than 100 ms is merged. The onset and cessation timing are shown by a rectangular window described the dashed line.
 - (g) The on-off timing of muscle activation produced by the algorithm (dashed line) and the actual timing of muscle contraction (solid line).
- The amplitude values of the simulated surface EMG signals shown in y-axis are normalized to the maximum value of amplitude.

8.5 Statistical Analysis of the Algorithm

The statistical characteristics of the algorithm are described by the two parameters: *Bias* and *Standard deviation*.

Bias is expressed by the following equation:

$$bias = t_i - t_0 \tag{8.13}$$

Where $i = 1, 2, 3 \dots N_{gc}$, N_{gc} is the number of the gait cycle. For the simulated surface EMG signal, N_{gc} is equal to 3. The t_i is the estimate of on-off timing of muscle activation obtained by the algorithm; t_0 is the known on-off timing of muscle activation. For the real surface EMG signal recorded from the gait experiment, t_0 is the mean of the t_i .

Standard deviation of the timing is defined by the equation:

$$\sigma_d = \sqrt{\frac{1}{N_{gc}} \sum_{i=1}^{N_{gc}} (t_i - \bar{t})^2} \quad 8.14$$

Where, \bar{t} is the mean of the t_i .

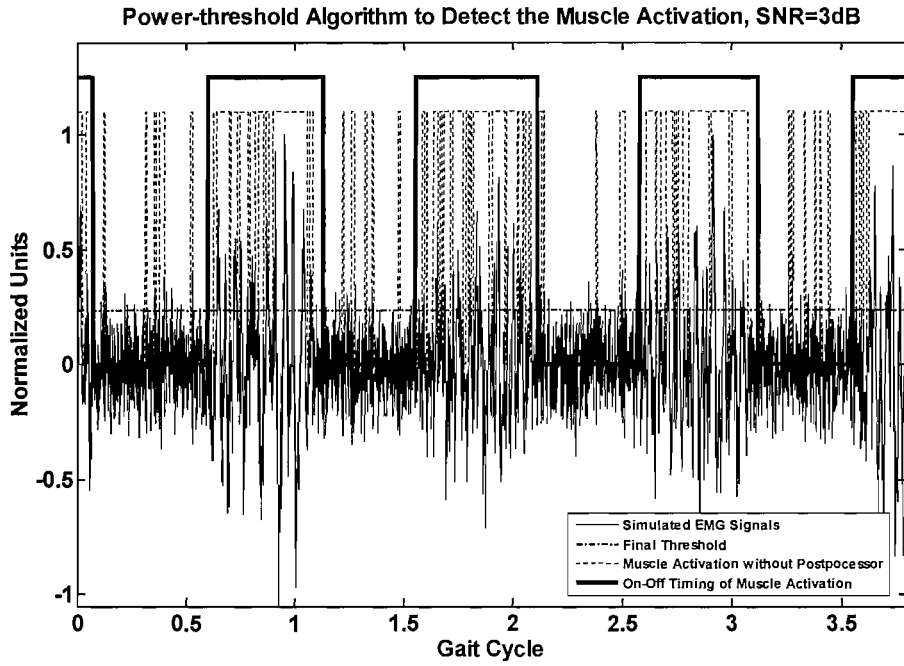
The standard deviations of the timing of muscle activation for simulated surface EMG signals with different signal-to-noise ratios (SNR=3 dB, 6 dB, 8 dB, 10 dB and 20 dB) are shown in Table 8-4. Results illustrate the standard deviation of the timing is lower than 20 ms for the signals with SNR greater than or equal to 3 dB. Moreover, the standard deviation of timing for the real data is given in Table 8-5. Results indicate the standard deviation of timing is lower than 25 ms. It is evident that the power-threshold algorithm is suitable for analysing the timing of muscle activity during gait analysis.

8.6 Applications of the Algorithm in the Analysis of the Muscle Activation Intervals

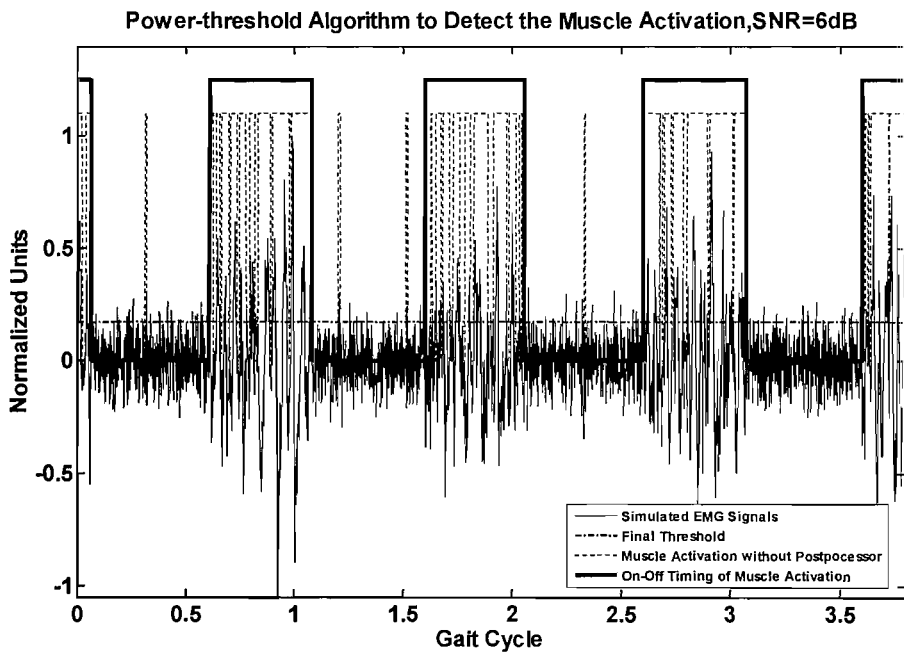
8.6.1 Detection the On-Off Timing of Muscle Activation of the Simulated Surface EMG Signals

The performance of the algorithm is shown in Figure 8-10 and statistical results are given in Table 8-4. In Figure 8-10, the on-off timings of muscle activation are depicted by the rectangular windows plotted by the bold solid line. All transitions without post-processing are displayed by the rectangular windows plotted by the dashed line. The final threshold is also displayed by the dash-dot line. In this case, the length of observation window is 8; the threshold coefficient is 1.8 (but is 1.2 when the SNR = 3 dB). In the post-

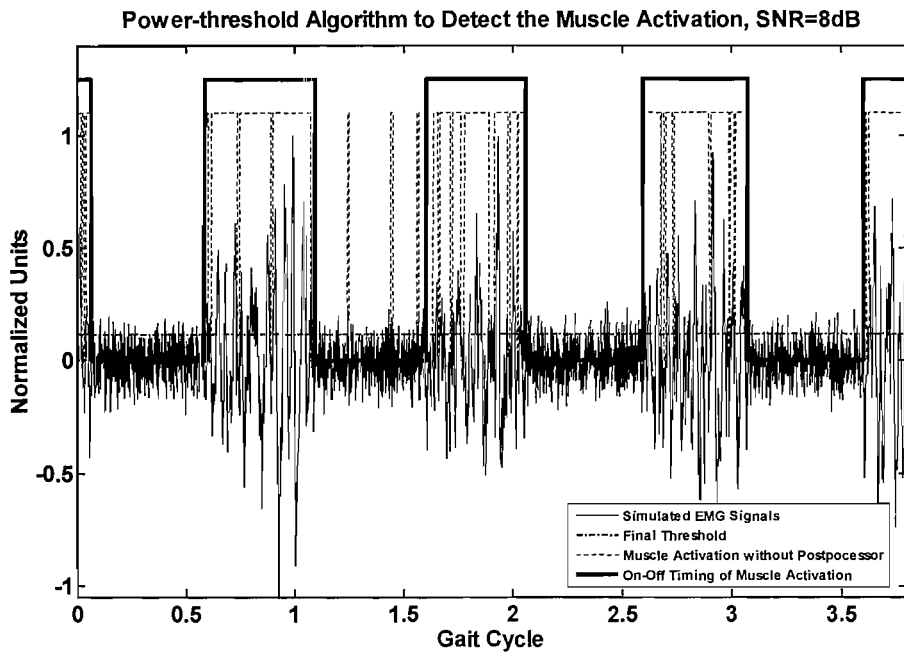
processor, all transitions less than 30 ms are rejected. The distance between two consecutive transitions lower than 100 ms are considered as belonging to the same contraction. Results illustrate that it is suitable to analyse the simulated surface EMG signals originated from the physically-based model.



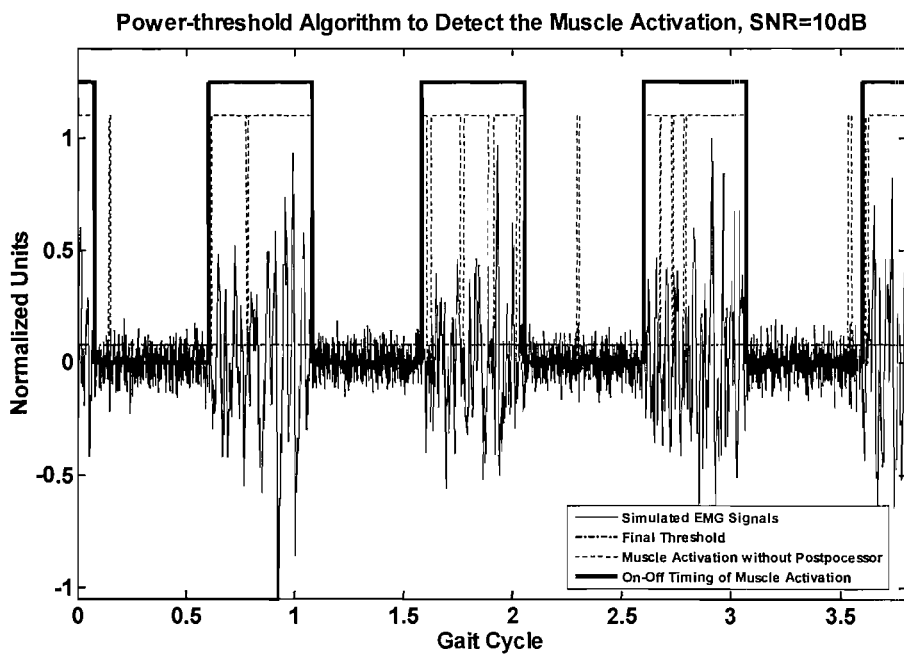
(a)



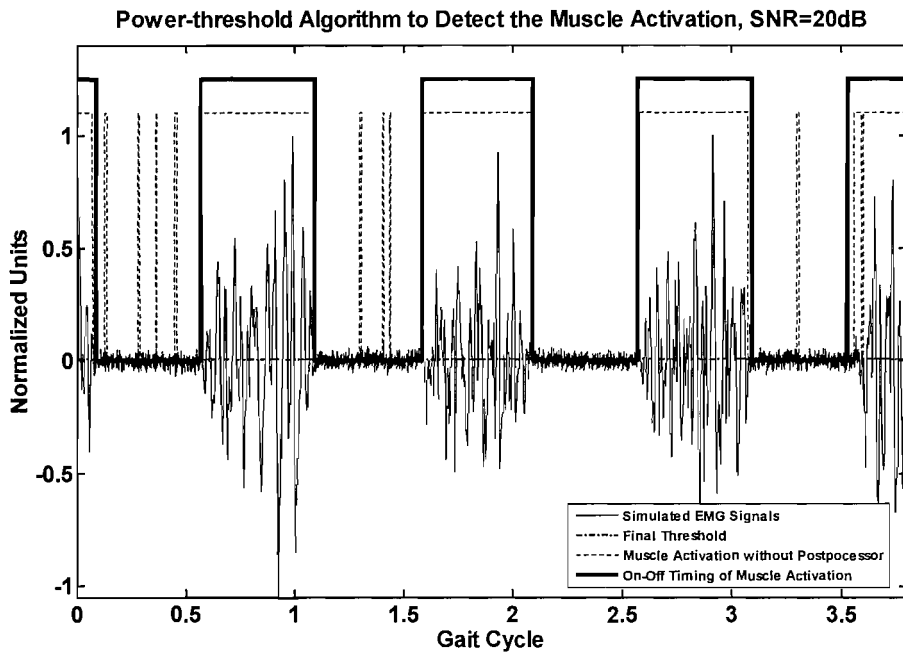
(b)



(c)



(d)



(e)

Figure 8-10 The performance of the algorithm on the simulated surface EMG signals with SNR = 3 dB, 6 dB, 8 dB, 10 dB, and 20 dB produced by the physically-based model.

Table 8-4 The standard deviation of the timing of muscle activation by using the algorithm. In this case, SNR = 3 dB, 6 dB, 8 dB, 10 dB, and 20 dB; the observation window w is 8 samples.

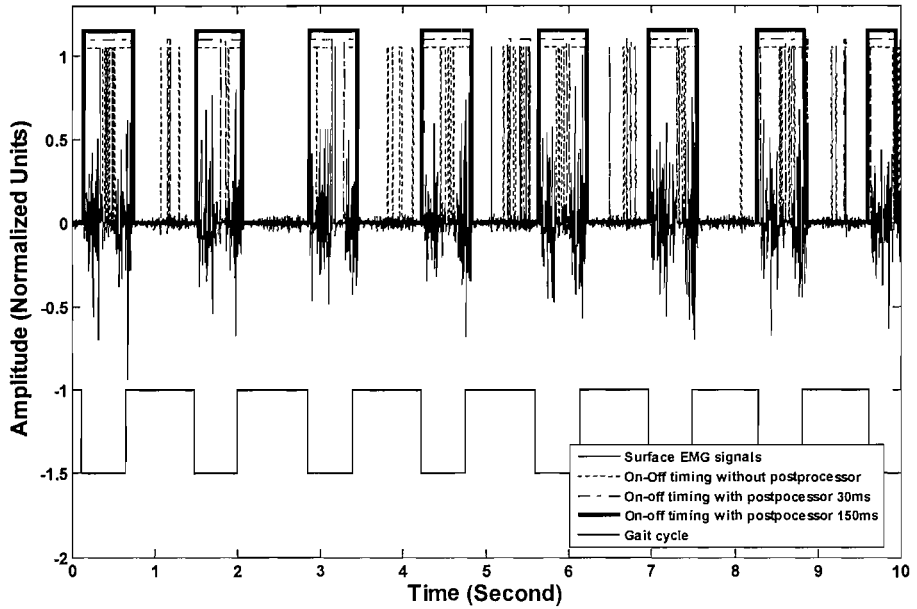
The Standard Deviation					
ms					
	SNR=3 dB	SNR=6 dB	SNR=8 dB	SNR=10 dB	SNR=20 dB
	$\lambda=1.2$	$\lambda=1.8$	$\lambda=1.8$	$\lambda=1.8$	$\lambda=1.8$
Standard deviation	16	9	12	11	5

8.6.2 Detection of On-Off Timing of Muscle Activation of Real Surface EMG Signals Recorded from the Gait Experiment

After examining the algorithm based upon a series of simulated surface EMG signals, it is necessary to test the algorithm in real-life clinical situations in order to fully assess the feasibility and validity of the new algorithm in practice. Hence, in this section, the algorithm is applied to the real surface EMG signals which are collected from the gait experiment addressed in Chapter 6. During the gait experiment, the surface EMG signals of three muscles and foot switch signals are recorded at the same time. Signal processing is used to improve the quality of the raw signals. For example, a band-pass filter was chosen to pre-process the raw surface EMG signal to eliminate the movement artefacts and cut off the high frequency components to reduce the aliasing phenomenon. The lower and upper cut-off frequencies were 8 Hz and 500 Hz, respectively.

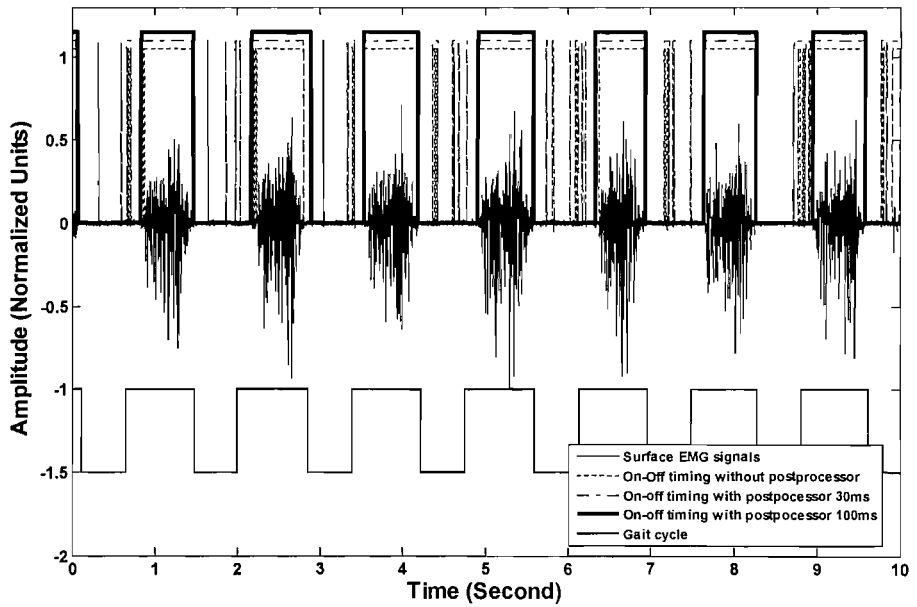
Figure 8-11 shows the muscle activation intervals of three muscles, tibialis anterior, gastrocnemius medialis and gastrocnemius lateral, during the gait cycle. On-off timings of muscle activation during walking are displayed by the rectangular windows plotted by the bold solid line. It is evident that three muscles are activated regularly related to the foot switches. Furthermore, the statistical results are shown in Table 8-5. In this case, the surface EMG signals recorded from the tibialis anterior muscle are chosen to assess the algorithm. Based upon the data recorded from 10 subjects, the standard deviations of muscle activation intervals are calculated and displayed, respectively. The standard deviation of timings of muscle activation is smaller than 25 ms, and the average is lower than 18 ms. The performance of the algorithm illustrate that it is suitable for the detection of muscle activation intervals during the gait cycle.

Muscle Activation Intervals Estimated by the Power-threshold Algorithm, Tibialis Anterior



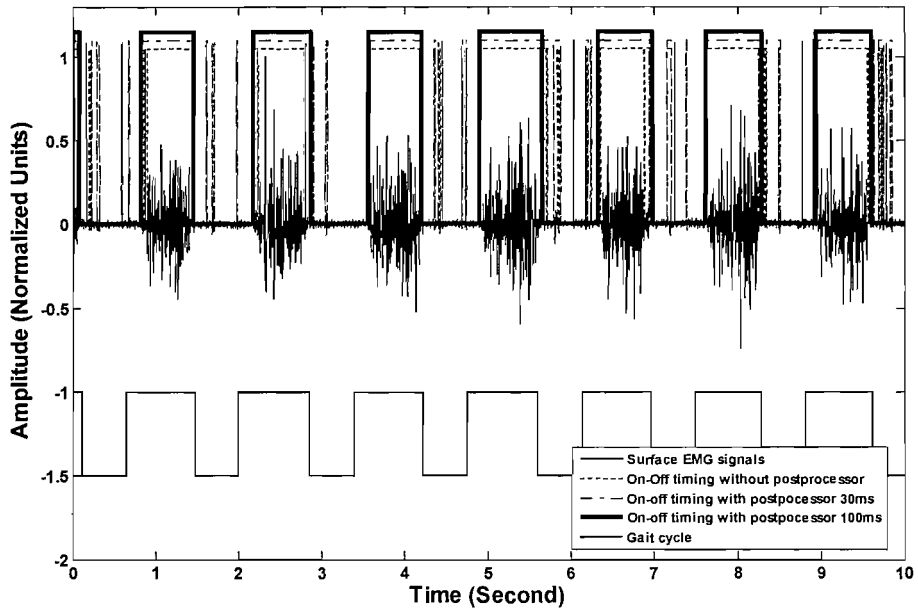
(a)

Muscle Activation Intervals Estimated by the Power-threshold Algorithm, Gastrocnemius Medialis



(b)

Muscle Activation Intervals Estimated by the Power-threshold Algorithm, Gastrocnemius Lateral



(c)

Figure 8-11 The performance of the power-threshold algorithm on the real surface EMG signal recorded from the gait experiment.

- (a) On-off timing of muscle activation of the tibialis anterior;
- (b) On-off timing of muscle activation of the gastrocnemius medialis;
- (c) On-off timing of muscle activation of the gastrocnemius lateral;

In the Figures, the surface EMG signals are shown plotted by the solid line. The foot switches are displayed by the rectangular windows plotted by the solid line under the surface EMG data. The on-off timings of muscle activation are displayed by the rectangular windows plotted by the bold solid line. All transitions without the post processor are depicted by the rectangular windows plotted by the dashed line. The on-off timings with part of the post processor, which rejects the transitions less than 30 ms, are also shown by the rectangular windows plotted by the dash-dot line.

Table 8-5 *The standard deviation of the timing of muscle activation produced by applying the algorithm to the real surface EMG data recorded from the tibialis anterior muscle of the healthy adults.*

The Standard Deviation		
Participants	Standard Deviation ms	Average ms
Subject 1	13	18
Subject 2	19	
Subject 3	23	
Subject 4	17	
Subject 5	18	
Subject 6	14	
Subject 7	21	
Subject 8	18	
Subject 9	17	
Subject 10	21	

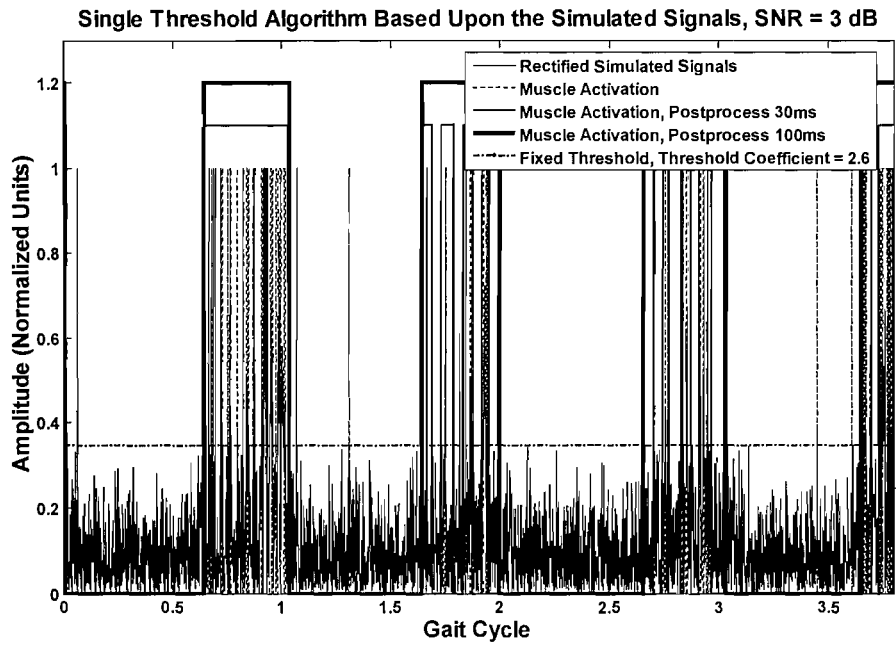
8.7 Comparison with Other Methods

The objective of this section is to examine the different algorithms and compare them with the power-threshold algorithm. The performances of the single-threshold algorithm, double-threshold algorithm and the algorithm presented in this study are assessed based upon a series of the simulated surface EMG signals. Comparing the bias and standard deviation of the timing of muscle activation achieved by using three approaches, it is obvious that the single-threshold algorithm and the double-threshold result in poor indications of the intervals of muscle activity when the simulated surface EMG signals originated from the physically-based model rather than a phenomenological one. The present algorithm maintains the standard deviation less than 15 ms when the SNR varies from 20 dB to 3 dB, which is shown in Table 8-4. Hence, the performance of the power-threshold

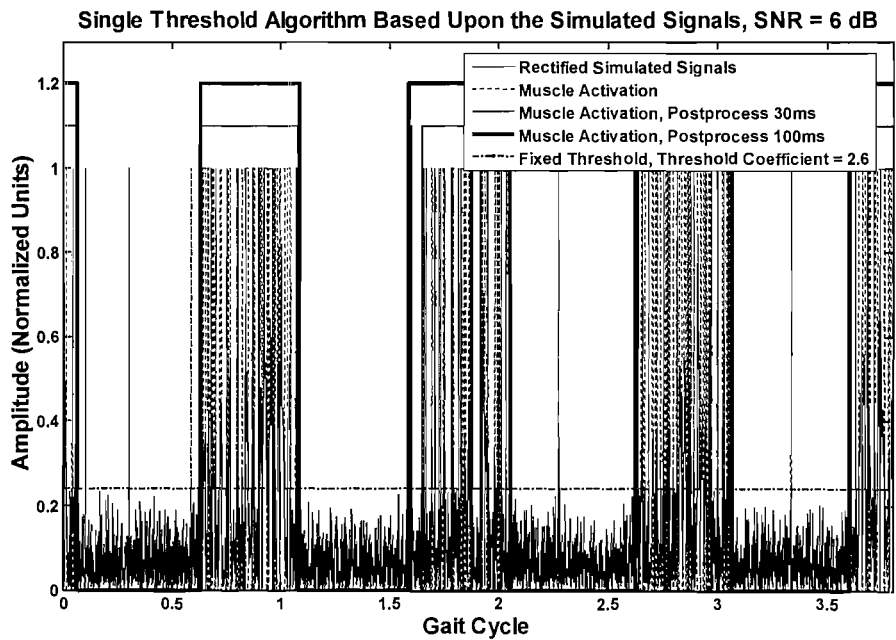
algorithm indicates that it is more suitable for the detection of muscle activation intervals during dynamic movement.

8.7.1 Comparison with the Single-threshold Algorithm

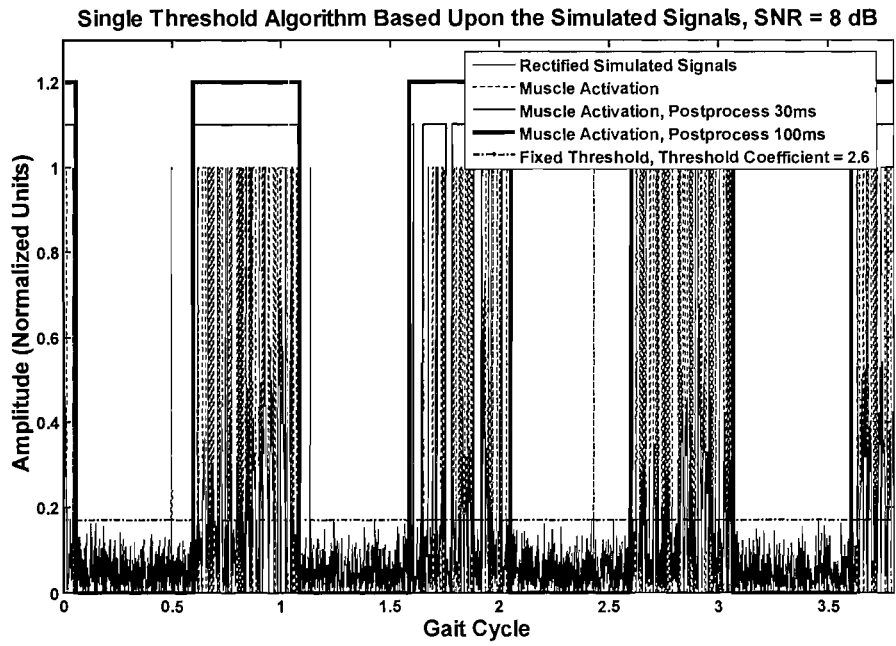
In the single-threshold approach, the fixed threshold is calculated by the equation $T_h = \mu_n + \gamma \cdot \sigma_n$, parameter γ plays a major role in the selection of the threshold and the typical range of the value for γ is from 2 to 3. The rectified simulated surface EMG signal is then compared with the threshold T_h . In this case, the value of parameter γ is changed from 2 to 3 in steps of 0.2, in order to achieve the best performance of the single-threshold algorithm applied to the simulated signal produced by the physically-based model. The standard deviations of on-off timing of muscle activation detected by using the single-threshold algorithm are shown in Table 8-6 when the value of the parameter γ varies from 2 to 3 in steps of 0.2 and the value of SNR alters from 3 dB to 20 dB. The result indicates that the better performance may occur when the value of γ is equal to 2.6. It is evident that the algorithm leads to a standard deviation of the timing greater than 40 ms when SNR is 3 dB and results in the worst performance when big spikes are present in the signal. The performance of the algorithm with $\gamma = 2.6$ applied to the simulated signal with different SNR (3 dB, 6 dB, 8 dB, 10 dB and 20 dB) is also presented by Figure 8-12 and Table 8-7. Obvious errors such as incorrect muscle activation estimation are presented due to large spikes. After eliminating the obvious errors by operator interaction, the standard deviation of the on-off timing is still up to 41.5 ms. The range of the bias of the on-off timing changes from -62 ms to 35 ms. The results show that the single-threshold algorithm is not satisfactory for the estimation of the muscle activation intervals on the basis of the simulated surface EMG signals generated from the physically-based model.



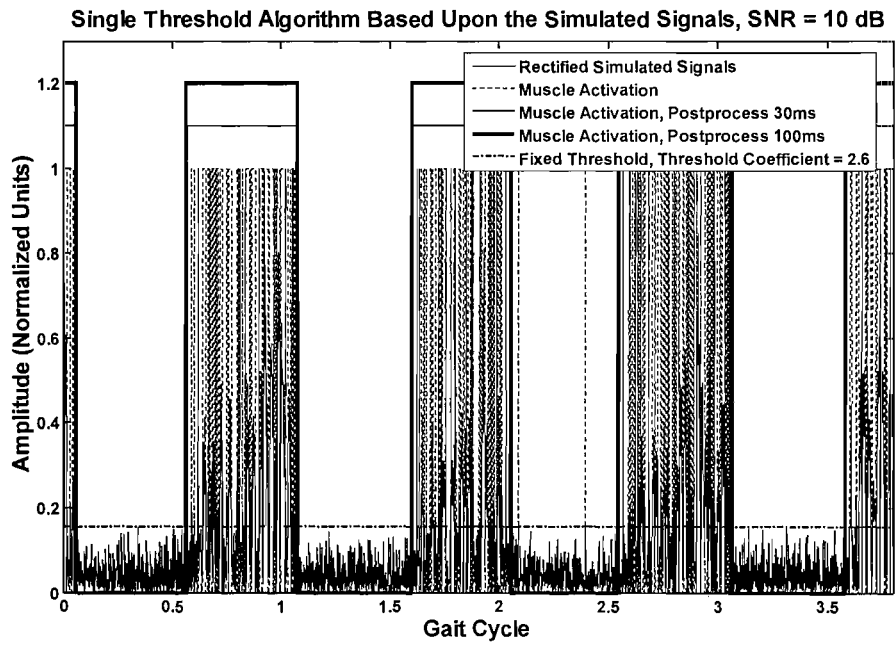
(a)



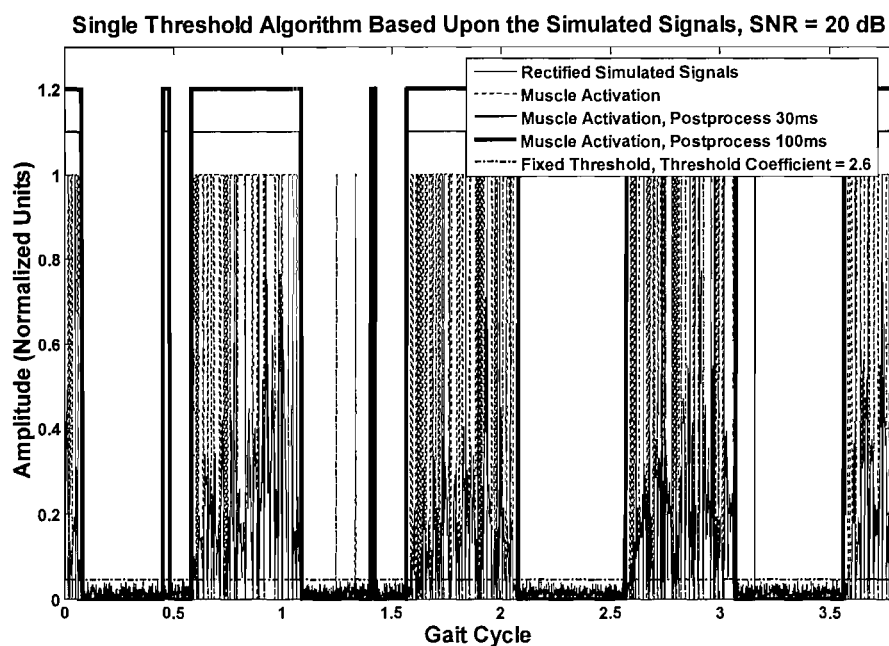
(b)



(c)



(d)



(e)

Figure 8-12 The results of the single-threshold algorithm on the simulated surface EMG signals with SNR = 3 dB, 6 dB, 8 dB, 10 dB 20 dB produced by the physically-based model.

In this case, the threshold coefficient of single threshold algorithm is $\gamma = 2.6$. The on-off timings of muscle activation are depicted by the rectangular windows plotted by the bold solid line. All transitions are shown by the rectangular windows plotted by the dashed line. The on-off timings with part of the post processor, which rejects the transitions shorter than 30 ms, are displayed by the rectangular windows plotted by the solid line. The fixed threshold is shown by the dash-dot line.

Table 8-6 The values of standard deviation of onset and cessation timing of the simulated signals with SNR = 3 dB, 6 dB, 8 dB, 10 dB and 20 dB are calculated by the use of the single-threshold algorithm with different threshold coefficients γ . In this case, $\gamma = 2.0, 2.2, 2.4, 2.6, 2.8, 3.0$.

			Threshold coefficient γ					
			2.0	2.2	2.4	2.6	2.8	3.0
Standard deviation	SNR=3 dB	On	30.0*	30.5*	25.9*	37.9	111.3	193.9
		Off	65.1*	51.0*	39.0*	41.5	66.3	80.7
	SNR=6 dB	On	15.6*	16.1*	17.7*	20.4	34.3	55.5
		Off	139.0*	14.6*	13.7*	13.7	13.7	14.7
	SNR=8 dB	On	98.4*	20.7*	20.7*	7.5	27.9	29.8
		Off	101.7*	10.6*	12.5*	13.4	13.4	32.9
	SNR=10 dB	On	137.1*	48.5*	31.7	25.1	25.2	24.0
		Off	81.6*	10.0*	16.4	16.4	18.5	20.5
	SNR=20 dB	On	109.8*	89.1*	88.2*	9.1*	6.6	7.1
		Off	104.1*	78.5*	68.4*	11.7*	13.0	13.7

* The obvious errors (the error due to large spikes) are eliminated by the observer before the computation of the value of standard deviation, in order to obtain correct muscle activation intervals and accurate statistical results. The results from selecting the threshold coefficient $\gamma = 2.6$ resulting in the minimum standard deviation for SNR greater than 3 dB are also highlighted.

Table 8-7 The bias and standard deviation of onset and cessation timing of muscle activation by using the single-threshold algorithm to analyse the simulated surface EMG signals produced by the physically-based model.

In this case, we choose the parameter $\gamma = 2.6$, the fixed threshold $T_h = \mu_n + \gamma \cdot \sigma_n = \mu_n + 2.6 \times \sigma_n$. 1st gc indicates the first, 2nd gc indicates the second, 3rd gc indicates the third cycle of the gait cycles, respectively; SD is the standard deviation of three gait cycles.

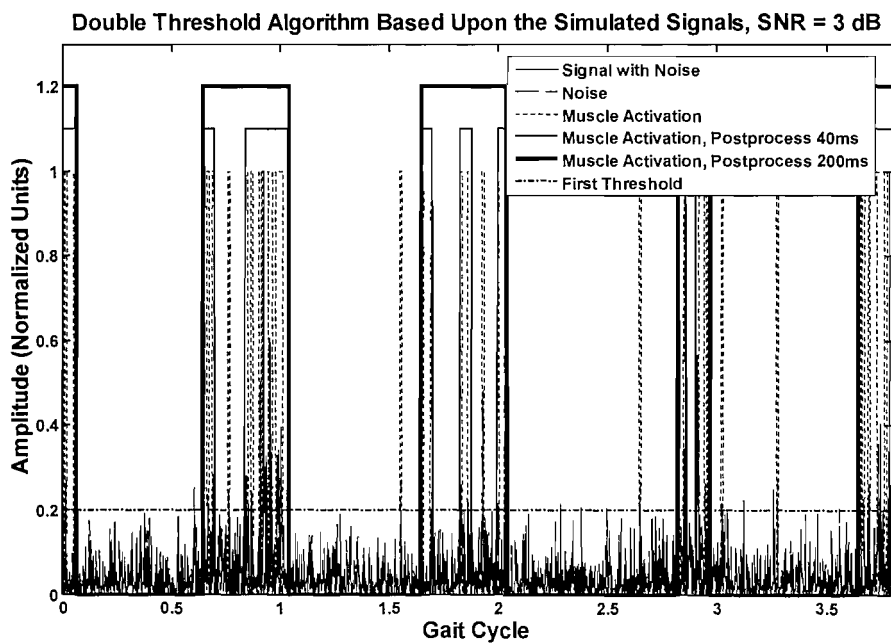
Bias and Standard Deviation									
$\gamma = 2.6$									
		Onset Timing				Cessation Timing			
		Bias ms			SD ms	Bias ms			SD ms
		1stgc	2ndgc	3rdgc		1stgc	2ndgc	3rdgc	
SNR	3 dB	35.0	35.0	43.0	37.9	-23.0	-62.0	-28.0	41.5
	6 dB	23.0	-19.0	19.0	20.4	21.0	-11.0	1.0	13.7
	8 dB	-5.0	-12.0	-1.0	7.5	19.0	-13.0	1.0	13.4
	10 dB	-18.0	22.0	-33.0	25.1	-4.0	-25.0	-13.0	16.4
	20 dB	1.0	-13.0	-9.0	9.1	-3.0	-9.0	-18.0	11.7

8.7.2 Comparison with the Double-threshold Algorithm

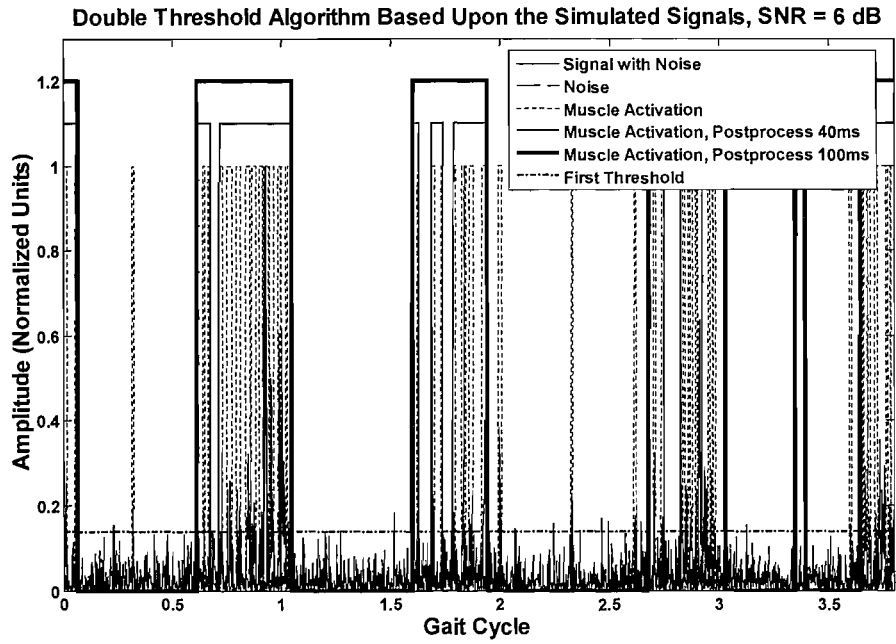
The double-threshold algorithm is derived on the basis of the whitened data that is assumed to have a Gaussian distribution. In the process of derivation of the algorithm, the surface EMG signal during voluntary contraction is simulated by a zero-mean, Gaussian distribution modulated by the muscle activity and corrupted by an independent zero-mean, Gaussian noise process. Hence, the simulated surface EMG signal produced by the physically-based model must be whitened for verifying the double-threshold algorithm. In this case, first, the simulated signal may be filtered by the whitening filter, then consecutive pairs of samples may be squared and summated, generating a

random process. The desired probability of false-alarm ($P_{false-alarm}$) is set to a typical value 0.05; the desired probability of detection ($P_{detection}$) is set to a value 0.95. The length of observation window (m) equals 5 samples, the second threshold (n_0) equals 1. The first threshold can be obtained by solving equation 8.5 with respect to P_η and equation 8.3 with respect to η . In the postprocessor, first transitions greater than 40 ms are considered as valid muscle contraction.

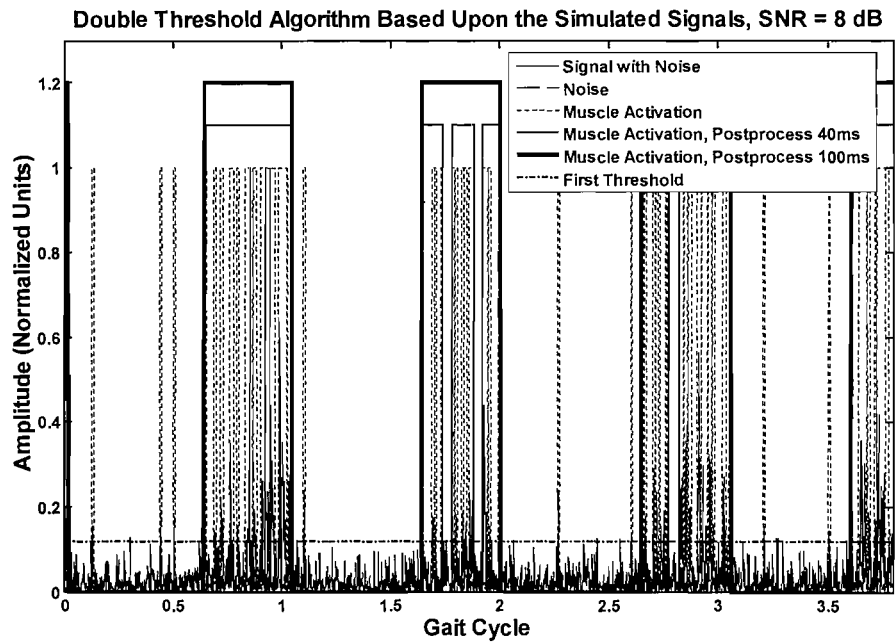
Figure 8-13 and Table 8-8 summarize the performance of the double-threshold algorithm used to analyse the simulated surface EMG signal when SNR varies from 3 dB to 20 dB. The standard deviation of the on-off timing of muscle activation provided in Table 8-8 fluctuates from 23.8 ms to 126.4 ms and indicates poor performance of the algorithm. This result indicates that the double-threshold is not satisfactory for analysing the simulated signals produced by the model based upon the physical structure. It is only appropriate for assessing the stochastic signals produced by a phenomenological model (The results have been shown in Table 8-1).



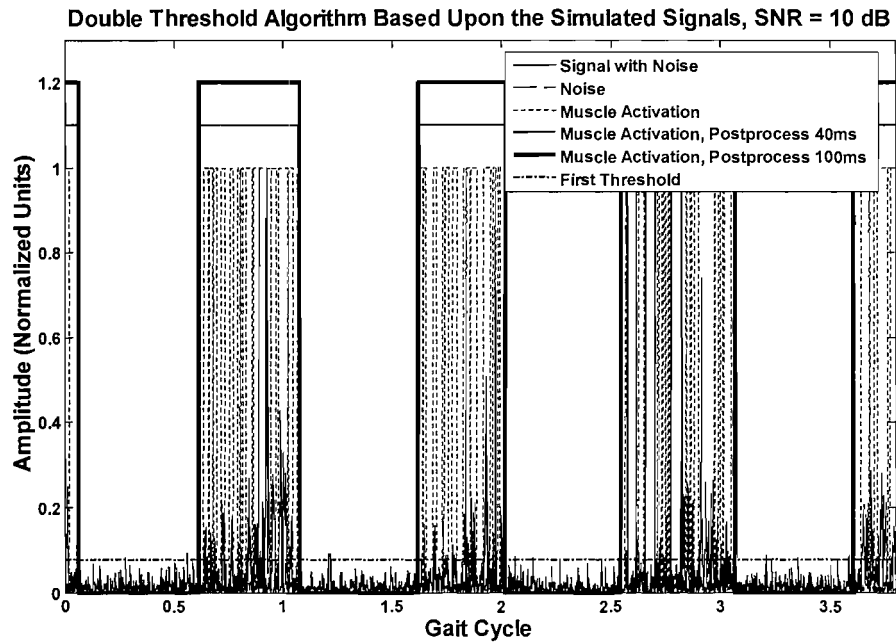
(a)



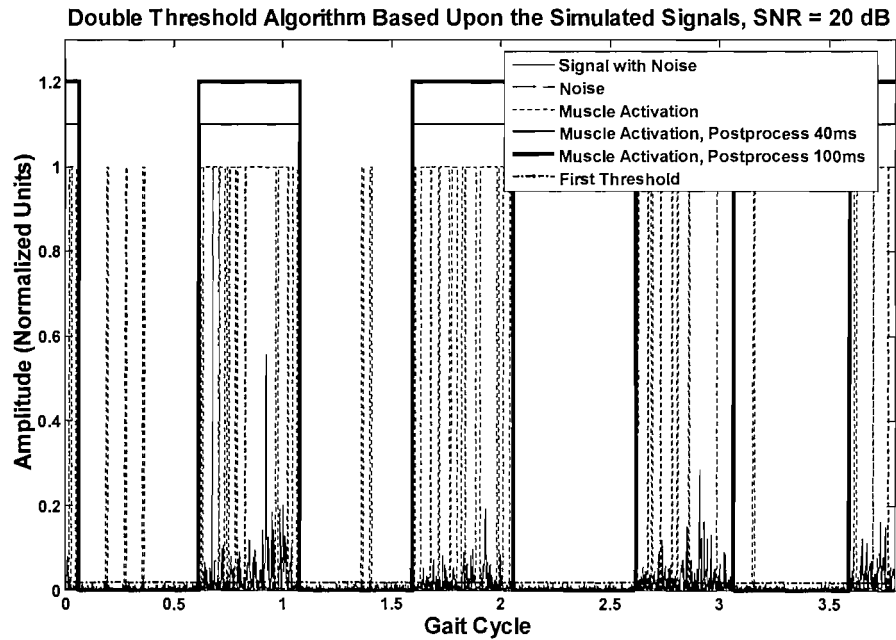
(b)



(c)



(d)



(e)

Figure 8-13 The results of the double-threshold algorithm on the simulated surface EMG signals with SNR = 3 dB, 6 dB, 8 dB, 10 dB and 20 dB produced by the physically-based model.

In this case, the length of observation window (m) is 5 samples; the second threshold (n) is 1. All the transitions may last more than 40 ms are considered as a valid activation in the post-processor. An additional post-processor is applied to overcome the worse results produced by the former double-threshold algorithm.

Table 8-8 The bias and standard deviation of onset and cessation timing of muscle activation by using the double-threshold algorithm.

Bias and Standard Deviation									
ms									
		Onset Timing				Cessation Timing			
		Bias			SD	Bias			SD
		ms				ms			
		1stgc	2ndgc	3rdgc		1stgc	2ndgc	3rdgc	
		SNR	3 dB	34.0		37.0	213.0	126.4	
	6 dB	0	-10.0	70.0	40.8	-15.0	-116.0	-29.0	69.6
	8 dB	32.0	36.0	40.0	36.1	-12.0	-54.0	-1.0	31.9
	10 dB	16.0	22.0	-56.0	35.9	7.0	-51.0	-3.0	29.8
	20 dB	37.0	18.0	41.0	33.5	-12.0	-32.0	-23.0	23.8

1st gc indicates the first, 2nd gc indicates the second, 3rd gc indicates the third cycle of the gait cycles, respectively; SD is the standard deviation of three gait cycles.

8.8 Results and Discussion

A muscle activation interval is an important parameter in the analysis of muscle activity during dynamic movements. From the signal processing point of view, the problem of timing detection is that of obtaining the presence of useful EMG signal in the noisy recording. This problem can be addressed with different methods, such as observation by an experienced operator, a fixed threshold or a double-threshold algorithm, and a generalized likelihood ratio test approach. A new method is proposed in this chapter and is used to detect the on-off timing of muscle activation, which is

based on the computation of the power of the surface EMG signals. The muscle activity is defined as a valid contraction when the power of the surface EMG signal within the observation window exceeds the final threshold described by the power of the noise, the threshold coefficient and the length of observation window.

The performances of the different approaches are strongly dependent upon the model used to produce the simulated surface EMG signal. Most previous methods are based upon a phenomenological model generating a stochastic signal, which is not efficient enough to interpret the real surface EMG signal. Therefore, the performances of previous methods assessed by a phenomenological model are not accurate enough to describe the characteristics of the methods. For example, the performance of the double-threshold algorithm based upon the stochastic signal produced by a phenomenological model shows good results in the analysis of the timing of muscle activation. However, the results of the double-threshold algorithm applied to the simulated EMG signals produced by a physically-based model appear worse; the standard deviation estimate of the timing alters from 23.8 ms to 126.4 ms when SNR changes from 20 dB to 3 dB. The new algorithm presented in this work is assessed by the simulated surface EMG signal originated from a physically-based model and shows better performance in the analysis of muscle activation intervals during dynamic movement. The algorithm is more reliable for clinical application to detect the timing of the surface EMG signal recorded from gait studies.

At present, the algorithm only provides a binary output, thus any abnormal amplitude of the surface EMG signal may not be recognized from the results. This implies that muscle activation with correct timing that corresponds to an incorrect or insufficient intensity of muscle contraction may not be considered as pathological muscle activity by the observer. In order to overcome this limitation, the output of the algorithm can also be described by a horizontal bar whose area may be shadowed by a grey-level scale. The

levels of grey depict the instantaneous power of the surface EMG signal. This work will be discussed and accomplished in future studies.

8.9 Summary

In this chapter, the features of traditional and new algorithms for detection of on-off timing of muscle activation using surface EMG signals have been described. As is evident from above descriptions, many approaches have been carried out in recent years in order to improve the accuracy of the indication and to make the methods less dependent upon the skill or experience of the operator. However, shortcomings of algorithms proposed previously have emerged by applying these algorithms to the simulated signals originated from the physically-based model. To overcome the shortcomings of the traditional methods, the power-threshold algorithm has been addressed in the Section 8.4. Section 8.6 indicated the performances of the algorithm applying to the simulated signals and real data recorded from the gait experiment. It is evident that the algorithm is more suitable than previous methods for the detection of the muscle activation intervals during gait analysis.

Chapter 9 Conclusions & Future Work

9.1 Surface EMG Acquisition & Measurement

The surface EMG technique offers a non-invasive and safe means of monitoring direct and associated muscle activity during dynamic movements. Both the magnitude and timing pattern of muscle activity can be displayed and allow objective quantification of muscle functions and possibly distinguish the different aspects of muscle activity. The surface EMG technique has been applied to many fields such as kinesiology, rehabilitation, physiology, bio-feedback, neurology, sports medicine, and ergonomics. One of them, the correlation between the surface EMG signal and the study of dynamic movements, especially in gait analysis, has been the topic of this study. The historical development of surface EMG and its key features were presented first. Physiological details of the surface EMG were then introduced and key definitions and concepts of gait analysis and basic functions of the gait have also been reviewed. Two main lower limb muscles,

tibialis anterior and gastrocnemius, participate in the support, swing and propulsion functions involved in the gait cycle, and their anatomy and control were discussed in detail.

The myoelectrical signal may be reduced due to the impedance of the body tissue, which is considered as a low-pass filter. The further the signal propagates through body tissue, the more higher-frequency components of signal may be absorbed. Hence, the magnitude of the myoelectrical signal recorded on the surface of the skin is very small in value so that it is easily contaminated by other electromagnetic signals in the recording environment. In order to decrease or eliminate common mode interference, noise and movement artefacts, many techniques have been introduced into surface EMG measurement. For example, two types of surface electrodes, floating and active electrodes, were recommended for recording. A differential amplifier able to eliminate the part of signal that is common to both recording electrodes was described on the basis of the two parameters of common mode rejection ratio and input impedance; surface electrode placement for recording the signal from the target muscles was recommended as well. In addition, band-pass and notch filters and their key parameters have been implemented both in the electronic circuitry and software.

9.2 Surface EMG Simulation Modelling

A simulation model provides an essential aid for assessing new methods and algorithms for processing the surface EMG signal. The performance of the algorithm can be examined by comparing actual or known values of parameters contained in the model with the values of parameters obtained by using the new method. A wide range of models has been addressed over recent decades by various research groups. However, only a few researchers

have attempted to relate the surface EMG to the phases of the gait cycle and to simulate the muscle activity on the basis of the gait patterns. In this study, a simulation model of the surface EMG signal for the analysis of muscle activity during the gait cycle has been generated. It covered most of the characteristics of the surface EMG, for example muscle fibre distribution and action, motor unit type, size, distribution, and recruitment, tissue anisotropy, electrode configuration, and gait phases. A series of surface EMG signals have been produced from the model and used to examine the algorithms to estimate muscle activation timing during the gait cycle.

9.3 Surface EMG Signal Processing

The information extracted from the surface EMG can be taken advantage of in many studies of muscle activity and motor control. The basic steps of the surface EMG signal processing, such as, sampling theorem, analog-to-digital conversion, quantification, normalization and spectral analysis, have been described respectively. Three main applications of the surface EMG signal processing, assessment of relative intensity, assessment of muscle activation intervals, and assessment of muscle function, were introduced. One of them, estimation of muscle activation intervals, referring to onset and cessation timing, has been discussed in depth. Many methods have been proposed in the literature and their performances vary considerably. To overcome the shortcomings of the traditional methods, the power-threshold algorithm to detect the on-off timing of muscle activation has been developed. The performance of the algorithm has been shown by comparing with other methods proposed previously on the basis of the simulated surface EMG. Furthermore, application to the real surface EMG signals recorded from the gait trials, the results clearly indicated that the algorithm is suitable for estimating the muscle activation intervals during dynamic movements.

9.4 Main Contributions of this Study

Key contributions were presented in section 1.7. In summary they are considered to be:

- Producing a comprehensive, physiologically-based simulation model of the surface EMG signal for the analysis of muscle activity during the gait cycle.
- Developing a novel power-threshold algorithm to detect the timing of muscle activation during the gait cycle.
- Designing and performing a gait experiment to investigate the muscle activity during dynamic movement. The data collected have been used to demonstrate the validity of the simulation model and to examine the power-threshold algorithm to detect the timing of muscle activation.

9.5 Future Work

9.5.1 Pathological Gait Analysis

Walking relies on activation timing and intensity of appropriate muscles to offer weight bearing stability, shock absorption and progression. A detailed study of individual muscle activity provides an aid to understanding normal or abnormal muscle functions and distinguish pathological gait from normal walking. The normal gait cycle can be disrupted in many ways. Pain, disuse, or direct injury may weaken the muscle functions. Brain or spinal cord injury may influence on the primary motor control and feedback pathway as well. Mixtures of inadequate, excessive, inappropriate activation timing or

out-of-phase muscle activity may result in pathological walking patterns. To treat the abnormal gait with an appropriate reconstructive procedure, the analysis of the surface EMG signals provides an easy and safe way to interpret the muscle activity.

Using the Vicon Motion Analysis System, the body movements recorded from healthy adults during the gait experiment described in Chapter 6 could be integrated with the surface EMG signals and used for visualising the gait cycle patterns and for cross-checking signal timings. The results may provide more valuable information for quantitative gait studies to identify the underlying causes for walking abnormalities in patients with cerebral palsy, stroke, head injury and other neuromuscular problems.

9.5.2 Surface EMG Analysis in the Study of Pathological Gait

9.5.2.1 Surface EMG Signal Simulation Modelling

In order to assess the algorithms to examine the abnormal muscle functions during the pathological gait, it is essential to create a simulation model with unusual parameter values. The simulation model used to produce the surface EMG signals of healthy adults during normal gait cycle has been described in Chapter 7. Based upon its existing modular parameters, which can be altered to suit the different requirement, the model can be modified to examine the algorithms to process pathological surface EMG signals. Generation of a simulation model to satisfy the various requirements in the analysis of abnormal walking would form a key future task.

9.5.2.2 Methods and Algorithms to Detect Muscle Activity

Different types of information are extracted for gait analysis from the surface EMG measurement. Most commonly, the researchers are interested

in two main types of data utilization. One is the presence or absence of the target muscle's activity during different phases of the gait cycle. The other is to relate some measure of the surface EMG signal intensity to muscle effort. The results of muscle activation timing lead to an understanding as to whether a particular muscle is activated at the appropriate timing in the gait sequence. Several approaches proposed previously to estimate the on-off timing of muscle activation have been addressed in Chapter 8. Because studies of normal gait are available, the on-off timing of the various muscles can be detected so that inappropriate firing of abnormal muscles during the pathological gait can be identified. The power-threshold algorithm derived from this study has been applied to the surface EMG signals recorded from healthy adults during normal walking. In future work, the power-threshold algorithm may also be used to detect the surface EMG signals recorded from the pathological gait to examine the abnormal muscle functions, for example, the estimation of muscle activation intervals of the cerebral palsy children with or without the treatment of BoNT/A.

9.6 Summary

The purpose of this study was to present the characteristics of the surface EMG signal and improve the analysis techniques and signal processing methods in order to explain the muscle activity during dynamic movements. An overview of the surface EMG, especially the development and applications of the surface EMG, has been introduced at the beginning of this thesis. The anatomy and physiological basis of the surface EMG, including the neuromuscular system, structure of the skeletal muscle, muscle fibre work, as well as motor unit properties and recruitment, was addressed in Chapter 2. The key definitions and concepts of gait analysis, one of the applications of the surface EMG technique, were set forth. Muscle control during normal gait also was described. Brief definitions and explanations of

some fundamentals of the surface EMG measurement and instrumentation, for example, surface electrodes, differential filter, input impedance, common mode rejection, and filters, have been illustrated in Chapter 4 in detail. Main applications of the surface EMG in clinical research, such as estimation of relative intensity, assessment of muscle activation intervals, and examination of muscle function were introduced. The basic methods of the surface EMG signal processing, signal acquisition, quantification, normalization and spectrum analysis, have been reviewed in Chapter 5.

A simulation model of the surface EMG signal for the analysis of muscle activity during the gait cycle on the basis of the physical structure was presented in Chapter 7. A series of simulated results, the single fibre action potential, motor unit action potential, motor unit action potential trains, as well as surface EMG signal during voluntary contractions, have been generated by input or modification of the values of the parameters contained in the model. In addition, the simulated surface EMG signals of the lower limb muscles during the gait cycle have been created. Comparison of the simulated signals with the real data recorded from the gait experiment described in Chapter 6, shows that the model described in this study can reproduce the surface EMG signals and is an efficient tool for assessing the effectiveness of new processing algorithms. The model could also have potential in combination with pathological information related to gait phases and could be adapted appropriately and used to investigate clinical problems.

Chapter 8 described a new approach, the power-threshold algorithm, to detect the muscle activation intervals in order to overcome the limitations of methods and algorithms proposed previously and to achieve an improved performance. The shortcomings of the previous methods have been examined based upon a series of simulated EMG signals. Derivation of the algorithm, the flowchart, basic parameters selection, post processor and statistical analysis, was addressed in Chapter 8. Comparing the algorithm

with the traditional approaches indicated that it is more suitable for examining the on-off timing of muscle activation and it promises to be a valuable tool for the analysis the muscle activation intervals in dynamic movements, especially during the gait cycle.

Both the simulation model and the power-threshold algorithm were presented on the basis of the normal surface EMG signals recorded from the healthy adults during normal dynamic movements. Chapter 9 indicated that the work might be extended to the analysis of abnormal surface EMG signals during the research field of pathological gait, such as in children with cerebral palsy. The model and algorithm could be utilized to process the surface EMG signals, which are recorded from the children with cerebral palsy treated by the BoNT/A. The various results between the children treated by BoNT/A and the children without the treatment of BoNT/A could demonstrate the influence (positive or negative) of BoNT/A on the study of cerebral palsy. That might provide an effective aid for clinicians and researchers in the domain of children cerebral palsy research.

Appendices

Appendix I: Abbreviations and Acronyms

Ach	Acetylcholine
A/D	Analog-to-digital
AR	Average Rectified
ATP	Adenosine Triphosphate
BoNT-A	Botulinum Toxin A
cm	Centimeter
CMRR	Common Mode Rejection Ratio
C₇	Seventh Cervical Vertebra
DA	Differential Amplifier
dB	Decibel
DFT	Discrete Fourier Transform
ECG	Electrocardiogram
EMG	Electromyogram
FFT	Fast Fourier Transformation
GC	Gait Cycle

GL	Gastrocnemius Lateral
GM	Gastrocnemius Medialis
Hz	Hertz
m	Meter
mm	Millimeter
ms	Millisecond
MU	Motor Unit
MUAP	Motor Unit Action Potential
mv	Millivolt
MVC	Maximum Voluntary Contraction
PSD	Power Spectral Density
RMS	Root Mean Square
s	Second
SD	Standard Deviation
SNR	Signal-to-noise Ratio
TA	Tibialis Anterior
2-D	Two-dimensional
3-D	Three-dimensional
μ	Micron
μm	Micrometer
μV	Microvolt
V	Velocity

Appendix II: Glossary of Terms

Acetylcholine

A white crystalline derivative of choline, $C_7H_{17}NO_3$, that is released at the ends of nerve fibres in the somatic and parasympathetic nervous systems and is involved in the transmission of nerve impulses in the body.

Actin

A protein found in muscle that together with myosin functions in muscle contraction.

Action Potential

Impulsive, electrical signal travelling along nerve and muscle fibres.

Anterior Horn

Also called ventral horn, a subdivision of gray matter in the anterior part of each lateral half of the spinal cord that contains neurons giving rise to motor fibres of the ventral roots of the spinal nerves.

ADP

An ester of adenosine that is converted to ATP for the storage of energy.

ATP

Adenosine Triphosphate, an adenosine-derived nucleotide, which supplies large amounts of energy to cells for various biochemical processes, for example, muscle contraction and sugar metabolism, through its hydrolysis to ADP.

Botulinum Toxin A

Botulinum Toxin A is a protein and synthesized as single polypeptide chains. It can be activated by proteolytic enzymes and produce a bi-chain molecule comprised of a heavy chain and a light chain connected by a disulphide bond. It acts by binding to the neuromuscular junction and blocks the release of the neurotransmitter acetylcholine from peripheral nerves.

Cerebral Palsy

Caused by an injury to the immature brain that generally happens during or shortly after birth. It can influence all functions of the brain, especially the motor cortex.

Coronal Plane

Relating to, or having the direction of the coronal suture or of the plane dividing the body into front and back portions.

Dorsiflexion

Causing the top of the foot towards the front of the leg.

Endplate

Region of muscle fibre underlying the motor nerve terminal which transmits neural impulses to a muscle.

Extension

The act of straightening or extending a limb, moving apart of two opposing surfaces in a paramedian plane.

Flexion

The act of bending a joint or limb by flexors in a paramedian plane, in order to bring together two anterior or posterior surfaces of limb.

Gastrocnemius

Gastrocnemius is situated on the back of the lower limb, its muscle bulks mainly in the upper half and the two fleshy bellies are an important factor in the shape of the calf. The two heads of gastrocnemius arise from the medial and lateral condyles of the femur. The medial head originates from behind the medial supracondylar ridge and the adductor tubercle on the popliteal surface of the femur; the lateral head arises from the outer surface of the lateral condyle of the femur just above and behind the lateral epicondyle. Its action is a mainly contribution in the plantarflexor of the ankle joint. It also produces the propelling force for movement such as running, walking, and jumping.

High Threshold Motor Unit

With large-diameter axons innervating fast type II muscle fibres supply fast, active muscle activities, such as running and jumping. Those units become fatigued easily.

Initial Swing

The phase of the swing period starts at the time when the foot is lifted from the ground and ends when the foot is opposite the other foot (stance foot), it might take approximately one-third of the swing period.

Isometric Contraction

Muscle contractions, in which the muscle length remains unaltered and the tension usually increases in order to overcome the resistance, are termed isometric.

Isotonic contraction

Muscle contractions, in which the muscle length obviously changes, although the tension produced remains more or less constant, are termed isotonic.

Loading Response

The phase begins at the moment of the initial contact and continues until the other foot is lifted to forward.

Lower Motor Neurone

Originating in the anterior horn of the spinal grey matter and its axon supplying skeletal muscle fibres. It is also used to define the neurones of the cranial motor nerves.

Lower Threshold Motor Unit

Innervating slow type I muscle fibres are recruited for sustaining muscle activity that maintains the posture of the body. These motor units are not easily fatigued.

Maximum Voluntary Contraction

The maximum value of voluntary contraction, which is a parameter utilized to normalize the surface EMG signal. The surface EMG signal can be normalized and represented from 0% to 100% by comparisons between the amplitude of surface EMG signals and the maximum voluntary contraction recorded from the target muscle. Its value can be obtained by requiring patient to make a resisted maximum contraction.

Mid-Stance

The phase of the stance period begins with the lifting of the other foot and continues until weight of body is moved to the forefoot.

Mid-Swing

The phase of the swing period happens at the moment when the swing foot is opposite the stance foot and ends when the swing limb is advanced until the tibia is vertical.

Motor Unit

The muscles are composed of many muscle fibres, which are united into functional units called motor units. It is the basic level of nerve system of the muscle.

Motor Unit Action Potential

Impulse, electrical signals produced by a motor unit.

Myosin

The commonest protein in muscle cells, responsible for the elastic and contractile properties of muscle. It combines with actin to form actomyosin.

Myofibrils

The threadlike fibrils that make up the contractile part of a striated muscle fibre.

Neuron

A cell composing the nervous system. Its salient features are its ability to open to ionic current when stimulated on its dendrites; to sum the incoming potentials in its cell body and to emit an action potential down its axonic part, if the potential accumulated is high enough.

Neuromuscular Junction

Connection area between motor nerve terminal and muscle fibre, where excitation spreads from axon to the muscle fibre.

Pathological Gait

An abnormal walking pattern, it may be produced by four modes of functional impairment, deformity, muscle weakness, sensory loss and pain.

Plantarflexion

The act of causing the dorsum of the foot to move away from the anterior surface of the leg.

Sarcomere

One of the segments into which a fibril of striated muscle is divided.

Sarcoplasmic Reticulum

In skeletal muscle, the calcium is injected into the intracellular fluid from a separate intracellular compartment which is defined as sarcoplasmic reticulum. It is an intracellular sack surrounding the myofibrils of a muscle cell.

Single Fibre Action Potential

Impulse, electrical signal produced by the depolarisation of the muscle fibre.

Skeletal Muscle

Also referred to as voluntary or striated muscle, is attached to the bones of the skeleton and produces movement at joints. Over one-third of the total human body mass consists of skeletal muscle.

Stance Phase

Employed to describe the period of a gait cycle during which the foot is on the ground.

Swing Phase

Represents the period of a gait cycle during which the foot is in the air and limb forwarding.

Terminal Stance

The phase of the stance period begins as heel is lifted and continues until the other foot touch the ground. It completes single limb support and moves the weight to the forefoot.

Terminal Swing

The phase of the swing period begins when the tibia is vertical and ends when the foot touches the ground.

Tibialis Anterior

A long fusiform muscle that is situated on the front of the leg lateral to the anterior border of the tibia, its action is a dorsiflexor of the foot at the ankle joint. It can balance the body on the foot when it works with other muscles in the leg. It is most superficial muscle and contributes most heavily to the surface EMG signal collected from the tibialis anterior muscle group.

Transverse Tubule System

Periodic invaginations of the plasma membrane that extend into the depths of the muscle fibre called the transverse tubule system.

Tropomyosin

A group of muscle proteins that bind to molecules of actin and troponin to regulate the interaction of actin and myosin.

Troponin

A calcium-regulated protein in muscle tissue occurring in three subunits with tropomyosin.

Voluntary Contraction

A kind of muscle activities, skeletal muscle is contracted under the normally controlling by individual volition of subject.

Appendix III: Papers Presented and Publications


W. Wang, A. De Stefano, R. Allen. '*A simulation model of the surface EMG signal for analysis of muscle activity during the gait cycle.*' Computers in Biology and Medicine. Accepted 14 April 2005. Available online 18 July 2005.

W. Wang, A. De Stefano, R. Allen. '*A simulation model of the surface EMG signal for analysis of muscle activity during the gait cycle*' MEDICON and HEALTH TELEMATICS 2004 Conference, Italy.

A. De Stefano, R. Allen, W. Wang, J.H. Burridge, V.T. Yule. '*Complex wavelet transform for EMG analysis during walking of children suffering of Cerebral Palsy*' World Congress on Medical Physics and Biomedical Engineering 2003, Sydney.

W. Wang, A. De Stefano, R. Allen. '*A model for simulation of the surface EMG signal for analysis of muscle activity during the gait cycle*'. IPEM Annual Scientific Meeting 2003, Bath.

Appendix IV: Ethics Approvals of Experiment

	University of Southampton	School of Health Professions and Rehabilitation Sciences										
		Professor Maureen J Simmonds, Head of School										
		<table border="0"> <tr> <td>University of Southampton</td> <td>Tel +44 (0)23 8059 2142</td> </tr> <tr> <td>Highfield</td> <td>Fax +44 (0)23 8059 5301</td> </tr> <tr> <td>Southampton</td> <td>Web www.sohp.soton.ac.uk/sohp/</td> </tr> <tr> <td>SO17 1BJ</td> <td></td> </tr> <tr> <td>United Kingdom</td> <td></td> </tr> </table>	University of Southampton	Tel +44 (0)23 8059 2142	Highfield	Fax +44 (0)23 8059 5301	Southampton	Web www.sohp.soton.ac.uk/sohp/	SO17 1BJ		United Kingdom	
University of Southampton	Tel +44 (0)23 8059 2142											
Highfield	Fax +44 (0)23 8059 5301											
Southampton	Web www.sohp.soton.ac.uk/sohp/											
SO17 1BJ												
United Kingdom												

19 May 2005

Wei Wang
School of Health Professions
University of Southampton

Dear Wei

Submission No: M05/04-02

Title: Analysis of muscle activity during the gait cycle based upon simulation and measurement of the surface EMG

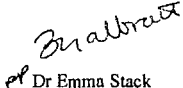
I am pleased to confirm **full approval** for your study has now been given. The Committee would like to suggest however that you may like to make your poster more eye-catching.

The approval has been granted by the School of Health Professions, University of Southampton School of Health Professions and Rehabilitation Sciences Internal Ethics Committee.

You are required to complete a University Research Governance Form and to receive insurance clearance before you begin data collection. I enclose a form which must be completed and sent to Jennifer Roemer in the Research Support Office (RSO) at the University along with a copy of this letter. Your project will be registered at the RSO, and then automatically transferred to the Finance Department for insurance cover. **You can not commence data collection until you have received a letter stating that you have received insurance clearance.**

Please note that you have ethics approval only for the project described in your submission. If you want to change any aspect of your project (e.g., recruitment or data collection) you must discuss this with your supervisor and you may need to request permission from the Ethics Committee.

Yours sincerely


 Dr Emma Stack
 Ethics Co-ordinator, SHPRS Ethics Committee

Enc.

Occupational Therapy Physiotherapy Podiatry
In a research led interdisciplinary environment

UNIVERSITY OF SOUTHAMPTON
INSTITUTE OF SOUND AND VIBRATION RESEARCH
HUMAN EXPERIMENTATION SAFETY AND ETHICS COMMITTEE

Human Experimentation Safety & Ethics Approval Number: 650

Title of Experiment: Analysis of muscle activity during the gait cycle based upon simulation and measurement of the surface EMG

The Committee has examined the safety and ethical aspects of the above experiment which has been submitted by: Wei Wang 15/04/05

The Planned experiment has been found satisfactory with the following actions to be taken prior to starting your experiment:

1. During shaving of the skin or other skin preparation, the researcher should wear protective gloves in case of contact with any body fluids.
2. Sticking plasters should be available to apply in case of any cuts of abrasions to the skin.

The proposed experiment may on start after written evidence has been provided to the secretary regarding the above comments.

The applicant is reminded that the consent forms, completed by all the subjects who participate in this experiment, must be provided to the Secretary of the Human Experimentation Safety and Ethics Committee by: 25/08/2005

****You are asked to record the Human Experimentation Safety & Ethics Approval Number on the completed subject consent forms against the appropriate heading. This number can be found at the top of this page****

Date: 25/05/05

Signed:*J. Winter*.....
Committee Secretary

cc: Professor Robert Allen

Wei Wang,
SPCG, ISVR, Building 13, Highfield,
University of Southampton,
Southampton, United Kingdom, SO17 1BJ
TEL: + 44 (0) 23 8059 4932
EMAIL: ww@isvr.soton.ac.uk

26 May 2005

For the secretary of

**HUMAN EXPERIMENTATION SAFETY AND ETHICS COMMITTEE OF THE
INSTITUTE OF SOUND AND VIBRATION RESEARCH**

Dear Emma,

I received Ethics Approval and reviewer comments about the experiment

Analysis of muscle activity during the gait cycle based upon simulation and measurement of the surface EMG

I appreciated these comments and would like to thank them for their help.

Answers to the reviewers

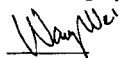
The first comment from the reviewers was requiring *protective gloves*.

In this experiment, the researchers will be asked to wear protective gloves for prevention of contact with any body fluids during proper skin preparation.

The second comment from the reviewers was about *sticking plasters*.

In this experiment, sticking plasters are available to apply in case of any cuts or abrasions to the skin.

Yours sincerely,
Wei Wang



Appendix V: Materials Involved in the Gait Experiment



University
Of Southampton

School of Health Professions and
Rehabilitation Sciences

PARTICIPANT
INFORMATION
SHEET

Participant Information Sheet

Analysis of muscle activity during the gait cycle based upon simulation and measurement of the surface EMG

Wei Wang

I am a PhD researcher at University of Southampton. I would like to invite you to take part in a research study. Before you decide it is important for you to understand why the research is being done and what it will involve. Please take time to read the following information carefully and discuss it with others such as friends, relatives, other participants, or your GP if you wish. Ask me if there is anything that is not clear or if you would like more information. Take time to decide whether or not you wish to take part. Thank you for your reading.

Consumers for Ethics in Research (CERES) publish a leaflet entitled 'Medical Research and You'. This leaflet gives more information about medical research and looks at some questions you may want to ask. A copy may be obtained from CERES, PO Box 1365, London, N16 0BW.

What is the purpose of the study?

The surface EMG (Electromyography) signal represents the characteristics of muscle function and provides information about muscle activity. Surface EMG recordings provide a safe, easy, and non-invasive measurement that allows objective quantification of the muscle activity and possibly differentiates the various phases of muscle activity. The analysis of this signal provides diagnostic information and can be used as an aid for choosing the most appropriate methods of treatment for muscle dysfunction. In the analysis of dynamic movement, the main use of EMG is to analyse the timing of muscle, or muscle group, activation and the intensity of muscle activity. The aim of our work is to utilize surface EMG to analyse the muscle activity in the gait cycle in order to choose the most appropriate methods of treatment for muscle dysfunction.

Why have I been chosen?

You have been chosen because you have no history of leg, ankle or foot injury affecting your normal walking. I am hoping to find 20 people who are interested in taking part in the research and who are aged between 18 and 65 years old.

Do I have to take part?

Taking part in the research is entirely voluntary. It is up to you to decide whether or not to take part. If you do decide to take part you will be given this information sheet and be asked to sign a consent form. If you decide to take part you are still free to withdraw at any time and without giving a reason.

What will happen to me if I take part?

If you take part in the study, I will contact you and answer any questions you might have and may arrange a visit to the Biomechanics Laboratory at the School of Health Professions & Rehabilitation Sciences (Building 45, Highfield Campus) if you wish.

On arrival at the Biomechanics Laboratory you will be shown the equipment used in the experiment and also be given all information about the procedure of the test. If you are happy to continue, you will be asked to sign a consent form. You will be asked to wear shorts because it is easy to attach surface EMG electrodes on your leg. You may bring your own shorts if you wish or I will provide them.

After skin preparation such as, shaving a small patch of hair and cleaning with an alcohol swab, I will mark the location of electrodes and reflective markers on your skin. Next I will attach the surface EMG electrodes and reflective markers on the marked placements, and place pressure sensitive pads on your toe and heel. Please note you will not be able to take part if you are allergic to electrodes, sticking plasters, cleansing wipes, or tapes. In total, seven surface EMG electrodes, five reflective markers and two pressure sensors will be placed on your leg, ankle and foot. Then I will connect the electrodes and foot pressure sensors to the pre-amplifiers and laptop computer.

You will be asked to walk normally on a treadmill while I record data. You will be allowed to rest between tests and we can stop at any time if you become tired. The total amount of time for the test (including preparation time) will be between 60 minutes and 90 minutes.

What are the possible benefits of taking part?

There will be no direct benefit to you from taking part in this research. However, the data collected from this study will provide valuable information for clinicians to develop techniques used to analyse muscle activity in order to assess muscle dysfunction.

What are the side effects of taking part?

There are no side effects from taking part in this study.

What if something goes wrong?

In the unlikely event that you will be harmed in any way by taking part, but if you feel the need to complain about any aspect of the way you have been treated during the course of this research, University complaints mechanisms are open to you. If you have any complaint please contact the research supervisor, Professor Robert Allen, on 023 8059 3746.

Will my taking part in this study be kept confidential?

All information that is collected about you during the course of the research will be kept strictly confidential. Any information about you that may be used in the research reports or publications will have your name and address removed so that you cannot be recognised.

Who is organising the research & reviewing the study?

The study is being organised through the University of Southampton and has been reviewed by both the Internal Ethics Committee of School of Health Professions & Rehabilitation Sciences and the Human Experiment Safety and Ethics Committee of Institute of Sound and Vibration Research.

What will happen to the results of the research study?

At the end of the research the data collected will be held at the University of Southampton in line with the policy for postgraduate research. The results will be presented at conferences and may be published in research papers in scientific journals. We hope this will help clinician or researchers to improve the technique of treatment of muscle dysfunction during movement. If you would like a copy of the published results at the end of the study please let me know.

Contact for Further Information

If you would like any further information please contact:

Wei Wang, Signal Processing & Control Group, Institute of Sound and Vibration Research,
Building 13, Highfield, University of Southampton, Southampton, SO17 1BJ.

Email: ww@isvr.soton.ac.uk

Professor Robert Allen, Room 3059, Signal Processing & Control Group, Institute of Sound
and Vibration Research, Building 13, Highfield, University of Southampton, Southampton,
SO17 1BJ.

Email: ra@isvr.soton.ac.uk

Thank you again for taking time to read this information!

Date:

Version: 2

Ethics Number: M05/04-02

Please tear off the slip below

Analysis of muscle activity during the gait cycle based upon simulation and measurement of
the surface EMG

Wei Wang

Dear Researcher,

Further to your information sheet regarding the above project I wish to confirm that I am
interested in taking part. I would be happy for you to contact me to discuss the project
further.

Please use the following contact details:

Name: _____

Email: _____

Or Telephone Number: _____

Or Address: _____



University
Of Southampton

School of Health Professions and
Rehabilitation Sciences

CONSENT
FORM

Title of Project

Analysis of Muscle Activity during the Gait Cycle Based Upon Simulation and Measurement of the Surface EMG

Name of Researcher

Wei Wang

Please initial box

I, _____
of _____ (address or department) _____
am happy to take part in the project 'Analysis of Muscle Activity during the Gait Cycle Based Upon Simulation and Measurement of the Surface EMG' to be conducted by Wei Wang during the period _____ to _____, 2005.

I confirm that I have read and understand the information sheet dated _____ (version __2__) for the above study and have had the opportunity to ask questions.

I understand that my participation is voluntary and that I am free to withdraw at any time, without giving any reason, without my medical care or legal rights being affected.

I understand that the data collected from me during the experiment will be stored at University of Southampton in line with the policy for postgraduate research.

I confirm that I have no known clinical problems affecting my legs, ankles, feet or my general mobility.

I confirm that I have no known allergies to surface EMG electrodes, sticking plasters, cleansing wipes, or attached tapes.

Name of Participant

Date

Signature

Researcher

Date

Signature

1 for participant; I for researcher

Version: 1
Ethics Number: M05/04-02



University
Of Southampton

Institute of Sound and
Vibration Research

CONSENT
FORM

Title of Project

Analysis of Muscle Activity during the Gait Cycle Based Upon Simulation and Measurement of the Surface EMG

Name of Researcher

Wei Wang

Please initial box

I, _____
of _____ (address or department)
am happy to take part in the project 'Analysis of Muscle Activity during the Gait Cycle Based Upon Simulation and Measurement of the Surface EMG' to be conducted by Wei Wang during the period _____ to _____, 2005.

I confirm that I have read and understand the information sheet dated _____ (version 2) for the above study and have had the opportunity to ask questions.

I understand that my participation is voluntary and that I am free to withdraw at any time, without giving any reason, without my medical care or legal rights being affected.

I understand that the data collected from me during the experiment will be stored at University of Southampton in line with the policy for postgraduate research.

I confirm that I have no known clinical problems affecting my legs, ankles, feet or my general mobility.

I confirm that I have no known allergies to surface EMG electrodes, sticking plasters, cleansing wipes, or attached tapes.

Name of Participant Date Signature

Researcher Date Signature

1 for participant; I for researcher

Version: 1
Ethics Number: 650

Appendix VI: Clinical Aspects of Treatment with Botulinum Toxin A

Since Dr Carl Lammanna first crystallized Botulinum neurotoxin type A (BoNT/A) in 1946, BoNT/A has become the most potent biological poison in the clinical research (*Moore, P, 1995*). The actions of BoNT/A on the neuromuscular junction produce neuromuscular blockade to cause the muscle weakness.

The method of injecting BoNT/A into muscles to treat the cerebral palsy in order to prevent longer term muscle shortening and permanent deformity is a promising medical treatment, which may defer or avoid corrective surgery treatment. However, it is essential to test the effects of the BoNT/A in randomized, controlled clinical trials before this treatment is utilized in the routine clinical application. These tests are applied not only in the effects of BoNT/A, but also in the improvement in mobility and reduction in the need for surgery.

Children who have cerebral palsy usually have no deformity at their birth, but as they grow, the spastic muscles generally cannot grow as rapidly as neighbouring structures, bringing about contractures, deformity and consequent impairment of function. A series of clinical trials are underway in order to explain the effects of the BoNT/A on the treatment of the cerebral palsy, for example, serial gait analysis with electro-goniometry to monitor changes at the hip, knee and ankle joints. (*Moore, P, 1995*). Early research results show that BoNT/A may change the pathogenesis of contractures in cerebral palsy and the improvement influences of BoNT/A on the muscles can be continued even after the parietic effects of the toxin have worn off.

References

Adrian, E D, "The electrical reaction of muscle before and after injury." Brain. vol. 39, pp 1 - 33, 1916.

Adrian, E D and Bronk, D W, "The discharge of impulse in motor nerve fibers II: The frequency of discharge in reflex and voluntary contractions." Journal of Physiology. vol. 67, pp 119 - 151, 1929.

Andreassen, S and Rosenfalck, A, "Relationship of Intracellular and Extracellular Action-Potentials of Skeletal-Muscle Fibers." Crc Critical Reviews in Bioengineering. vol. 6, no. 4, pp 267 - 306, 1981.

Armagan, O, Tascioglu, F, and Oner, C, "Electromyographic biofeedback in the treatment of the hemiplegic hand - A placebo-controlled study." American Journal of Physical Medicine & Rehabilitation. vol. 82, no. 11, pp 856 - 861, 2003.

Baher, H, Analog & digital signal processing. Chichester: Wiley, 1990.

Basmajian, J V, "Control and training of individual motor units." Science. vol. 141, pp 440 - 441, 1963.

Basmajian, J V, Muscles alive: their functions revealed by electromyography. 2nd. Baltimore: Williams & Wilkins, 1967.

Basmajian, J V and De Luca, C J, *Muscle Alive: Their functions revealed by electromyography*. 5th. Baltimore: Williams and Wilkins, 1985.

Berry, C M, Grundfest, H, and Hinsey, J C, "The electrical activity of regenerating nerves in the cat." *Journal of Neurophysiology*. vol. 7, pp 103 - 115, 1944.

Bogey, R A, Barnes, L A, and Perry, J, "Computer Algorithms to Characterize Individual Subject Emg Profiles During Gait." *Archives of Physical Medicine and Rehabilitation*. vol. 73, no. 9, pp 835 - 841, 1992.

Bogey, R A, Perry, J, Bontrager, E L, and Gronley, J K, "Comparison of across-subject EMG profiles using surface and multiple indwelling wire electrodes during gait." *Journal of Electromyography and Kinesiology*. vol. 10, no. 4, pp 255 - 259, 2000.

Bonato, P, "Recent advancements the analysis of dynamic EMG data." *IEEE Engineering in Medicine and Biology Magazine*. vol. 20, no. 6, pp 29 - 32, 2001.

Bonato, P, D'Alessio, T, and Knaflitz, M, "A statistical method for the measurement of muscle activation intervals from surface myoelectric signal during gait." *IEEE Transactions on Biomedical Engineering*. vol. 45, no. 3, pp 287 - 299, 1998.

Bonato, P, Roy, S H, Knaflitz, M, and De Luca, C J, "Time-frequency parameters of the surface myoelectric signal for assessing muscle fatigue during cyclic dynamic contractions." *IEEE Transactions on Biomedical Engineering*. vol. 48, no. 7, pp 745 - 753, 2001.

Booker, H E, Rubow, R T, and Coleman, P J, "Simplified feedback in neuromuscular retraining: an automated approach using EMG signals." *Achieves of Physical Medicine*. vol. 50, pp 621 - 625, 1969.

Brach, J S, Kriska, A M, Newman, A B, and VanSwearingen, J M, "A new approach of measuring muscle impairment during a functional task: Quadriceps muscle activity recorded during chair stand." *Journals of Gerontology Series A-Biological Sciences and Medical Sciences*. vol. 56, no. 12, pp M767 - M770, 2001.

Broman, H, DeLuca, C J, and Mambrito, B, "Motor Unit Recruitment and Firing Rates Interaction in the Control of Human Muscles." *Brain Research*. vol. 337, no. 2, pp 311 - 319, 1985.

Brown, B H, *Medical physics and biomedical engineering*. Bristol: Institute of Physics Publishing, 1999.

- Brown, W F, *Clinical electromyography*. 2nd. Boston: Butterworth-Heinemann, 1993.
- Brucker, B S and Bulaeva, N V, "Biofeedback effect on electromyography responses in patients with spinal cord injury." *Archives of Physical Medicine and Rehabilitation*. vol. 77, no. 2, pp 133 - 137, 1996.
- Budzynski, T, Stoyva, J, and Adler, C, "Feedback-induced muscle relaxation: Application to tension headache." *Journal of Behavior Therapy and Experimental Psychiatry*. vol. 1, pp 205 - 211, 1970.
- Burke, R E, Levine, D N, Tsairis, P, and Zajac, F E, "Physiological Types and Histochemical Profiles in Motor Units of Cat Gastrocnemius." *Journal of Physiology-London*. vol. 234, no. 3, pp 723 - &, 1973.
- Buurke, J H, Hermens, H, Roetenberg, D, Harlaar, J, Rosenbaum, D, and Kleissen, R F M, "Influence of hamstring lengthening on muscle activation timing." *Gait & Posture*. vol. 20, no. 1, pp 48 - 53, 2004.
- Buurke, J H, Hermens, H J, Erren-Wolters, C V, and Nene, A V, "The effect of walking aids on muscle activation patterns during walking in stroke patients." *Gait & Posture*. vol. 22, no. 2, pp 164 - 170, 2005.
- Clancy, E A, Morin, E L, and Merletti, R, "Sampling, noise-reduction and amplitude estimation issues in surface electromyography." *Journal of Electromyography and Kinesiology*. vol. 12, no. 1, pp 1 - 16, 2002.
- Cram, J R, "Surface Emg Recordings and Pain-Related Disorders - A Diagnostic Framework." *Biofeedback and Self-Regulation*. vol. 13, no. 2, pp 123 - 138, 1988.
- Cram, J R, "The history of surface electromyography." *Applied Psychophysiology and Biofeedback*. vol. 28, no. 2, pp 81 - 91, 2003.
- Cram, J R, Kasman, G S, and Holtz, J, *Introduction to surface electromyography*. Gaithersburg: Aspen, 1998.
- D'Alessio, T and Conforto, S, "Extraction of the envelope from surface EMG signals." *IEEE Engineering in Medicine and Biology Magazine*. vol. 20, no. 6, pp 55 - 61, 2001.
- Davis, R C, *Manual of surface EMG laboratory for psychological studies*. Canada: Montreal: Allen. Memorial Institute of Psychiatry, 1952.
- DeLuca, C J, "Use of the Surface Emg Signal for Performance Evaluation of Back Muscles." *Muscle & Nerve*. vol. 16, no. 2, pp 210 - 216, 1993.

DeLuca, C J, "Decomposition of the Emg Signal Into Constituent Motor Unit Action-Potentials." *Muscle & Nerve*. vol. 18, no. 12, pp 1492 - 1493, 1995.

DeLuca, C J, "The use of surface electromyography in biomechanics." *Journal of Applied Biomechanics*. vol. 13, no. 2, pp 135 - 163, 1997.

DeLuca, C J and Jabre, J F, "Emg Signal Decomposition - A New Technique for Studying Individual Motor Unit Action-Potentials at Different Stages of Contraction." *Electroencephalography and Clinical Neurophysiology*. vol. 60, no. 5, pp 101 - 101, 1985.

DeLuca, C J and Jabre, J F, "A Technique for the Detection, Decomposition and Analysis of Complex Emg Signals." *Muscle & Nerve*. vol. 9, no. 6, pp 572 - 573, 1986.

DeLuca, C J, Lefever, R S, Mccue, M P, and Xenakis, A P, "Behavior of Human Motor Units in Different Muscles During Linearly Varying Contractions." *Journal of Physiology-London*. vol. 329, no. AUG, pp 113 - 128, 1982a.

DeLuca, C J, Lefever, R S, Mccue, M P, and Xenakis, A P, "Control Scheme Governing Concurrently Active Human Motor Units During Voluntary Contractions." *Journal of Physiology-London*. vol. 329, no. AUG, pp 129 - 142, 1982b.

DeLuca, C J and Merletti, R, "Surface Myoelectric Signal Cross-Talk Among Muscles of the Leg." *Electroencephalography and Clinical Neurophysiology*. vol. 69, no. 6, pp 568 - 575, 1988.

Dimitrov, G V and Dimitrova, N A, "Precise and fast calculation of the motor unit potentials detected by a point and rectangular plate electrode." *Medical Engineering & Physics*. vol. 20, no. 5, pp 374 - 381, 1998.

Dimitrov, G V, Disselhorst-Klug, C, Dimitrova, N A, Schulte, E, and Rau, G, "Simulation analysis of the ability of different types of multi-electrodes to increase selectivity of detection and to reduce cross-talk." *Journal of Electromyography and Kinesiology*. vol. 13, no. 2, pp 125 - 138, 2003.

Dimitrova, N A and Dimitrov, G V, "Amplitude-related characteristics of motor unit and M-wave potentials during fatigue. A simulation study using literature data on intracellular potential changes found in vitro." *Journal of Electromyography and Kinesiology*. vol. 12, no. 5, pp 339 - 349, 2002.

Dimitrova, N A and Dimitrov, G V, "Interpretation of EMG changes with fatigue: facts, pitfalls, and fallacies." *Journal of Electromyography and Kinesiology*. vol. 13, no. 1, pp 13 - 36, 2003.

- Dimitrova, N A, Dimitrov, G V, and Nikitin, O A, "Longitudinal variations of characteristic frequencies of skeletal muscle fibre potentials detected by a bipolar electrode or multi-electrode." *Journal of Medical Engineering & Technology*. vol. 25, no. 1, pp 34 - 40, 2001.
- Drost, G, Stegeman, D F, Schillings, M L, Horemans, H L D, Janssen, H M H A, Massa, M, Nollet, F, and Zwarts, M J, "Motor unit characteristics in healthy subjects and those with postpoliomyelitis syndrome: A high-density surface EMG study." *Muscle & Nerve*. vol. 30, no. 3, pp 269 - 276, 2004.
- Duchene, J and Goubel, F, "Surface Electromyogram During Voluntary Contraction - Processing Tools and Relation to Physiological Events." *Critical Reviews in Biomedical Engineering*. vol. 21, no. 4, pp 313 - 397, 1993.
- Duchene, J and Hogrel, J Y, "A model of EMG generation." *IEEE Transactions on Biomedical Engineering*. vol. 47, no. 2, pp 192 - 201, 2000.
- Duchenne, G B and Kaplan, E B, *Physiology of movement*. Philadelphia: WB Saunders, 1949.
- Erler, K, Anders, C, Fehlberg, G, Neumann, U, Brucker, L, and Scholle, H C, "Measurement of results of a special hydrotherapy during in-patient rehabilitation after implantation of a total knee arthroplasty." *Zeitschrift fur Orthopadie und Ihre Grenzgebiete*. vol. 139, no. 4, pp 352 - 358, 2001.
- Farina, D, Arendt-Nielsen, L, Merletti, R, and Graven-Nielsen, T, "Assessment of single motor unit conduction velocity during sustained contractions of the tibialis anterior muscle with advanced spike triggered averaging." *Journal of Neuroscience Methods*. vol. 115, no. 1, pp 1 - 12, 2002.
- Farina, D and Merletti, R, "A novel approach for precise simulation of the EMG signal detected by surface electrodes." *IEEE Transactions on Biomedical Engineering*. vol. 48, no. 6, pp 637 - 646, 2001.
- Farina, D and Merletti, R, "Methods for estimating muscle fibre conduction velocity from surface electromyographic signals." *Medical & Biological Engineering & Computing*. vol. 42, no. 4, pp 432 - 445, 2004.
- Farina, D, Merletti, R, and Enoka, R M, "The extraction of neural strategies from the surface EMG." *Journal of Applied Physiology*. vol. 96, no. 4, pp 1486 - 1495, 2004.
- Farina, D, Mesin, L, Martina, S, and Merletti, R, "A surface EMG generation model with multilayer cylindrical description of the volume conductor." *IEEE Transactions on Biomedical Engineering*. vol. 51, no. 3, pp 415 - 426, 2004.

Ferrario, V F, Tartaglia, G M, Maglione, M, Simion, M, and Sforza, C, "Neuromuscular coordination of masticatory muscles in subjects with two types of implant-supported prostheses." *Clinical Oral Implants Research*. vol. 15, no. 2, pp 219 - 225, 2004.

Floyd, W F and Silver, P, "The function of the erector spinae muscles in certain movements and postures in man." *Journal of Physiology*. vol. 129, pp 184 - 203, 1955.

Fuglevand, A J, Winter, D A, Patla, A E, and Stashuk, D, "Detection of Motor Unit Action-Potentials with Surface Electrodes - Influence of Electrode Size and Spacing." *Biological Cybernetics*. vol. 67, no. 2, pp 143 - 153, 1992.

Gabriel, C, Gabriel, S, and Corthout, E, "The dielectric properties of biological tissues .1. Literature survey." *Physics in Medicine and Biology*. vol. 41, no. 11, pp 2231 - 2249, 1996.

Gabriel, D, Basford, J R, and An, K N, "Assessing fatigue with electromyographi spike parameters." *IEEE Engineering in Medicine and Biology Magazine*. vol. 20, no. 6, pp 90 - 96, 2001.

Gage, J R, *Gait analysis in cerebral palsy*. London: Mac Keith Press, 1991.

Gamet, D, Duchene, J, Garaponbar, C, and Goubel, F, "Electromyogram Power Spectrum During Dynamic Contractions at Different Intensities of Exercise." *European Journal of Applied Physiology and Occupational Physiology*. vol. 61, no. 5-6, pp 331 - 337, 1990.

Gasser, H S and Newcomer, H S, "Physiological action currents in the phrenic nerve. an application of the thermionic vacuum tube to nerve physiology." *American Journal of Physiology*. vol. 57, pp 1 - 26, 1921.

Gazzoni, M, Farina, D, and Merletti, R, "A new method for the extraction and classification of single motor unit action potentials from surface EMG signals." *Journal of Neuroscience Methods*. vol. 136, no. 2, pp 165 - 177, 2004.

Gosling, J A, Harris, P F, Humpherson, J R, Whitmore, I, and Willan, P L T, *Human anatomy*. London: Wolfe Publishing, 1994.

Green, E E, Walters, E D, Green, A, and Murphy, G, "Feedback techniques for deep relaxation." *Psychophysiology*. vol. 6, pp 371 - 377, 1969.

Helal, J N and Bouissou, P, "The Spatial Integration Effect of Surface Electrode Detecting Myoelectric Signal." *IEEE Transactions on Biomedical Engineering*. vol. 39, no. 11, pp 1161 - 1167, 1992.

Henneman, E, Somjen, G, and Carpenter, D O, "Functional significance of cell size in spinal motoneurons." *Journal of Neurophysiology*. vol. 28, pp 560 - 580, 1965.

Hermens, H J, Freriks, B, Merletti, R, Stegeman, D, Blok, J, Rau, G, Disselhorst-Klug, C, and Hagg, G, European recommendations for surface electromyography. Roessingh Research and Development, 1999a.

Hermens, H J, Merletti, R, and Freriks, B, "European activities on surface electromyography." *Proceedings of the first general SENIAM workshop*, Italy: Torino. 1996.

Hermens, H J, Merletti, R, Rix, H, and Freriks, B, The state of the art on signal processing methods for surface electromyography. Roessingh Research and Development, 1999b.

Hermens, H J, Stegeman, D, Blok, J, and Freriks, B, State of the art on modelling methods for surface electromyography. Roessingh Research and Development, 1998.

Hodges, P W and Bui, B H, "A comparison of computer-based methods for the determination of onset of muscle contraction using electromyography." *Electromyography and Motor Control-Electroencephalography and Clinical Neurophysiology*. vol. 101, no. 6, pp 511 - 519, 1996.

Inman, V T, "Human Locomotion (Reprinted from *Can Med Assoc J*, Vol 94, Pg 1047, 1966)." *Clinical Orthopaedics and Related Research*. no. 288, pp 3 - 9, 1993.

Inman, V T, *Human walking*. Baltimore: Williams & Wilkins, 1981.

Inman, V T, Saunders, J B, and Abbott, L C, "Observations on the function of the shoulder joint." *Journal of Bone and Joint Surgery*. vol. 26, pp 1 - 30, 1944.

Jacobson, E, "Electrical measurement concerning muscular contraction (tonus) and the cultivation of relaxation in man: relaxation times of individuals." *American Journal of Physiology*. vol. 108, pp 573 - 580, 1934.

Johnson, H E and Garton, W H, "Muscle re-education in hemiplegia by use of electromyographic device." *Archives of Physical Medicine and Rehabilitation*. vol. 54, pp 320 - 322, 1973.

Jonkers, I, Nuyens, G, Seghers, J, Nuttin, M, and Spaepen, A, "Muscular effort in multiple sclerosis patients during powered wheelchair manoeuvres." *Clinical Biomechanics*. vol. 19, no. 9, pp 929 - 938, 2004.

- Kasman, G, "Using surface electromyography." *Rehab Management Magazine*. 2002.
- Kleine, B U, Blok, J H, Oostenveld, R, Praamstra, P, and Stegeman, D F, "Magnetic stimulation-induced modulations of motor unit firings extracted from multi-channel surface EMG." *Muscle & Nerve*. vol. 23, no. 7, pp 1005 - 1015, 2000.
- Knutson, L M, Soderberg, G L, Ballantyne, B T, and Clarke, W R, "A Study of Various Normalization Procedures for Within Day Electromyographic Data." *Journal of Electromyography and Kinesiology*. vol. 4, no. 1, pp 47 - 59, 1994.
- Landau, L D and Lifshitz, E M, *Electrodynamics of continuous media*. 2nd. Oxford: Pergamon, 1984.
- Lauer, R T, Stackhouse, C, Shewokis, P A, Smith, B T, Orlin, M, and McCarthy, J J, "Assessment of wavelet analysis of gait in children with typical development and cerebral palsy." *Journal of Biomechanics*. vol. 38, no. 6, pp 1351 - 1357, 2005.
- Lenman, J A R, Ritchie, A E, and Simpson, J A, *Clinical electromyography*. 4th. Edinburgh: Churchill Livingstone, 1987.
- Levin, O S, Khutorskaya, O E, Amosova, N A, Smolentseva, I G, and Shtock, V N, "Clinical and electromyographical analysis of peculiarities of parkinsonian syndrome in multiple system atrophy and Parkinson's disease." *Zhurnal Nevropatologii I Psikhiatrii Imeni S S Korsakova*. vol. 103, no. 11, pp 4 - 9, 2003.
- Lim, H K, Lee, D C, Mckay, W B, Priebe, M M, Holmes, S A, and Sherwood, A M, "Neurophysiological assessment of lower-limb voluntary control in incomplete spinal cord injury." *Spinal Cord*. vol. 43, no. 5, pp 283 - 290, 2005.
- Lowery, M M, Stoykov, N S, Taflove, A, and Kuiken, T A, "A multiple-layer finite-element model of the surface EMG signal." *IEEE Transactions on Biomedical Engineering*. vol. 49, no. 5, pp 446 - 454, 2002.
- Malmo, R B, Shagass, C, Bellanger, D J, and Smith, A A, "Motor control in psychiatric patients under experimental stress." *Journal of Abnormal and Social Psychology*. vol. 46, pp 539 - 547, 1951.
- Martin, T P, Bodinefowler, S, Roy, R R, Eldred, E, and Edgerton, V R, "Metabolic and Fiber Size Properties of Cat Tibialis Anterior Motor Units." *American Journal of Physiology*. vol. 255, no. 1, pp C43 - C50, 1988.

- Matthews, G G, Cellular physiology of nerve & muscle. Palo Alto: Blackwell Scientific, 1986.
- McComas, A J, Skeletal muscle: form and function. Champaign, IL: Human Kinetics, 1996.
- Merletti, R, Bottin, A, Cescon, C, Farina, D, Gazzoni, M, Martina, S, Mesin, L, Pozzo, M, Rainoldi, A, and Enck, P, "Multichannel surface EMG for the non-invasive assessment of the anal sphincter muscle." *Digestion*. vol. 69, no. 2, pp 112 - 122, 2004.
- Merletti, R, Farina, D, Gazzoni, M, and Schieroni, M P, "Effect of age on muscle functions investigated with surface electromyography." *Muscle & Nerve*. vol. 25, no. 1, pp 65 - 76, 2002.
- Merletti, R, Lo Conte, L, Avignone, E, and Guglielminotti, P, "Modeling of surface myoelectric signals - Part I: Model implementation." *IEEE Transactions on Biomedical Engineering*. vol. 46, no. 7, pp 810 - 820, 1999a.
- Merletti, R and LoConte, L R, "Surface EMG signal processing during isometric contractions." *Journal of Electromyography and Kinesiology*. vol. 7, no. 4, pp 241 - 250, 1997.
- Merletti, R, Roy, S H, Kupa, E, Roatta, S, and Granata, A, "Modeling of surface myoelectric signals - Part II: Model-based signal interpretation." *IEEE Transactions on Biomedical Engineering*. vol. 46, no. 7, pp 821 - 829, 1999b.
- Merlo, A, Farina, D, and Merletti, R, "A fast and reliable technique for muscle activity detection from surface EMG signals." *IEEE Transactions on Biomedical Engineering*. vol. 50, no. 3, pp 316 - 323, 2003.
- Merlo, E, Pozzo, M, Antonutto, G, di Prampero, P E, Merletti, R, and Farina, D, "Time-frequency analysis and estimation of muscle fiber conduction velocity from surface EMG signals during explosive dynamic contractions." *Journal of Neuroscience Methods*. vol. 142, no. 2, pp 267 - 274, 2005.
- Micera, S, Vannozzi, G, Sabatini, A M, and Dario, P, "Improving detection of muscle activation intervals." *IEEE Engineering in Medicine and Biology Magazine*. vol. 20, no. 6, pp 38 - 46, 2001.
- Moore, P, Handbook of botulinum toxin treatment. London: Blackwell Science Ltd, 1995.
- Nandedkar, S D and Sanders, D B, "Measurement of the Amplitude of the Emg Envelope." *Muscle & Nerve*. vol. 13, no. 10, pp 933 - 938, 1990.

- Nandedkar, S D, Sanders, D B, and Stalberg, E V, "Simulation and Analysis of the Electromyographic Interference Pattern in Normal Muscle .1. Turns and Amplitude Measurements." *Muscle & Nerve*. vol. 9, no. 5, pp 423 - 430, 1986.
- Nandedkar, S D and Stalberg, E, "Simulation of Single Muscle-Fiber Action-Potentials." *Medical & Biological Engineering & Computing*. vol. 21, no. 2, pp 158 - 165, 1983.
- Nandedkar, S D, Stalberg, E V, and Sanders, D B, "Simulation Techniques in Electromyography." *IEEE Transactions on Biomedical Engineering*. vol. 32, no. 10, pp 775 - 785, 1985.
- Neafsey, E J, Hull, C D, and Buchwald, N A, "Preparation for Movement in Cat .1. Unit-Activity in Cerebral-Cortex." *Electroencephalography and Clinical Neurophysiology*. vol. 44, no. 6, pp 706 - 713, 1978.
- Northrop, R B, *Signals and systems analysis in biomedical engineering*. Boca Raton, Fla.: CRC Press, 2003.
- Ohanian, H C, *Classical electrodynamics*. Boston, Mass: Allyn and Bacon, 1988.
- Okada, M, "An electromyographic estimation of the relative muscular load in different human postures." *Journal of Human Ergology*. vol. 1, no. 1, pp 75 - 93, 1973.
- Palastanga, N, Field, D, and Soames, R, *Anatomy and human movement: structure and function*. 4th. Oxford: Butterworth-Heinemann, 2002.
- Perry, J, "Determinants of Muscle Function in the Spastic Lower-Extremity." *Clinical Orthopaedics and Related Research*. no. 288, pp 10 - 26, 1993.
- Perry, J, "Gait Analysis - Technology and the Clinician." *Journal of Rehabilitation Research and Development*. vol. 31, no. 1, pp R7 - R7, 1994.
- Perry, J, "The use of gait analysis for surgical recommendations in traumatic brain injury." *Journal of Head Trauma Rehabilitation*. vol. 14, no. 2, pp 116 - 135, 1999.
- Perry, J, Bontrager, E L, Bogey, R A, Gronley, J K, and Barnes, L A, "The Rancho Emg Analyzer - A Computerized System for Gait Analysis." *Journal of Biomedical Engineering*. vol. 15, no. 6, pp 487 - 496, 1993.
- Perry, J, Burnfield, J M, Gronley, J K, and Mulroy, S J, "Toe walking: Muscular demands at the ankle and knee." *Archives of Physical Medicine and Rehabilitation*. vol. 84, no. 1, pp 7 - 16, 2003.

- Perry, J, Garrett, M, Gronley, J K, and Mulroy, S J, "Classification of Walking Handicap in the Stroke Population." *Stroke*. vol. 26, no. 6, pp 982 - 989, 1995.
- Perry, J, Gronley, J K, Newsam, C J, Reyes, M L, and Mulroy, S J, "Electromyographic analysis of the shoulder muscles during depression transfers in subjects with low-level paraplegia." *Archives of Physical Medicine and Rehabilitation*. vol. 77, no. 4, pp 350 - 355, 1996.
- Perry, J, Hoffer, M M, Antonelli, D, Plut, J, and Lewis, G, "Kinesiological Evaluations of Hip Muscles in Cerebral-Palsy with Crouched Gait." *Journal of Bone and Joint Surgery-American Volume*. vol. 57, no. 7, pp 1023 - 1023, 1975.
- Perry, J, *Gait analysis: normal and pathological function*. Thorofare, NJ: SLACK Incorporated, 1992.
- Pratt, F H, "The all-or-none principle in graded response of skeletal muscle." *American Journal of Physiology*. vol. 44, pp 517 - 542, 1917.
- Price, J P, Clare, M H, and Ewerhardt, R H, "Studies in low backache with persistent spasm." *Achieves of Physical Medicine*. vol. 29, pp 703 - 709, 1948.
- Priez, A, Duchene, J, and Goubel, F, "Duchenne Muscular-Dystrophy Quantification - A Multivariate-Analysis of Surface Emg." *Medical & Biological Engineering & Computing*. vol. 30, no. 3, pp 283 - 291, 1992.
- Proakis, J G, *Advanced digital signal processing*. New York: Macmillan, 1992.
- Pullman, S L, Goodin, D S, Marquinez, A I, Tabbal, S, and Rubin, M, "Clinical utility of surface EMG - Report of the Therapeutics and Technology Assessment Subcommittee of the American Academy of Neurology." *Neurology*. vol. 55, no. 2, pp 171 - 177, 2000.
- Reusch, J, Cobb, S, and Finesinger, J E, "Studies on muscular tension in the neuroses." *Transactions of the American Neurological Association*. vol. 67, pp 186 - 189, 1941.
- Roeleveld, K, Blok, J H, Stegeman, D F, and vanOosterom, A, "Volume conduction models for surface EMG; Confrontation with measurements." *Journal of Electromyography and Kinesiology*. vol. 7, no. 4, pp 221 - 232, 1997.
- Roetenberg, D, Buurke, J H, Veltink, P H, Forner Cordero, A, and Hermens, H J, "Surface electromyography analysis for variable gait." *Gait & Posture*. vol. 18, no. 2, pp 109 - 117, 2003.

- Rosenfalck, P, "Intra- and extracellular potential fields of active nerve and muscle fibers." *Acta Physiologica Scandinavica*. vol. 321, pp 1 - 168, 1969.
- Saitou, K, Masuda, T, and Okada, M, "Muscular unit size and fiber density deduced from simulation of inverse analysis of surface electromyograms." *Japanese Journal of Physical Fitness and Sports Medicine*. vol. 53, no. 4, pp 391 - 401, 2004.
- Sanders, F K and Whitteridge, D, "Conduction velocity and myelin thickness in regenerating nerve fibres." *Journal of Neurophysiology*. vol. 105, pp 152 - 172, 1946.
- Schulte, E, Farina, D, Merletti, R, Rau, G, and Disselhorst-Klug, C, "Influence of muscle fibre shortening on estimates of conduction velocity and spectral frequencies from surface electromyographic signals." *Medical & Biological Engineering & Computing*. vol. 42, no. 4, pp 477 - 486, 2004.
- Stashuk, D W, "Simulation of Electromyographic Signals." *Journal of Electromyography and Kinesiology*. vol. 3, no. 3, pp 157 - 173, 1993.
- Staudenmann, D, Kingma, I, Stegeman, D F, and van Dieen, J H, "Towards optimal multi-channel EMG electrode configurations in muscle force estimation: a high density EMG study." *Journal of Electromyography and Kinesiology*. vol. 15, no. 1, pp 1 - 11, 2005.
- Stegeman, D F, Blok, J H, Hermens, H J, and Roeleveld, K, "Surface EMC models: properties and applications." *Journal of Electromyography and Kinesiology*. vol. 10, no. 5, pp 313 - 326, 2000.
- Stylianou, A P, Luchies, C W, and Insana, M F, "EMG onset detection using the maximum likelihood method. 2003 Summer Bioengineering Conference." Florida, 1075 - 1076,
- Sutherland, D H, "Gait Analysis in Cerebral-Palsy." *Developmental Medicine and Child Neurology*. vol. 20, no. 6, pp 807 - 813, 1978.
- Sutherland, D H, "The evolution of clinical gait analysis part I: kinesiological EMG." *Gait & Posture*. vol. 14, no. 1, pp 61 - 70, 2001.
- Sutherland, D H, "The evolution of clinical gait analysis - Part II - Kinematics." *Gait & Posture*. vol. 16, no. 2, pp 159 - 179, 2002.
- Sutherland, D H, "The evolution of clinical gait analysis part III - kinetics and energy assessment." *Gait & Posture*. vol. 21, no. 4, pp 447 - 461, 2005.
- Sutherland, D H and Cooper, L, "Crouch Gait in Spastic Diplegia." *Developmental Medicine and Child Neurology*. vol. 19, no. 1, pp 119 - 120, 1977.

- Sutherland, D H and Davids, J R, "Common Gait Abnormalities of the Knee in Cerebral-Palsy." *Clinical Orthopaedics and Related Research*. no. 288, pp 139 - 147, 1993.
- Sutherland, D H, Kaufman, K R, Campbell, K, Ambrosini, D, and Wyatt, M, "Clinical use of prediction regions for motion analysis." *Developmental Medicine and Child Neurology*. vol. 38, no. 9, pp 773 - 781, 1996.
- Sutherland, D H and Lescooper, A S, "Pathomechanics of Progressive Crouch Gait in Spastic Diplegia." *Orthopedic Clinics of North America*. vol. 9, no. 1, pp 143 - 154, 1978.
- Sutherland, D H, Olshen, R, Cooper, L, and Woo, S L Y, "The Development of Mature Gait." *Journal of Bone and Joint Surgery-American Volume*. vol. 62, no. 3, pp 336 - 353, 1980.
- Sutherland, D H, Olshen, R, Cooper, L, Wyatt, M, Leach, J, Mubarak, S, and Schultz, P, "The Pathomechanics of Gait in Duchenne Muscular-Dystrophy." *Developmental Medicine and Child Neurology*. vol. 23, no. 1, pp 3 - 22, 1981.
- Sutherland, D H, Zilberfarb, J L, Kaufman, K R, Wyatt, M P, and Chambers, H G, "Psoas release at the pelvic brim in ambulatory patients with cerebral palsy: Operative technique and functional outcome." *Journal of Pediatric Orthopaedics*. vol. 17, no. 5, pp 563 - 570, 1997.
- Tanji, J and Kato, M, "Discharges of Single Motor Units at Voluntary Contraction of Abductor Digiti Minimi Muscle in Man." *Brain Research*. vol. 45, no. 2, pp 590 - &, 1972.
- Thextun, A J, "A randomisation method for discriminating between signal and noise in recordings of rhythmic electromyographic activity." *Journal of Neuroscience Methods*. vol. 66, no. 2, pp 93 - 98, 1996.
- Togawa, T and Tamura, T, *Biomedical transducers and instruments*. Boca Raton: CRC Press, 1997.
- Travell, J G and Simons, D G, *Myofascial pain and dysfunction: the trigger point manual*. Baltimore: Williams & Wilkins, 1983.
- Trueblood, P R, "Partial body weight treadmill training in persons with chronic stroke." *Neurorehabilitation*. vol. 16, no. 3, pp 141 - 153, 2001.
- Turker, K S, "Electromyography - Some Methodological Problems and Issues." *Physical Therapy*. vol. 73, no. 10, pp 698 - 710, 1993.
- Tyldesley, B and Grieve, J, I, *Muscles nerves and movement in human occupation*. 3rd. Oxford: Blackwell Science, 2002.

van Putten Jr, J D, "EMG onset determination using a maximum likelihood method. Proceeding. 1st Joint BMES/EMBS Conference." GA, 571 - 1999.

Whatmore, G and Ellis, R M, "Some motor aspects of schizophrenia: an EMG study." American Journal of Psychiatry. vol. 114, pp 882 - 889, 1958.

Yang, J F and Winter, D A, "Electromyographic Amplitude Normalization Methods - Improving Their Sensitivity As Diagnostic-Tools in Gait Analysis." Archives of Physical Medicine and Rehabilitation. vol. 65, no. 9, pp 517 - 521, 1984.